

GHENT UNIVERSITY

MASTER THESIS

**Opinion dynamics on social networks with
stubborn actors**

Author:

Nina BOTTE

Supervisor:

Prof. Dr. Luis E.C. ROCHA

Co-Supervisor:

Prof. Dr. Jan RYCKEBUSCH

*A thesis submitted in partial fulfillment of the requirements
for the degree of Master of Science in Physics and Astronomy*

in the

Faculty of SCIENCE
Department of PHYSICS AND ASTRONOMY

Academic year 2020-2021

Acknowledgments

At times, our own light goes out and is rekindled by a spark from another person. Each of us has cause to think with deep gratitude of those who have lighted the flame within us.

—Albert Schweitzer

First and foremost, I would like to thank my supervisor Prof. Luis E.C. Rocha for his support, feedback and useful insights during the course of this year. This thesis would not be of the same quality if it wasn't for his insightful remarks. I learned a tremendous deal, not only about social physics and network science, but also about organizing, structuring and reporting relevant results. I would not have been able to learn these things without his guidance.

I also want to give special thanks to my co-supervisor Prof. Jan Ryckebusch. Not only for his support during my thesis, but mostly for the enthusiastic and passionate way in which he teaches all his classes. His dedication to his students and his willing to learn them valuable insights in the wonderful world of physics are truly admirable.

I am especially thankful to Yolan. He helped me with every possible problem I encountered during my physics education. If it was not for him, I would still be a (very poor) programming beginner. His patience and talent for explaining things in an understandable way are incredibly valuable. I do not only want to thank him for all his help during my study and my thesis, but also for being the great friend he is. This thesis, but also myself, would not have been the same without him.

Beside Yolan, I want to give credit to all of my other friends. They make my life valuable, joyful and are a true enrichment.

Finally, I would like to thank my family, and especially my parents. They have unbelievable faith in me and support me in every single way. I feel great gratitude for how they raised me and for all the opportunities that they have given me, and are still giving me every single day.

Nina Botte.

Abstract

The past decade, the rise of social media has become undeniable. More and more people are getting engaged on some type of social media platform and hence, it is probably not wrong to say that nowadays most of us have, beside our real life, a virtual life on social media. This rapidly increased engagement on social media undoubtedly has many advantages. However, every upside has a downside and social media is no different. This thesis deals with the impact of social media on the formation and evolution of opinions in society.

Social media allows for the spread of information at a faster pace and at an unprecedented scale. However, people are still bound by time- and cognitive constraints. In order to handle the information overflow, social media companies design filtering algorithms that can fine-tune and individualize the information someone is exposed to. This filtering and individualizing of information may have some potentially dangerous downsides in the sense that people might get trapped in “echo chambers” that confirm their own beliefs. It is important to know the effects of such algorithmic personalization on the appearance and formation of phenomena such as polarization, spread of extremism, formation of echo chambers, etc.

People are, however, more than sheep that thoughtlessly follow their shepherd (contrary to what some books might lead us to believe). They are capable of critical thinking and may be hesitant to change their current opinion. This aspect of potential stubbornness should not be ignored.

In this thesis toy models are designed to investigate the interplay between network structure, filtering algorithms and individual resistance to change in the evolution of two competing opinions. We will investigate whether network properties such as community structure and clustering coefficient may enhance or hamper the formation of echo chambers. We will use some basic filtering algorithms to determine their possible effects on the appearance of echo chambers and we will investigate the impact of individual stubbornness. Beside that, we will also pay some attention to the possible ways of distributing the opinions and how this may affect the opinion dynamics in the system.

Finally, we will test the model on real-world networks. Some question that may arise are: Do the results agree with those obtained from the theoretical network models? What are the similarities or differences in the results? What are the possible underlying reason/structures for these similarities/differences?

Samenvatting

Sociale media zijn bijna niet meer weg te denken uit ons dagelijks leven. De laatste tientallen jaren is het gebruik van sociale media, zowel op persoonlijk vlak als op professioneel vlak, in snel tempo toegegenomen. Tegenwoordig kan men zeggen dat (bijna) iedereen, naast zijn werkelijke leven, een virtueel leven op sociale media leidt. Het gebruik van sociale media heeft ongetwijfeld veel voordelen. Goed en kwaad gaan echter vaak hand in hand en men kan niet ontkennen dat het gebruik van sociale media ook veel potentiële, soms onbekende, nadelen kent. Eén van die, tot nog toe, onbekende kanten van sociale media is de impact die het heeft op de dynamica van opinies in de maatschappij.

Het is bekend dat mensen niet enkel hun mening uit zichzelf vormen, maar sterk beïnvloed worden door onder andere de mensen rond hen, hun omgeving, hun opvoeding,... Sociale media laten onmiddellijke interacties toe tussen mensen van overal op de wereld, zonder daarbij belemmerd te worden door fysieke en/of tijdsbegrenzingen. Dit kan een potentieel grote impact hebben op hoe meningen zich vormen en hoe ze evolueren.

Door het toenemende gebruik van sociale media worden deze echter overspoeld door informatie. Om hun gebruikers niet het gevoel te geven dat ze verdronken in wat ze te zien krijgen op hun sociale media platform, gebruiken deze sociale media platformen filtering algoritmen. Deze filtering algoritmen filteren, zoals de naam al impliceert, en individualiseren de informatie die iemand te zien krijgt op zijn/haar tijdslijn. Een gebruiker op sociale media krijgt dus niet alle berichten die zijn/haar vrienden posten te zien, maar enkel een selectie die onder andere gemaakt wordt op basis van de gebruiker zijn/haar sociale media geschiedenis. Dit filteren/individualiseren kan, mogelijk, grote gevolgen hebben. Zo zou het kunnen leiden tot de vorming van “echo kamers” waar gebruikers gevangen raken tussen ideeën die hun eigen visie versterken. Dit kan op zijn beurt polarisatie in de maatschappij, opkomst van extremisme, enzovoort bevorderen. Het is daarom uiterst belangrijk om de impact van deze filtering algoritmen grondig in kaart te brengen.

Mensen zijn echter ook in staat om kritisch te denken, soms ook over-kritisch of selectief kritisch, maar dat terzijde. Dit kritisch denken kan ertoe leiden dat mensen niet zomaar hun mening veranderen omdat hun vrienden en/of omgeving dat suggereren. Ze zijn meer overtuigd van hun eigen gelijk of menen dat hun eigen visie een correcter standpunt inneemt. Deze individuele koppigheid zou men niet mogen verwaarlozen in het ontwerpen van modellen die de dynamica van opinies op sociale media willen onderzoeken.

In deze thesis wordt gebruik gemaakt van “toy models” die de interactie tussen verschillende netwerk modellen, filtering algoritmen en individuele terughoudenheid om van mening te veranderen onderzoeken in de evolutie van twee opinies. Er worden verschillende netwerk modellen geïntroduceerd die de impact van onder andere clustering en/of groepsstructuur op de evolutie van opinies en de vorming van echo kamers moeten onderzoeken. Daarnaast wordt er gebruik gemaakt van enkel simpele filtering algoritmen om hun impact op de dynamica van de opinies te onderzoeken. Tot slot wordt er een

notie van koppigheid in het systeem geïntroduceerd om mogelijke effecten hiervan in kaart te kunnen brengen.

Naast het bovenstaande zal er ook kort aandacht gespendeerd worden aan hoe de twee verschillende opinies verdeeld worden over het systeem. Is er bijvoorbeeld een verschil tussen de twee meningen willekeurig over het systeem te verspreiden versus deze in een meer groepsstructuur te verdelen? Om de thesis te besluiten zal het opinie-dynamica model, dat in de thesis gebruikt werd, getest worden op netwerken verkregen van data uit de werkelijke wereld (bv. van email data of telefoonnetwerken). Er zal nagegaan worden of de resultaten van deze werkelijke netwerken gelijkenissen, dan wel verschillen, vertonen met de data verkregen van de netwerk modellen.

Table of Contents

Acknowledgments	ii
Abstract	iii
Samenvatting	iv
Table of Contents	vii
List of Figures	x
List of Tables	xi
1 Introduction	1
1.1 Complex networks	2
1.2 Opinion dynamics	3
1.3 Statistical and social physics	4
1.4 This thesis: hypotheses and goals	5
2 Networks	7
2.1 Definition and network measurements	7
2.1.1 Adjacency matrix	7
2.1.2 Degree and degree distribution	8
2.1.3 Connectivity	9
2.1.4 Assortative and disassortative networks	9
2.1.5 Network distances	10
2.1.6 Clustering coefficient and transitivity	11
2.1.7 Network communities	12
2.1.8 Modularity	13
2.2 Network models	15
2.2.1 The Erdős-Rényi model	15
2.2.2 The Watts-Strogatz model	17
2.2.3 The stochastic block model	18
2.3 Real-world social networks	20

3 Opinion dynamics	23
3.1 Binary models	23
3.1.1 The majority model	24
3.1.2 The probabilistic majority model	24
3.1.3 The voter model	25
3.2 Continuous models	25
3.2.1 The classical models	25
3.2.2 Bounded confidence models	26
3.3 Algorithmic personalization	27
3.4 The activation mechanism: Static to temporal	28
3.5 The presence of stubborn actors	29
3.5.1 Stubbornness in bounded confidence models	30
3.5.2 Stubbornness in binary models	31
4 Materials and methods in this thesis	33
4.1 Network models	33
4.2 Real-world networks	35
4.3 Opinion dynamics model	36
5 Results	39
5.1 Network structure	39
5.1.1 Balanced starting conditions	39
5.1.2 Unbalanced starting conditions	42
5.1.3 Formation of echo chambers versus community structure	48
5.2 Stubborn actors	50
5.2.1 Including a stubbornness parameter	50
5.2.2 The majority threshold model	64
5.3 Random versus community distributed opinions	69
5.3.1 Evolution of the prevalence of the opinions	69
5.3.2 Echo chambers	72
5.4 Real-world networks	77
5.4.1 The Last.fm on-line social network	77
5.4.2 The PGP trust network	79
6 Discussion	81
7 Conclusion	85
Appendices	86
A Network measurements: Derivations	87
A.1 Modularity	87
A.1.1 Simple form of network modularity	87
A.1.2 Modularity change after merging two communities	88

B Network models: Derivations	89
B.1 The Erdős-Rényi model	89
B.1.1 Degree distribution	89
B.1.2 Average degree	89
B.1.3 Poisson form of the degree distribution	90
B.1.4 Diameter	91
B.2 The Watts-Strogatz model	91
B.2.1 The regular ring lattice	91

List of Figures

4.1	Degree distribution $P(k)$ of the two real-world networks used in this thesis.	36
5.1	Evolution of the prevalence of opinion A ($P_A(t)$) over time for an initial 50/50 opinion distribution.	40
5.2	Distribution of the fraction of friends (nearest neighbors, nn) of node i with the same opinion B at $t = 500$, $\langle P_B^{\text{nn}} \rangle$, for an initial 50/50 opinion distribution.	41
5.3	Evolution of the prevalence of opinion A ($P_A(t)$) over time for an initial 20/80 opinion distribution.	44
5.4	Evolution of the prevalence of opinion A ($P_A(t)$) over time for an initial 20/80 opinion distribution for a WS model with $N = 10^3$ or $N = 10^4$, $\langle k \rangle = 6$ and $\beta = 0.01$. The PR filtering algorithm is used.	45
5.5	Distribution of the fraction of friends (nearest neighbors, nn) of node i with the same opinion B at $t = 500$, $\langle P_B^{\text{nn}} \rangle$, for an initial 20/80 opinion distribution.	46
5.6	Relation between the formation of echo chambers and community structure (modularity Q).	49
5.7	Formation of echo chambers versus fraction of completely stubborn actors for the PR filtering algorithm and an initial 50/50 opinion distribution.	51
5.8	Formation of echo chambers versus fraction of completely stubborn actors for the REF and REC filtering algorithms and an initial 50/50 opinion distribution.	52
5.9	Formation of echo chambers versus fraction of completely stubborn actors for the PR and REC filtering algorithms and an initial 20/80 opinion distribution.	55
5.10	Evolution of the prevalence of opinion A ($P_A(t)$) over time for an initial 20/80 opinion distribution, using the PR filtering algorithm and comparing three different fractions of completely stubborn actors ($\text{fracRes} = 0$, $\text{fracRes} = 0.4$ and $\text{fracRes} = 0.8$).	57
5.11	Formation of echo chambers versus the stubbornness parameter of all the nodes, r , for the PR filtering algorithm and an initial 50/50 opinion distribution.	59
5.12	Formation of echo chambers versus the stubbornness parameter of all the nodes, r , for the REF and REC filtering algorithms and an initial 50/50 opinion distribution.	60
5.13	Formation of echo chambers versus the stubbornness parameter of all the nodes, r , for the PR and REC filtering algorithms and an initial 20/80 opinion distribution.	62
5.14	Evolution of the prevalence of opinion A ($P_A(t)$) over time for an initial 20/80 opinion distribution, using the PR filtering algorithm and comparing three different values of the stubbornness parameter r of all the nodes ($r = 0$, $r = 0.4$ and $r = 0.8$).	63

5.15	Formation of echo chambers versus the threshold parameter of all the nodes, T , for the PR filtering algorithm and an initial 50/50 opinion distribution. The majority threshold model is implemented.	65
5.16	Formation of echo chambers versus the threshold parameter of all the nodes, T , for the REF and REC filtering algorithms and an initial 50/50 opinion distribution. The majority threshold model is implemented.	66
5.17	Evolution of the prevalence of opinion A ($P_A(t)$) over time for an initial 50/50 opinion distribution. Results for one simulation of the majority threshold model with $T = 0$	68
5.18	Evolution of the prevalence of opinion A ($P_A(t)$) over time for making a fraction equal to 0.1 of the communities single opinion A communities, while the others get an initial 50/50 opinion distribution. Results are compared to the case where the total initial opinion distribution (55/45) is randomly distributed over each community.	70
5.19	Average prevalence of opinion A before and after the time evolution versus the fraction of single opinion A communities. Community distributed cases are compared to the corresponding randomly distributed cases for both a high modularity and a low modularity network. Results for the REC and PR filtering algorithms.	72
5.20	Distribution of the fraction of friends (nearest neighbors, nn) of node i with the same opinion B at $t = 500$. 10% of the communities is given a single opinion, opinion A, while the remaining communities get an initial 50/50 opinion distribution. The community distributed case is compared to the corresponding randomly distributed case (55/45) for both a high modularity and a low modularity network. Results for the REC and PR filtering algorithms.	74
5.21	Distribution of the fraction of friends (nearest neighbors, nn) of node i with the same opinion B at $t = 500$. 50% of the communities is given a single opinion, opinion A, while the remaining communities get an initial 50/50 opinion distribution. The community distributed case is compared to the corresponding randomly distributed case (75/25) for both a high modularity and a low modularity network. Results for the REC and PR filtering algorithms.	76
5.22	Formation of echo chambers versus fraction of completely stubborn actors for the PR and REC filtering algorithms and an initial 50/50 opinion distribution. The Last.fm on-line social network is compared to corresponding network models.	78
5.23	Distribution of the fraction of friends (nearest neighbors, nn) of node i with the same opinion B at $t = 500$. The SBM-WS with heterogeneous community sizes is compared to the SBM-WS with a single community size. Results are compared to the real-world Last.fm network with similar clustering and modularity. Results for the REC and PR filtering algorithms.	79
5.24	Formation of echo chambers versus fraction of completely stubborn actors for the PR and REC filtering algorithms and an initial 50/50 opinion distribution. The PGP trust network is compared to corresponding network models.	80

List of Tables

5.1 Network models used in Fig. 5.6.	48
--	----

Chapter 1

Introduction

The past decade social media has become ever more important in our daily lives. Nowadays most of us have, beside a real-world life, a virtual life on social media. This increased engagement on social media may have a huge impact on the formation of opinions, not only on the individual scale, but also on a broader, societal scale.

It is known that individuals not only form their opinions through self-reflection, but also through interactions with other people and with their surroundings [66]. The broad range of interactions people undergo on social media with people from all over the world can thus not be underestimated in the process of opinion formation. The understanding of the role of social media on the emergence of polarization and extremism in society is of uttermost importance.

It is also known that some people change their opinions more easily than others, that is, once in a while you encounter somebody that is really stubborn and persistent towards its own opinion. It is important to understand the effects of individual resistance on the formation and evolution of opinions. When designing models of opinion dynamics on social networks, this individual stubbornness should not be ignored.

One important feature of opinion dynamics on social media is the use of algorithmic personalization. Social media allow for simultaneous or asynchronous interactions between people without geographical constraints and thus allow for the spread of information at a faster pace and at an unprecedented scale [66]. People are, however, still bound by temporal and cognitive constraints. In order to assure a more pleasant/convenient experience on their platforms, social media companies use algorithms to order/filter the posts on an individual's time-line according to what might be relevant to that individual [66]. It is of great importance to know the possible effects of these filtering algorithms on the evolution of opinions in the population.

Opinion dynamics models have two important layers. On one hand, we introduce social networks to describe the underlying structure of social interactions; on the other hand, we need appropriate opinion dynamics/formation models to reproduce the opinion dynamics and opinion formation processes found in real life.

Section 1.1 gives an introduction to the first layer, namely that of complex networks. The second layer, the opinion dynamics layer, is introduced in Section 1.2. Section 1.3 introduces concepts such as statistical and social physics. Finally, in Section 1.4, the hypotheses and goals of this thesis are summarized and discussed.

1.1 Complex networks

Complex networks have become more and more popular for analyzing complex, dynamical systems. They are used in fields such as physics, economics, social sciences, biology, etc [23]. These different fields are very diverse, but they have at least one common ground: they often deal with a large number of variables/components that interact with each other. In other words, in all these fields one encounters complex systems, systems where it is not possible to predict collective behavior based on the properties of the individual components alone [25]. Complex systems often display phenomena such as non-linearity, emergence, spontaneous order,...

One of the tools to deal with these complex systems and to give us more insight in the possible underlying structures are complex networks. A network, also often called a graph (both terms will be used in this thesis), is a structure composed of nodes or vertices and a set of links or edges that indicate the interactions between the nodes (in this thesis terms like agent, actor, user, individual, people, etc will be interchangeably used to denote the nodes; edges will usually just be called edges) [25].

Representing/modeling a complex system as a graph makes the system appear more simple and tractable, while it still includes the non-linearity of these systems. One can find the language to describe networks in mathematical graph theory. However, complex systems in real-life situations often deal with a huge number of components, so the use of statistical and high-performance computing tools is inevitable [25]. One could argue that the study of complex networks lies somewhere at the intersection of mathematical graph theory and statistical physics [24].

The advantage of working with network models is that they reduce the level of complexity encountered in the real world, so that one can treat these systems in a more practical way. However, we still want our models to display properties similar to the ones seen in real systems [25]. Since many real systems are not static but evolve in time, this means that we do not only need to deal with static networks but also with temporal networks. Temporal networks are networks where the edges are not always active, but instead become active for some periods of time [45]. In temporal networks time becomes an explicit element in the network representation [45]. Static networks have been widely studied and are often convenient for their analytic tractability, whereas temporal networks are, in some cases, more realistic [25].

Some other important concepts in network theory are the degree distribution, clustering/community structure, connectivity, etc. These concepts will be explained in depth in Chapter 2, Section 2.1, but let us already anticipate a bit on the case of social networks. It is found that many real-life social systems have a power-law degree distribution [57]. This heterogeneous or scale-free degree distribution repre-

sents one of the three general properties of social networks. The other two are short distances and high clustering. These two are also referred to as “small world phenomenon” (note that in the literature the term “small world” sometimes only refers to the property of short distances, however, in this thesis, we will use it to indicate both a high clustering and short distances) [57]. Ideally, our theoretical network should exhibit these three properties. Some theoretical networks, that are thoroughly studied, do not possess all of them. However, they might still be used, because of their simplicity and ability to produce analytic results. When using these models one must always bear in mind their limitations to reproduce some properties encountered in real social systems.

Some examples of theoretical network models used in this thesis are the Erdős-Rényi network, the stochastic block model and the Watts-Strogatz model. These will be explained thoroughly in Chapter 2, Section 2.2.

1.2 Opinion dynamics

The formation of an individual’s opinion is the result of the interplay of many factors such as self-reflection, peer pressure, the individual’s personality (eg. stubbornness), the information someone is exposed to, etc. Opinion dynamics models should try to capture these complex processes in a simplified way. Several models have been developed ranging from simple binary models to more complex, continuous approaches [71].

The basic idea of all opinion dynamics models is that the nodes or agents in a social network have a variable that represents their opinion and that is updated according to some predefined rules. These models are a simplification of real-world opinion dynamics. It is however shown that they display a lot of aspects of real opinion formation such as agreement, transitions between order (consensus) and disorder (fragmentation), polarization, formation of echo chambers (clusters of people with the same opinion), etc [71].

The opinion of the agents in the model can be either discrete or continuous. This thesis deals with models where each agent can have one of the two opinions, A or B, and thus only deals with the case of discrete opinions. This might come across as a huge simplification of the real-world complexity of opinion formation, but also in real life people often have to choose between two competing opinions (eg. republicans or democrats, cat or dog, renting or buying a house,...).

The rules that determine how an agent updates his or her opinion can include many different aspects. They can, for example, be as simple as a majority rule (i.e. the majority model: if the majority of your neighbors have a certain opinion, you adopt that opinion as well) or can include a more probabilistic way of updating. A small overview of possible opinion dynamics models is given in Chapter 3, Section 3.1 and Section 3.2.

One can also include a resistance parameter that determines the hesitation of an agent to change to a new opinion and/or a parameter that determines the influence of an agent on others. Furthermore, the agents can have a parameter that determines whether they are active or not. The introduction of

stubborn actors will be discussed in Chapter 3, Section 3.5; the activation mechanism of nodes is discussed in Chapter 3, Section 3.4.

Since this thesis deals with the particular case of opinion dynamics on on-line social platforms, it is important to define/set up different filtering algorithms. The filtering algorithms that real social media companies use, are corporate secrets, but we know that there are three main principles of content curation: popularity, semantic and collaborative filtering [66]. Popularity filtering refers to the practice of promoting content that is popular across the platform; semantic filtering means that post similar to previous consumed posts are recommended and collaborative filtering suggests posts that are similar to the ones our friends consume [66]. In Chapter 3, Section 3.3 a detailed description of the filtering algorithms used in this thesis will be given.

1.3 Statistical and social physics

Another important tool in the study of opinion dynamics/formations in large groups of people is the use of statistical physics. This branch of physics offers a framework that relates microscopic properties of atoms, molecules,... to macroscopic observed behavior and has a wide field of applications inside and outside the world of physics. The observation that large number of people display collective, ‘macroscopic’ behavior begged for the use of the concepts and insights developed in statistical physics [71]. The application of the theory of statistical physics on social phenomena is referred to as social physics or sociophysics. The ‘microscopic’ constituents are now individual humans who interact with a limited number of other individuals and in that way form complex, ‘macroscopic’ groups such as human societies. These ‘macroscopic’ groups display stunning regularities, transitions from disorder to order, the emergence of consensus, universality, etc [15]. The statistical physics approach of these social systems tries to explain the found regularities at large scale as collective effects of the interactions among these individuals [71].

The statistical approach of social phenomena has one big difficulty compared to the description of gases and other physical phenomena. In regular physics, the microscopic constituents are ‘simple’ atoms or molecules, whose dynamics and interactions with each other are often well known and can be put in relatively simple laws with only a few parameters [16]. Humans, on the other hand, are far from simple entities and the dynamics of a single individual are far from known [16]. Even if the dynamics/behavior of individuals would be well known, the interactions between them would still be complicated and it would be impossible to describe them with simple laws and only a few parameters [16]. Hence, it may seem that extracting useful and qualitative information out of social models is a nearly impossible and almost hopeless task [16]. The use of statistical physics may, however, also offer a way out. In most situations the qualitative (and sometimes even quantitative) properties of large scale phenomena do not depend on the microscopic details of the process [16][41]. Instead, the relevant aspects for the global behavior are often higher level features such as symmetries, conservation laws, dimensionality, etc [16]. This introduces a concept of universality [41]. With this universality in mind, one can proceed to build models of human/social behavior where only the simplest and most important properties of single individuals and their interactions are taken into account [16]. An important factor herein is the comparison with real/empirical data to investigate whether or not the trends seen in real

life are compatible with the outputs generated by the models [16][69]. This interplay between theory, model, experiment and real-life data is not only an important factor in social physics, but also in regular physical research and science in general.

1.4 This thesis: hypotheses and goals

This thesis will try to investigate the interplay between the social network structure and the individual resistance to change in the evolution of two competing opinions. On one hand, we want to determine the influence of different network structures on the formation and evolution of opinions, whereas, on the other hand, we would like to investigate the effect of stubborn actors in the network. Since this thesis deals with opinion dynamics on social media, the effect of filtering algorithms must also be included.

In one of their previous papers (“*Modelling opinion dynamics in the age of algorithmic personalization*”, [66]) Perra and Rocha investigated both the effect of different filtering algorithms and different network topologies on the formation and evolution of two competing opinions. They also considered the effect of nudging (meaning that one opinion is pushed to all agents in the network). Their main findings were that the algorithmic filtering could not break the status quo when the prevalence of opinions was equally distributed in the population and that topological correlations (such as high clustering coefficient) could result in the formation of echo chambers [66]. On the other hand, a more heterogeneous contact pattern hampers this formation of echo chambers [66]. If the two opinions were, initially, not equally distributed, one of the filtering algorithms (namely semantic filtering) caused a further increase in the predominant opinion [66]. In the case of nudging, they found that the opinions in the population moved to the nudged opinion relatively fast, even in the case of small nudging [66]. They, however, did not investigate the effect of stubborn actors in the network, nor did they investigate networks with a community structure. This thesis will build on their model and incorporate these new features. We will compare networks that have a community structure and relatively low clustering to networks without community structure, but with a high clustering coefficient (a detailed description of concepts like clustering coefficient and community structure will be given in Chapter 2, Section 2.1). We want to investigate whether networks with community structure are able to form echo chambers, such as one can observe in networks with a high clustering coefficient. We will also pay some attention to networks that have both a high clustering coefficient and community structure. Can we observe echo chambers in those kinds of networks? If yes, can we determine which property might be the main driver for the formation of echo chambers: high clustering or community structure?

On the other hand, we want to determine the impact of stubborn actors on the formation and evolution of opinions in the network. Some interesting questions that may come to mind are: Is there an interplay between network structure and stubbornness? What about the possible interplay between the filtering algorithms and the introduction of stubborn actors?

Chapter 2

Networks

2.1 Definition and network measurements

Networks or graphs are conceptually simple and flexible objects that are made of a set of nodes/vertices V and a set of edges/links E , where the elements of E determine connections between elements of V [22]

$$E \subseteq \{\{x, y\} | x, y \in V\}. \quad (2.1)$$

If self-loops are not allowed, we need the following condition on the elements of E

$$E \subseteq \{\{x, y\} | x, y \in V \text{ and } x \neq y\}. \quad (2.2)$$

A graph with no self-loops is a simple graph. The nodes x and y of an edge $\{x, y\}$ are called the endpoints of the edge. It is possible that nodes are not joined by any edge, such nodes are called isolated or disconnected. If two or more edges have the same pair of endpoints, the graph is called a multi-graph. This thesis is not concerned with multi-graphs, nor are self-loops allowed. Graphs in which the edges have an orientation are called directed graphs [22]. If the edges have weights w_{ij} , one speaks of a weighted graph.

A graph can be represented in different ways. One of the most common ways is by use of the adjacency matrix.

2.1.1 Adjacency matrix

The adjacency matrix \mathbf{A} is a $N \times N$ matrix (for a graph with N nodes) where the elements indicate whether two nodes are connected by an edge or not [25]

$$A_{ij} = \begin{cases} 1 & \text{if nodes } i \text{ and } j \text{ are connected,} \\ 0 & \text{otherwise.} \end{cases} \quad (2.3)$$

For a simple, undirected graph, the adjacency matrix is symmetric ($A_{ij} = A_{ji}$) with zeros on the diagonal ($A_{ii} = 0$). Directed graphs can have asymmetric adjacency matrices. If we are dealing with

weighted graphs, the elements of the adjacency matrix are the weights w_{ij} of the edges

$$A_{ij} = \begin{cases} w_{ij} & \text{if nodes } i \text{ and } j \text{ are connected,} \\ 0 & \text{otherwise,} \end{cases} \quad (2.4)$$

with, generally, $0 \leq w_{ij} \leq 1$ [25].

2.1.2 Degree and degree distribution

The adjacency matrix contains a lot of information such as the degree of a node. The degree k_i of a node i is the number of edges attached to node i or, in other words, k_i represents the number of nearest neighbors of node i . The degree can be easily obtained from the adjacency matrix [25]

$$k_i = \sum_{j=1}^N A_{ij} . \quad (2.5)$$

In the case of a directed graph one can differentiate between the number of incoming edges k_i^{in} and the number of outgoing edges k_i^{out} of node i . These are called the in-degree and out-degree respectively and are defined as [25]

$$k_i^{\text{in}} = \sum_{j=1}^N A_{ji} , \quad k_i^{\text{out}} = \sum_{j=1}^N A_{ij} . \quad (2.6)$$

The total degree of node i is then $k_i = k_i^{\text{in}} + k_i^{\text{out}}$. For weighted graphs the degree is easily generalized to the weighted degree s_i , often called strength [47]

$$s_i = \sum_{j=1}^N w_{ij} . \quad (2.7)$$

From the degree of the nodes in the network one can construct the degree distribution. The degree distribution $P(k)$ represents the fraction of nodes with a degree k or, in other words, the degree distribution gives the probability that a randomly selected node has a degree k [59]. The average degree can be obtained from the degree distribution [25]

$$\langle k \rangle = \frac{1}{N} \sum_{i=1}^N k_i = \sum_k k P(k) , \quad (2.8)$$

where N is the total number of nodes in the network. The degree distribution allows us to classify networks. The two most important classes are homogeneous and heterogeneous networks. Homogeneous networks have a bell curved degree distribution, eg. a Poisson distribution. In this case, most of the nodes have a degree close to the average degree $\langle k \rangle$ [8]. Heterogeneous networks, on the other hand, have a power-law degree distribution, $P(k) \sim k^{-\gamma}$. They are also referred to as scale-free networks, since they do not possess a characteristic length scale or, in this case, the average degree is not a characteristic scale for the network [8][25].

2.1.3 Connectivity

In physics literature, the degree of a node is often called the connectivity [24][29]. This is different from the mathematical/graph definition of connectivity, where connectivity refers to the minimum number of nodes or edges that need to be removed to separate the remaining nodes in isolated subgraphs.

Two nodes u and v of a graph are connected if there exist a path between them. If the two nodes are connected by a path that contains only one edge, the two nodes are called adjacent.

The average degree $\langle k \rangle$ is a global measurement of the connectivity of the network [23]. If the average connectivity $\langle k \rangle$ is too small (this is, if there are too few edges), there will be many isolated nodes and only a few clusters with a small number of nodes. If more and more edges are added to the network, the small clusters will grow and will tend to connect to each other to form larger clusters. At some critical value of the connectivity, most nodes will be connected into a giant cluster (the giant component), which characterizes the percolation of the network [24].

2.1.4 Assortative and disassortative networks

Another concept that is closely related to the degree of a node is the notion of assortative and disassortative networks. More precisely, the notion of assortativity and disassortativity has to do with degree correlations.

The joint degree distribution $P(k, k')$ is the probability that an arbitrary edge connects a node with degree k to a node with degree k' [24]. The conditional probability $P(k|k')$, which is another way to express dependencies between node degrees, is the probability that an arbitrary neighbor of a node with degree k has a degree k' [24]

$$P(k|k') = \frac{\langle k \rangle P(k, k')}{k P(k)} . \quad (2.9)$$

The average degree of the nearest neighbors of nodes with degree k can be computed as [24]

$$k_{nn}(k) = \sum_{k'} k' P(k'|k) . \quad (2.10)$$

If there are no degree correlations, k_{nn} is independent of k . Such a network is called a neutral network [24]. If $k_{nn}(k)$ is an increasing function of k , nodes with a high degree tend to connect to nodes with a high degree and the network is classified as assortative. If instead $k_{nn}(k)$ is a decreasing function of k , nodes with a high degree tend to connect to nodes with a low degree and the network is called disassortative [24].

The terms assortativity and disassortativity are also often used without taking degree correlations into account. Instead, one may look at a particular node property to classify networks as either assortative or disassortative [73]. In this way, an assortative network is a network where nodes tend to connect to other nodes with similar properties as themselves, whereas in a disassortative network nodes tend to connect to nodes with different properties [73].

2.1.5 Network distances

Several measurements quantify the notion of length and distance in a network/graph. We start with the definition of a path: a path is a sequence of distinct nodes, such that adjacent nodes in the sequence are adjacent nodes in the network [39]. The length of a path is defined as the number of edges in the path [39]. A geodesic path, often called the shortest path, between two nodes is the path between two nodes i and j with minimum length (the geodesic path is not necessarily unique) [24]. The length of the geodesic path between the two nodes i and j is called the geodesic distance or shortest distance d_{ij} [24]. Geodesic distance is often just called distance [39]. The notion of distance enables to define several global network measurements such as average distance, diameter and radius.

Average distance

The average distance is the mean value of the geodesic distance d_{ij} [24]

$$\langle d \rangle = \frac{1}{N(N-1)} \sum_{i \neq j} d_{ij}. \quad (2.11)$$

This definition, however, diverges if there are unconnected nodes in the network (unconnected nodes have, by definition, a distance equal to infinity) [24]. This problem could be avoided by only including connected pairs in the sum, but this introduces a distortion for networks with a lot of unconnected pairs of nodes. These networks will then have a small average distance, which is only expected for networks with lots of connections [24]. Instead, another definition of average distance can be used: the global efficiency E [24]

$$E = \frac{1}{N(N-1)} \sum_{i \neq j} \frac{1}{d_{ij}}. \quad (2.12)$$

This measurement quantifies the efficiency of the network in sending information between nodes [24]. This assumes that the efficiency of sending information between two nodes is reciprocal to their distance. The harmonic mean of the geodesic distances is now defined as the reciprocal of the global efficiency [24]

$$h = \frac{1}{E}. \quad (2.13)$$

Diameter and radius

The diameter $diam(G)$ of a network G is the maximum distance between any pair of nodes [39]. The eccentricity of a node is the maximum distance from that node to any other node. The radius $rad(G)$ is the minimum eccentricity among all nodes of G . Note that the diameter is the maximum eccentricity among all nodes in G [39].

2.1.6 Clustering coefficient and transitivity

The clustering coefficient is another important measure of network topology. It is a measure for the number of triangles in a network and determines the connectivity in the neighborhood of a node i : if a node i has a high clustering coefficient, its neighbors are likely to be directly connected to each other [53].

A triangle is defined as a loop of length three, this is a sequence of nodes x, y, z, x such that $\{x, y\}$, $\{y, z\}$ and $\{z, x\}$ are edges of the network. The clustering coefficient is thus a way to measure the degree to which nodes in a network tend to cluster [53]. The local clustering coefficient of a node i is defined as [25]

$$cc_i = \frac{2n_i}{k_i(k_i - 1)}, \quad (2.14)$$

where n_i is the number of edges that actually exist between the nodes in the neighborhood of i and $k_i(k_i - 1)/2$ is the maximum number of edges that could exist between them (this expression is only valid for an undirected graph, since for a directed graph $e_{ij} \neq e_{ji}$ and we have $k_i(k_i - 1)$ possible edges between the neighbors of node i). The average clustering coefficient is then given as the average of the local clustering coefficients [59]

$$\langle cc \rangle = \frac{1}{N} \sum_{i=1}^N cc_i, \quad (2.15)$$

where N denotes the number of nodes in the network. The clustering coefficient is, beside a measure for the connectivity in the network, also linked to the robustness, or resilience against random damage, of the network [43][48][53].

A measure that is closely related to the clustering coefficient is the transitivity T , defined as (valid for undirected, unweighted networks) [24][59]

$$T = \frac{3 \times \text{number of triangles in the network}}{\text{number of connected triples of nodes in the network}}. \quad (2.16)$$

A connected triple is defined as a set of three nodes with at least two edges between them, so that each node can be reached from the other two (either directly or indirectly) [59]. The factor three arises from the fact that each triangle contributes to three different connected triples in the network: one centered at each node in the triangle [24].

Let us denote the number of triangles as N_Δ and the number of connected triples as N_3 . These two numbers can be obtained from the adjacency matrix [24]

$$N_\Delta = \sum_{k>j>i} A_{ij} A_{ik} A_{jk}, \quad (2.17)$$

$$N_3 = \sum_{k>j>i} (A_{ij} A_{ik} + A_{ji} A_{jk} + A_{ki} A_{kj}), \quad (2.18)$$

where A_{ij} are the elements of the adjacency matrix. It is possible to define the transitivity of one node as [24]

$$T_i = \frac{N_\Delta(i)}{N_3(i)}, \quad (2.19)$$

where $N_\Delta(i)$ represents the number of triangles that involve node i and $N_3(i)$ is the number of connected triples with i as the central node [24]

$$N_\Delta(i) = \sum_{k>j} A_{ij} A_{ik} A_{jk}, \quad (2.20)$$

$$N_3(i) = \sum_{k>j} A_{ij} A_{ik}. \quad (2.21)$$

It is not too hard to see that $N_\Delta(i)$ counts the number of edges between the neighbors of i and that $N_3(i)$ is equal to $k_i(k_i-1)/2$, where k_i is the degree of node i . It is then obvious that the local clustering coefficient cc_i (Eq. (2.14)) of a node and the transitivity T_i (Eq. (2.19)) of a node define the same quantity [24]. In the case of the average clustering coefficient $\langle cc \rangle$ and the global transitivity T this is, however, not the case. The difference between the two definitions is that the average of Eq. (2.16) gives the same weight to each triangle in the network, whereas Eq. (2.15) gives the same weight to each node [59]. This may lead to slightly different values since nodes with a higher degree may possibly be involved in a higher number of triangles than nodes with a lower degree [24].

2.1.7 Network communities

Network communities are another feature that (complex) networks may posses. A community inside a network is loosely defined as a set of nodes that are more densely connected to nodes inside that set than to the other nodes in the network [67]. More strictly, a community is defined based on two hypotheses: the connectedness hypothesis and the density hypothesis [9]. In short, the connectedness hypothesis means that each member of a community should be reached through each other member of the same community [9]. The density hypothesis implies that nodes inside a community are more likely to be linked to other nodes inside that community than to nodes outside the community [9]. The density hypothesis narrows what could be considered a community, but it does not uniquely define it. Several community definitions are consistent with the density hypothesis. Let us consider three possible definitions: maximum cliques, strong communities and weak communities [9].

Maximum cliques

A clique is a complete subgraph, where a complete subgraph is defined as a set of nodes of the network where each node in the set is directly connected to all the other nodes in the same set [9]. A community based on this definition would then be the largest clique in the network. This definition of community might, however, be too restrictive and, beside that, large cliques do not appear very frequent in networks [9].

Strong communities

A strong community is defined such that each node inside the community has more edges to other nodes inside the same community than to nodes outside the community [9][24]. Let us denote a community as C and let i be a node inside the community C . If we define the internal degree $k_i^{\text{int}}(C)$ as the number of edges that connect node i with other nodes in C and the external degree $k_i^{\text{ext}}(C)$ as the number of edges that connect node i with nodes outside C , then we have the following condition for C to be a strong community [9]

$$k_i^{\text{int}}(C) > k_i^{\text{ext}}(C), \quad \forall i \in C. \quad (2.22)$$

Weak communities

A weak community is a community where the sum of the internal degree of all the nodes in the community exceeds the sum of the external degree of all the nodes in the community [9][24]. We thus have the following condition for a weak community C [9]

$$\sum_{i \in C} k_i^{\text{int}}(C) > \sum_{i \in C} k_i^{\text{ext}}(C). \quad (2.23)$$

2.1.8 Modularity

The modularity Q is a measurement that represents the quality of a particular division of a network into different communities [24]. It was proposed after the fundamental problem arised for real networks concerning how to best divide the network into its constituent communities [24]. Generally, no a priori information is available about the number of existing communities in real networks [24].

The modularity of a network with N nodes and L edges and partitioned into n_c communities is calculated as follows. Each community has N_c nodes and L_c edges ($c = 1, \dots, n_c$) [9]. The modularity of a community Q_c is then calculated by measuring the difference between the network's real wiring diagram (which is given by the adjacency matrix A_{ij}) and the expected number of edges between i and j if the network is randomly wired (where i and j are two nodes that lie in the same community C_c) [9]. This last quantity is given by p_{ij} , which is obtained by randomizing the original network while keeping the expected degree of each node unchanged [9]. Hence, the modularity of a community Q_c

becomes [9]

$$Q_c = \frac{1}{2L} \sum_{(i,j) \in C_c} (A_{ij} - p_{ij}), \quad (2.24)$$

where the factor $\frac{1}{2L}$ is a normalization factor. Using [9]

$$p_{ij} = \frac{k_i k_j}{2L}, \quad (2.25)$$

we can derive a simpler form for Q_c [9]

$$Q_c = \frac{L_c}{L} - \left(\frac{k_c}{2L} \right)^2, \quad (2.26)$$

where L_c is the total number of edges in the community C_c and k_c is the total degree of the nodes in this community [9].

To generalize this idea to the whole network, we sum Eq. (2.26) over all n_c communities [9]

$$Q = \sum_{c=1}^{n_c} \left[\frac{L_c}{L} - \left(\frac{k_c}{2L} \right)^2 \right]. \quad (2.27)$$

The derivation of this formula, and thus of Eq. (2.26), can be found in Appendix A.1, Section A.1.1. The modularity Q can have values in the interval $[-1, 1]$ and has the following properties [9]: (i) The higher the value of Q for a certain partition, the better the corresponding community structure. This idea is used in community detection algorithms, where modularity is maximized in order to find the optimal community structure; (ii) A modularity Q equal to zero corresponds to the situation where all nodes are put in the same community, this is, if the whole network is put into a single community. Then the two terms in Eq. (2.27) become equal and Q vanishes; (iii) If every node is put into a separate community, the first term in Eq. (2.27) vanishes and we are left with n_c negative terms. Hence, this situation corresponds to a negative modularity.

Modularity is often used in community detection algorithms. It is thus important to be aware of the limitations of modularity. One of the biggest shortcomings of modularity maximization as community detection is its resolution limit. Modularity maximization forces small communities into larger ones [9]. If two communities A and B are merged, the modularity changes by [9]

$$\Delta Q_{AB} = \frac{l_{AB}}{L} - \frac{k_A k_B}{2L^2}, \quad (2.28)$$

where l_{AB} is the number of direct edges that connect nodes in community A with nodes in community B ; k_A and k_B are the total degree of nodes in communities A and B respectively. The derivation of this formula is found in Appendix A.1, Section A.1.2. If A and B are distinct communities, they should remain distinct when Q is maximized [9]. This is however not always the case. Consider the case where $\frac{k_A k_B}{2L} < 1$ and there is at least one edge between A and B ($l_{AB} \geq 1$), then $\Delta Q_{AB} \geq 0$ and the modularity increases by merging the two communities [9]. Assume for simplicity that $k_A = k_B = k$,

then modularity is increased by merging A and B if

$$k \leq \sqrt{2L}, \quad (2.29)$$

and if there is at least one edge between the two communities; even if A and B are distinct communities [9]! Eq. (2.29) is called the resolution limit: communities that are smaller than this limit will not be detected by modularity maximization [9].

2.2 Network models

In order to study the topological structures of real-world networks, several theoretical network models have been developed. These theoretical models usually have a simpler representation and well known properties that can be derived analytically. They are widely studied and used extensively. The study of complex networks relies heavily on the knowledge and understanding of these models. In this section we will review some of the most important ones.

2.2.1 The Erdős-Rényi model

In 1959 the two mathematicians Paul Erdős and Alfréd Rényi proposed a model to generate simple random networks [24]. Independently of them, Solomonoff and Rapoport already proposed the model in 1951. The model constructs random networks with N nodes in the following way [4]: (i) Start with N disconnected nodes; (ii) For each pair of nodes, connect them with a predefined probability p .

If $p = 1$, we obtain a network with the maximum number of edges $N(N - 1)/2$. This is called the fully connected network.

Degree distribution and average degree

The degree distribution of the random network with N nodes is given by

$$P(k) = \binom{N-1}{k} p^k (1-p)^{N-1-k}. \quad (2.30)$$

The derivation can be found in Appendix B.1, Section B.1.1. From this we can calculate the average degree of the network. The expected mean degree is given by [81]

$$\begin{aligned} \langle k \rangle &= \sum_{k=0}^{N-1} k P(k) \\ &= \sum_{k=0}^{N-1} k \binom{N-1}{k} p^k (1-p)^{N-1-k}. \end{aligned} \quad (2.31)$$

This equation can be simplified to $\langle k \rangle = (N - 1)p$, and for $N \gg 1$ this approximately becomes $\langle k \rangle \approx Np$. The derivation of this result can be found in Appendix B.1, Section B.1.2.

Most real networks are sparse, which means that $\langle k \rangle \ll N$. In this case the degree distribution of the random network is well approximated by a Poisson distribution [7]

$$P(k) = e^{-\langle k \rangle} \frac{\langle k \rangle^k}{k!}. \quad (2.32)$$

The derivation can be found in Appendix B.1, Section B.1.3.

Average clustering coefficient

The average clustering coefficient (Eq. (2.16)) of the Erdős-Rényi network is given by [18]

$$\langle cc \rangle = \frac{\binom{N}{3} p^3}{\binom{N}{3} p^2} = p = \frac{\langle k \rangle}{N - 1}. \quad (2.33)$$

This can be easily understood since choosing three nodes out of N is given by $\binom{N}{3}$. The chance that they are connected by three edges is given by p^3 , which gives the number of triangles; the chance that they are connected by two edges is p^2 , which determines the number of connected triples (recall that this model creates random networks with no self-loops and no edge duplicates). If the average degree $\langle k \rangle$ is constant, the average clustering constant goes as $\langle cc \rangle \sim \mathcal{O}(1/N)$, which becomes small for large networks [18].

Diameter and average distance

A heuristic derivation of the diameter of a random network goes as follows. Consider a random network with average degree $\langle k \rangle$, then a node in this network has on average [7]

- $\langle k \rangle$ nodes at distance one ($d = 1$),
- $\langle k \rangle^2$ nodes at distance two ($d = 2$),
- $\langle k \rangle^3$ nodes at distance three ($d = 3$),
- ...,
- $\langle k \rangle^d$ nodes at distance d .

The number of nodes at a distance d cannot exceed the number of nodes N in the network. We thus obtain the following equation from which the maximum distance or diameter d_{\max} can be obtained

$$N \approx \langle k \rangle^{d_{\max}}, \quad (2.34)$$

or

$$d_{\max} \approx \frac{\ln N}{\ln \langle k \rangle}. \quad (2.35)$$

A more precise calculation can be found in Appendix B.1, Section B.1.4. Eq. (2.35) might, however, be a better approximation to the average distance $\langle d \rangle$ between two randomly chosen nodes [7]. This is

because d_{\max} is often dominated by a few extreme paths, whereas $\langle d \rangle$ is averaged over all node pairs and thus suppresses these fluctuations [7]. Hence, the average distance of a random network is defined by [7]

$$\langle d \rangle \approx \frac{\ln N}{\ln \langle k \rangle}. \quad (2.36)$$

Since for large N , $\ln N \ll N$, we find that the average distance is a lot smaller than the size of the network. Generally, the logarithmic dependence of the average distance $\langle d \rangle$ on the network size N is one of the two defining properties of what is referred to as the “small world phenomenon”; the other property is a high clustering coefficient [30].

To summarize: the random Erdős-Rényi network has a bell shaped degree distribution which approximates a Poisson distribution for $N \gg 1$; the average clustering coefficient becomes small for large networks and the average distance depends logarithmic on the system sizes. The Erdős-Rényi network thus possesses one of the two properties of the “small world phenomenon”, a short average distance.

Real social networks, however, usually display the “small world phenomenon” and thus have both a short average distance and a high clustering coefficient. The question then rises: Can we construct a model that has both of these properties? The answer is yes and this is exactly what Duncan Watts and Steve Strogatz did.

2.2.2 The Watts-Strogatz model

In 1998, Duncan Watts and Steve Strogatz constructed a network model that generates random networks with small world properties, such as high clustering and short average distances. Their model achieves this by interpolating between a regular ring lattice and a random network [78]. The construction goes as follows [78]: (i) Start with a regular ring lattice with N nodes, each connected to $K = 2m$ neighbors (m on each side); (ii) For each node i , rewire each edge that connects i with its $K/2$ rightmost neighbors with a probability β . Rewiring is done in such a way that self-loops and edge duplication are avoided.

The probability β allows us to tune the graph between a regular lattice ($\beta = 0$) and a random network ($\beta = 1$) [78]. Usually, the following condition is required for the number of neighbors K : $N \gg K \gg \ln N \gg 1$. The first inequality assures sparse networks, whereas the second inequality guarantees that a random graph will be connected (thus the network is not so sparse that it becomes disconnected) [78].

The regular ring lattice ($\beta = 0$) has an average clustering coefficient $\langle cc(0) \rangle$ and an average path length $\langle d(0) \rangle$ equal to [78]

$$\langle cc(0) \rangle = \frac{3(K-2)}{4(K-1)} \approx \frac{3}{4} \text{ for } K \gg 1, \quad \langle d(0) \rangle \approx \frac{N}{2K}. \quad (2.37)$$

The derivations of these formulas can be found in Appendix B.2, Section B.2.1. The regular ring lattice thus has a high clustering coefficient and an average path length that grows linearly with the system size N .

The random network ($\beta = 1$), on the other hand, has a low clustering coefficient $\langle cc(1) \rangle$ and a small average path length $\langle d(1) \rangle$ (Eq. (2.33) and Eq. (2.36)) [78]

$$\langle cc(1) \rangle \approx \frac{K}{N} \ll 1, \quad \langle d(1) \rangle \approx \frac{\ln N}{\ln K}. \quad (2.38)$$

Watts and Strogatz then showed by numerical simulation that the average distance for the networks with $0 < \beta < 1$ is comparable with the average distance of a random graph (which is small), even for small β [58]. The clustering coefficient is approximately given by [10]

$$\langle cc \rangle \approx \langle cc(0) \rangle (1 - \beta)^3, \quad (2.39)$$

where $\langle cc(0) \rangle$ is given by Eq. (2.37). This can be seen in the following way: (i) The probability that none of the three edges of the original triangles in the regular lattice are rewired is $(1 - \beta)^3$; (ii) The probability that edges are rewired back to each other is negligible.

For rather small values of β , the clustering coefficient remains high. The model of Watts and Strogatz is thus able to generate random networks with a high clustering coefficient and short average distances. The Watts-Strogatz network has a homogeneous, bell shaped degree distribution with an average degree equal to $\langle k \rangle = K$ [10].

2.2.3 The stochastic block model

The stochastic block model (SBM) is a random graph model that is able to produce networks containing a community structure. The stochastic block model originates in social sciences and was developed to describe group structures in friendship networks [36]. The idea behind the development of this model is that often in real networks, there are groups of nodes that are more densely interconnected with each other than with the rest of the network [24]. Hence, these networks posses a modular/community structure and this is exactly the structure that is easily modeled by the stochastic block model. The stochastic block model is also often used as a benchmark for community detection algorithms [2].

The stochastic block model in its most simple form is defined by the following parameters [19]: (i) The number of nodes N ; (ii) A partition of the node set $\{1, 2, \dots, N\}$ into k disjoint subsets C_1, \dots, C_k ; these groups are the communities; and (iii) A symmetric $k \times k$ matrix M ; the diagonal elements M_{ii} , $i = 1, \dots, k$, represent the edge probabilities inside the community C_i and the off-diagonal elements M_{ij} , $i, j = 1, \dots, k$ with $i \neq j$, give the edge probabilities between nodes in community C_i and nodes in community C_j .

There are no real restrictions on the edge probabilities, which makes the stochastic block model a general model that is capable of reproducing many different network structures [50]. However, the edge probabilities inside a community are often taken to be bigger than the probabilities between communis-

ties ($M_{ii} > M_{ij}$, $i \neq j$). In this way, the stochastic block model generates a network with community structure. A stochastic block model that fulfills this condition is called an assortative SBM [52]. A disassortative stochastic block model refers to the case where the edge probabilities between the communities are higher than those inside the communities ($M_{ii} < M_{ij}$, $i \neq j$) [40].

The stochastic block model includes the Erdős-Rényi model [19]. This can be seen in the two different ways. First, consider the case where $k = 1$, thus we only have one community and all nodes belong to this community. The matrix M then reduces to one number p and we are left with the parameters N and p of the Erdős-Rényi model [19]. Second, assume we have more than one group or community, $k > 1$, and assume that every element of the matrix M is the same, $M_{ij} = p$, $\forall i, j$ [19]. Again, we are left with the parameters N and p of the Erdős-Rényi model. In both cases, the mathematical properties of the Erdős-Rényi model are obtained: a Poisson degree distribution, an average distance that is logarithmic with the system size N , vanishing clustering coefficient for large N , etc [19]. The structure within the groups or communities of the stochastic block model is that of a random graph, while the structure between the communities is that of a random bipartite graph [19].

The stochastic block model can be fitted to data [19]. Given a choice of the number of communities k and an observed network G , the stochastic block model can be used to infer the latent community structure and the edge probability matrix M [19]. One of the shortcomings of fitting the SBM to infer the community structure, is that real-world networks often have a heterogeneous or power-law degree distribution. Since the SBM is made of random networks inside each group and random bipartite networks between each pair of groups, the degree distribution of the full network is always a mixture of Poisson distributions [19]. The consequence of this is that if a network possesses a more skewed degree distribution, then fitting the SBM to the data will most likely give poor results [50]. The reason behind this is one of the main assumptions of the stochastic block model: the edge probabilities only depend on which group the node belongs to [19]. In other words, nodes that belong to the same group are stochastically equivalent, meaning that they have equivalent connectivity patterns to other nodes [19]. However, a network with a skewed degree distribution violates this assumption of edge independence [19]. To say it in the words of Karrer and Newman: “Just as the fitting of a straight line to intrinsically curved data is likely to miss important features of the data, so a fit of the simple stochastic block model to the structure of a complex network is likely to miss much [...].” (Karrer and Newman, p.1, [50]). Karrer and Newman proposed a variation of the SBM, the degree corrected SBM, that deals with this limitation. We will not discuss their variation, since that would lead us too far astray, but interested readers can find more detailed information in [50].

An extension that we are going to explore a bit deeper is the stochastic Watts-Strogatz block model (SBM-WS).

The stochastic Watts-Strogatz block model (SBM-WS)

The stochastic block model is a flexible model and there are many different extensions. One extension that is used in this thesis is a stochastic block model that uses the Watts-Strogatz model instead of the Erdős-Rényi model to construct the constituent communities. In this way, we obtain a version of

the stochastic block model that has both a community structure and a high clustering coefficient.

The construction of the model is very similar to that of the regular stochastic block model. For a SBM-WS with n_c communities of specified sizes, we first construct n_c Watts-Strogatz networks (for each constituent Watts-Strogatz network the rewire probability β and the mean degree $\langle k \rangle$ are specified), then edges are (with some predefined probability) randomly added between the different Watts-Strogatz communities. The result is a network that can be tuned to have both a community structure and a high clustering coefficient. This is different from the regular stochastic block model that can only account for a community structure and lacks a high clustering.

2.3 Real-world social networks

The models discussed in the sections above, describe real-world networks in an idealized, simplified way. They may posses some of the characteristics of real-world networks, but they certainly do not always describe real-world networks appropriately. The question then arises: What are the main properties/characteristics of real-world networks, and more specifically of real-world social networks? Another important question that can be asked is whether or not there is a significant difference between off-line social networks and on-line social networks?

As discussed briefly in the introduction, it is found that real-world networks often posses three characteristic properties. These are the two properties of the “small world phenomenon”, namely a short average distance and a high clustering coefficient, and a heterogeneous or power-law degree distribution [21]. These properties are valid for both off-line and on-line social networks [80]. Lets discuss them in a bit more detail.

Short average distance

In the late 1960’s Stanley Milgram performed a, what is now famous, experiment [59]. He asked randomly selected people in Boston and Omaha to forward a letter to a distant target person. The letter could, however, only be sent to acquaintances, thought to be closer to the target person [21]. The remarkable result of this experiment was that the average number of steps between the sender and the target person was only around six. This phenomenon is now often referred to as “six degrees of separation” [21].

This phenomenon is also observed in many other real-world networks: in most real-world networks it is possible to go from one node to another node through a number of edges that is small compared to the system size [21]. Such networks usually have an average distance that depends logarithmically on the system size instead of linearly [59]. A short average distance facilitates a fast transmission of information [59][80].

High clustering coefficient

In real-world social networks, one often observes the pattern that two friends of an individual are also friends of each other [21]. In graph terminology, this is translated into a high clustering coefficient (which quantifies a large number of triangles in the network) [21]. This property is not only found in social networks, but also in a wide variety of different real-world networks [21].

Heterogeneous or power-law degree distribution

Many real-world networks are found to have a power-law degree distribution [21]

$$P(k) \sim k^{-\gamma}, \quad (2.40)$$

where the exponent γ often lies between 2 and 3. Networks with a power-law degree distribution are also called heterogeneous or scale-free networks. The term scale-free refers to the fact that there is no characteristic scale in the network. Compared to the homogeneous network, where each node has a degree close to the average degree $\langle k \rangle$ (hence, this average degree serves as a characteristic scale of the system), the heterogeneous network has many nodes with a low degree and a few nodes with a very high degree (these nodes are referred to as hubs). If the exponent γ is smaller or equal to two ($\gamma \leq 2$), the average degree diverges [60]. Simple scale-free networks with an exponent smaller than two, however, cannot exist, since the largest hubs grow faster than the network size N [8]. If $2 < \gamma < 3$ (which is the case for most real-world networks), there is a finite average degree, but a diverging variance [60]. A diverging variance means that the fluctuations around the average can be arbitrary large, which makes this average degree no longer a characteristic scale for the system [8].

It should be noted that not all real-world networks have a heterogeneous degree distribution. And even if the degree distribution is heterogeneous or fat-tailed, it does not always need to follow a power-law. The degree distribution can eg. also be a power-law with an exponential cut-off, a log-normal distribution, a stretched exponential, etc [60].

These three main characteristics are valid for on- and off-line social networks. Another property that is found in most on- and off-line networks is the appearance of a giant component, this is, most nodes belong to the same connected component [51]. They also often posses a modular/community structure [33][54].

There are, however, some properties that are different between on-line and off-line social networks. One of them might be the degree correlations/mixing pattern. It is commonly assumed and accepted that most real-life social networks have an assortative mixing pattern (this distinguishes them from other real-world networks, eg. biological networks [24], which often have a disassortative pattern) [46][80]. For a long time, it was thought that this is also valid for on-line social networks. However, recent research has shown that a lot of on-line social networks display disassortative mixture [46][80]. This discrepancy between real-life social networks and on-line social networks may be explained as follows. In real life, ‘ordinary people’ often want to be friends with celebrities, however, the celebrities

usually prefer to stay within their own circles [46][80]. The ‘ordinary people’ do not have access to these circles and we are left with the situation where ‘ordinary people’ interact with ‘ordinary people’ and celebrities hang out among other celebrities; hence, an assortative structure. In on-line social networks, ‘ordinary people’ can easily connect with the celebrity and vice-versa, the celebrity wants to show his/her importance/influence by the number of fans [46][80]. This leads to a disassortative mixing pattern.

Chapter 3

Opinion dynamics

The study of opinion dynamics in a group of people, as mentioned in the introduction, has two major layers: a network layer and an opinion dynamics layer. The network layer, which describes the underlying structure and correlations between the agents/people, is intensively described in the previous chapter, Chapter 2. The current chapter focuses on the second layer, that of the opinion dynamics models. These models need to describe, in a simplified way, how opinions are formed and how they evolve in a group of people that interact in a certain way. Hence, these opinion dynamics are the dynamics that run on the underlying network structure.

Some major attention will be given to the content curation/filtering algorithms used by social media companies (Section 3.3). This is needed because this thesis deals with opinion dynamics on on-line social media, so the aspect of filtering cannot be ignored in the formation and evolution of opinions.

We will also discuss the activation mechanism (Section 3.4). This is the mechanism that describes the timings in which content/information is exchanged between users [66]. Such a mechanism changes the network from a static one to a temporal one, where nodes become active and inactive over time.

Several models have been proposed; here we will review some of the most important ones, with the main focus on the models used in this thesis. There are two major groups of opinion dynamics models, namely binary/discrete models and continuous approaches. These will be discussed in Section 3.1 and Section 3.2, respectively. This thesis only deals with binary opinion dynamics models, so these will be thoroughly described; the continuous models will be quickly reviewed in order to give a more complete overview.

Finally, in Section 3.5, the introduction of stubborn actors is discussed.

3.1 Binary models

Binary models are models where each agent can have one of the two opinions A or B. A binary model could reflect real-life cases where there exist two competing opinions, such as a vote in an election system with two competing candidates or choosing between Windows and Linux [61].

In this section, some binary models will be discussed; note, however, that the models described here are far from all the models that currently exist.

3.1.1 The majority model

One of the simplest opinion dynamics models is the binary majority model. Each agent has one of the two opinions A or B. Initially, these opinions can be equally distributed or not. If the distribution is not equal, but instead eg. 80/20, there is a predominant opinion and a minority opinion. The following updating rule is imposed on the network: each agent/individual adopts the majority opinion of his/her nearest neighbors [61]. Initially each agent is assigned an opinion; then the opinions are evolved in time: each individual iteratively updates his/her opinion according to the majority opinion of his/her direct neighbors [61].

Several studies have been performed on this kind of model, searching for answers on several questions such as: What are the conditions that drive the system to converge to unanimity; and, Does an opinion, that is initially a majority opinion, remain a majority opinion in the final state [61]?

Most of these studies conclude that, at the end of the opinion evolution, a complete consensus state is obtained where all the agents adopt the same opinion [61]. This is even the case when the opinions are equally and randomly distributed in an Erdős-Rényi network (with the side note that the degree needs to be high enough), as was shown by Benjamini et al. [12]. It is also found that the rate of convergence increases with increasing edge density and that if the network is sparse enough, consensus will not be reached and the two opinions coexist [61]. This can be explained by the fact that if the network is sparse enough, we may have disconnected parts; each of these disconnected groups may evolve to a different consensus opinion, so that over the entire network different opinions coexist [61].

3.1.2 The probabilistic majority model

The probabilistic majority model is similar to the majority model, but has, as the name suggests, a more probabilistic nature. In this model the fraction of neighbors of user i with opinion A, p_A , and the fraction of neighbors with opinion B, p_B , are determined. Then, the opinion of user i is updated: he/she takes on opinion A (or B) with a probability equal to p_A (or p_B) [66].

For example, if 70% of the neighbors of user i have an opinion A (and thus 30% of the neighbors have opinion B), user i will update his/her opinion to opinion A with a probability equal to 0.7 and to opinion B with a probability equal to 0.3 [66]. User i no longer simply updates his/her opinion according to the majority opinion carried by his/her neighbors, but the majority opinion still has a higher probability to be taken on by this user.

This model is no longer deterministic, but has a level of randomness, which is an important component of opinion dynamics [66].

3.1.3 The voter model

Another simple binary model is the voter model. The model works as follows: each agent in the network has a binary opinion (A or B); at each time step, an agent is randomly selected along with one of its neighbors and, subsequently, the agent adopts the opinion of this neighbor [16]. The agent thus mimics its neighbor [16].

The pressure of the majority is only felt in an averaged way, in the sense that a neighbor that carries the majority opinion has more chance to be randomly selected [16].

Lots of studies have been performed on this model. In this thesis, however, we will not make use of the voter model. Hence, we will not go into further detail. Interested readers are referred to [16], [32] and related references therein.

3.2 Continuous models

In continuous opinion dynamics models, the opinion variable of the agents in the network is no longer discrete, in contrast to binary or discrete models, but takes real values (often in the interval $[0, 1]$ or $[-1, 1]$).

Some concepts that are valid for the discrete models no longer apply (eg. the concept of a majority/minority opinion or the concept of equality of opinions); hence, they require a bit of a different framework [16].

The basis of most continuous models is a set of N nodes or agents, each having an opinion x_i represented by a real number that takes values in some interval [16]. In contrast to discrete/binary models, all agents usually start with different opinions [16]. The possible outcomes are more complex than in the discrete models and often have opinion clusters emerging in the final states (where opinion clusters refer to clusters of nodes with the same opinion) [16]. The number of opinion clusters can be one (consensus), two (polarization) or more (fragmentation) [16].

Several models have been proposed, we will only discuss a fraction of them.

3.2.1 The classical models

In the classical model, there are N nodes/agents, each with an opinion x_i and each node i gives a weight w_{ij} to all its neighbors (with $w_{ij} \geq 0$; this weight may for example represent the importance/influence of the neighbors) [44]. The most simple model has fixed weights w and the updating rule is [44]

$$x(t+1) = Wx(t) , \quad (3.1)$$

where W is the fixed stochastic matrix which contains the weights w_{ij} , $x(t)$ is the opinion profile at time t (this is a N -dimensional vector containing the opinions x_i of each node at time t) and $x(t+1)$ is the opinion profile at time $t+1$.

Friedkin and Johnsen proposed a variation of this model [34][35]. The model they proposed assumes that an agent i adheres to its initial opinion to a certain degree g_i and is influenced by others by a susceptibility of $1 - g_i$ [44]. This variation thus has the following updating rule (in matrix notation) [44]

$$x(t+1) = Gx(0) + (\mathbb{1} - G)Wx(t), \quad (3.2)$$

where G is the diagonal matrix which contains the g_i and $\mathbb{1}$ is the identity matrix. If all the g_i are equal to zero, we obtain the model of Eq. (3.1) [44].

A possible time variant extension is [44]

$$x(t+1) = W(t)x(t), \quad (3.3)$$

where now the weights are time dependent. This model can be used for situations in which so called “hardening of positions” occur [44]. This means that, over time, the agents put more and more weight on their own opinion and less weight on the opinion of others [44].

3.2.2 Bounded confidence models

In bounded confidence models, each node has, beside an opinion x_i , a threshold ϵ_i , also called an uncertainty or tolerance (ϵ can be the same for all nodes or can be different for each node) [16][26]. This threshold determines which opinions of neighbors are close enough to the agent’s opinion in order to influence that agent; opinions that are beyond this threshold are ignored [26]. In other words, an agent with opinion x_i is only affected/influenced by those neighbors which have an opinion in the interval $[x_i - \epsilon, x_i + \epsilon]$ [16].

The two most popular bounded confidence models are the Deffuant model and the Hegselmann-Krause model [16].

The Deffuant model

Assume we have a population of N agents, each with an opinion x_i that takes real values in the interval $[0, 1]$ [16]. Furthermore, the threshold ϵ is the same for all the agents. At each time step, an agent i is randomly selected together with one of its neighbors j (which is also randomly selected) [16]. If the opinions of the two nodes i and j are too far apart nothing happens; this is the case if $|x_i(t) - x_j(t)| \geq \epsilon$. If instead $|x_i(t) - x_j(t)| < \epsilon$, then the opinions are updated to [16][28]

$$\begin{aligned} x_i(t+1) &= x_i(t) + \mu[x_j(t) - x_i(t)], \\ x_j(t+1) &= x_j(t) + \mu[x_i(t) - x_j(t)]. \end{aligned} \quad (3.4)$$

The parameter μ is called the convergence parameter; its value lies in the interval $[0, 1/2]$ [16].

The model is based on a compromise strategy: after some discussion and a constructive debate, the opinions of the two agents move closer to each other [16]. The final state is a situation where several opinion clusters coexist. This is because the opinions move closer and closer to each other in several clusters; once each cluster is sufficiently far apart from the others (the difference in opinions between all agents in the two clusters is larger than ϵ), they no longer interact with each other [16]. Only agents inside the same cluster keep on interacting with each other, which makes the opinions inside a cluster converge to a single value [16]. Usually, the number and sizes of the clusters depends on the threshold ϵ , whereas μ determines the convergence rate [16].

The Hegselmann-Krause model

The Hegselmann-Krause model is similar to the Deffuant model. Again, there are N agents, each with an opinion x_i and a constant threshold ϵ [16]. Each agent interacts with those neighbors with an opinion in the interval $[x_i - \epsilon, x_i + \epsilon]$ [16]. The difference with the Deffuant model lies in the updating rule [16]. In the Deffuant model, only the opinion of one randomly selected neighbor is taken into account, whereas the Hegselmann-Krause model considers all compatible neighbors [16]. The updating rule becomes [16]

$$x_i(t+1) = \frac{\sum_{j:|x_i(t)-x_j(t)|<\epsilon} A_{ij} x_j(t)}{\sum_{j:|x_i(t)-x_j(t)|<\epsilon} A_{ij}}, \quad (3.5)$$

where A_{ij} are the elements of the adjacency matrix. This model thus takes the average opinion of the compatible neighbors into account [16].

The dynamics of this model is similar to the Deffuant model and the final state is also characterized by a number of stationary opinion clusters [16]. The number of clusters decreases if ϵ increases and above a critical value ϵ_c of the threshold, there can only be one cluster [16].

There are, of course, many other variations of the bounded confidence model. As mentioned earlier, the threshold ϵ can be different for each node, so that each node has an opinion x_i and a threshold ϵ_i or the confidence interval can be made asymmetric $[x_i - \epsilon_l, x_i + \epsilon_r]$ with $\epsilon_l \neq \epsilon_r$ [44]. Another extension is the relative agreement interaction model. Interested readers are referred to [26] and [27].

3.3 Algorithmic personalization

On-line social platforms use algorithms to order and filter the posts that appear on the time-line of an individual [66]. They do this in order to make the experience on their platforms more pleasant, interesting and convenient [66]. If social media companies would not use any kind of filtering, there would be too much content to handle and process for the social media user [14]. This in turn would make the on-line social experience unpleasant and inconvenient; the user might feel overwhelmed by the number of information he/she is exposed to [14]. The reason behind this is that people are cognitive and time constrained [66]; hence, there is only a limited amount of information that humans can process [14].

The downside of such algorithmic filtering is that it fine-tunes the information it shows based on the user. Even two users with the same friends may then be exposed to different content, based on their previous activities and history [14]. This may lead to the formation of echo chambers in which users get ‘trapped’ in content that confirms their own mindset [14].

It is important to know and be aware of the possible impacts of algorithmic personalization on the formation and evolution of opinions. Perra and Rocha partly investigated the role of such algorithms on the dynamics of opinions in several networks in [66]. Since filtering algorithms are often not transparently shared by social media companies, they proposed several personalization algorithms based on three simple ways of filtering [66]: (i) Popularity filtering: promoting content that is popular across the platform; (ii) Semantic filtering: promoting posts that are similar to previous consumed posts; (iii) Collaborative filtering: promoting content that people similar or close to us consume.

The following paragraph briefly reviews the filtering algorithms that Perra and Rocha proposed.

At every time t each platform user has a hidden list $L_i(t)$ that contains all the opinions/posts that he/she received from his/her friends [66]. The filtering algorithm then selects S items from this list and shows them on the user’s time-line (this is the fundamental idea behind algorithmic personalization: only showing a fraction of the possible posts [66]). The following selection methods are used [66]: (i) the reference filtering algorithm (REF): randomly select S items from the list $L_i(t)$; (ii) the old filtering algorithm (OLD): the S oldest post in $L_i(t)$ are displayed on the time-line of the user; (iii) the recent filtering algorithm (REC): shows the S most recent items from $L_i(t)$; and (iv) the preference filtering algorithm (PR): sorts the hidden list $L_i(t)$ according to the current opinion of the user and selects the first S elements. This filtering algorithm is based on semantic filtering.

Perra and Rocha showed that the REF, OLD and REC filtering algorithms behave similar in many cases and that the PR filtering algorithm often displays different behavior (such as a larger formation of echo chambers compared to the other three filtering algorithms) [66]. In this thesis the REC and REF filtering algorithms are used as a reference/benchmark algorithm and the PR filtering algorithm is used as the main filtering algorithm.

3.4 The activation mechanism: Static to temporal

Most of the simple opinion dynamics models make use of a static network in which users are always active and always exchanging opinions. In this kind of model the opinion dynamics might go as follows: each time step a random user is selected after which his/her opinion is updated according to the opinion dynamics model that is implemented. Another possibility is updating all users at the same time during each time step.

It might, however, be more realistic if nodes/users become active/inactive over time. This would be a better representation of real social media platforms, where users are active for some periods of time and then become inactive again. This kind of activation mechanism of the users gives the network a

temporal character. The underlying network structure does not change (each user/node has a fixed number of neighbors that does not change over time, so no new friends are made or, conversely, no old friends are being defriended), but by making users active and inactive the exchange of information between users becomes time dependent and depends on which users are active and which are not. Hence, this does affect the network structure in some way, because if a user, for example, does not become active for a long period of time, he/she does not participate in the exchange of information/opinions and the network structure behaves like if this user/node is absent. This may affect the dynamics, since it may seem as if the network has a different average degree and some properties like connectivity, clustering coefficient, etc may behave differently.

In this thesis we follow the same activation mechanism as was proposed in the paper of Perra and Rocha [66]. Every time step users are made active with some probability p_i (thus, every time step, each node becomes active with a probability p_i). In this thesis the activation probability is set equal to $p = 0.1$, which is constant for all the nodes. Perra and Rocha chose activation probabilities that are extracted from a power-law ($F(p) \sim p^{-1.5}$, with $p \in [0.01, 1]$) [66]. They did this based on the analyses of real social networks that shows that the propensity of users to start an on-line social interaction follows a heterogeneous distribution [65][66]. However, they also showed that using a constant activation probability p over the entire population yields results that are qualitatively similar (at least in their case) [66].

For simplicity, this thesis implements the constant activation probability variant. It might however be an interesting extension to switch to the heterogeneous activation probabilities and investigate the possible impacts on the dynamics.

If a user is active, he/she first spreads his current opinion to all his/her neighbors. Then, the active user updates his own opinion according to the opinions on his/her time-line [66]. This updating goes according to the implemented opinion dynamics model (eg. majority model, probabilistic majority model,...). In every time step the updating of all active nodes is done simultaneously [66].

3.5 The presence of stubborn actors

It is well known that in real life, you can find people that are persistent towards their own opinion and that are not open to opinions of others. They are convinced that they carry the truth with them and that other people, with different world-views, are not capable of giving them any new and useful insights. They are close-minded in contrast to people with an open-mind that are willing to learn from others and to reconsider their beliefs. Of course this is put a bit simplistic and there are many shades of gray between this black and white statement. However, there are groups in society, often with more extreme opinions, that are known to be inflexible towards changing that (extreme) opinion (being stubborn and being extreme does not need to go hand in hand, you can be stubborn without being extreme and vice versa; however, it is often widely accepted that there is some kind of correlation/link between people with extreme opinions and being more persistent towards these opinions compared to people with more moderate beliefs; this idea of correlating extreme people with a stubborn character is often used in models [26][27][75]) (having some resistance to change your opinion to any other opinion does not necessarily need to be a bad thing, it can be seen as a form of critical thinking and as a form of

taking things with a grain of salt).

Knowing the impact of stubborn groups on the opinions of others is of great importance, especially with the rise of social media which makes the reach of more extreme and persistent groups a lot bigger. Before the era of social media, one could maybe argue that these extreme and stubborn groups are often isolated and therefore would not reach too many people. So their impact could only be of a minor nature (this is only a statement that could have been given, there are of course plenty of examples throughout human history that may contradict this argument; to only mention a few: Nazism in the 1930s and 1940s, the Ku Klux Klan in the late 19th and begin 20th century, the rise of communism in the 20th century, etc, all examples of groups that can be considered extreme and that have had a (relatively) wide reach and a significant impact on society). Today, this possible argument is no longer valid; social media enables the contact with all sorts of beliefs and all sorts of people with almost no (time and spatial) constraints. Extreme and stubborn groups that may have been isolated before no longer need to be so and this may have huge, and largely unknown, impacts.

What is the impact of having stubborn/extreme people in your society? Does it matter if the stubborn people are grouped together or if they are distributed evenly throughout your system? Are there ways to reduce the possible impacts of stubbornness and/or extremism? Can these stubborn groups lead to polarization or even overtake the opinions in the system? Or is introducing some kind of stubbornness, on the other hand, a protective factor towards extremism/polarization? To answer these questions, several models have been proposed to include some kind of stubbornness/resistance in the system under study.

3.5.1 Stubbornness in bounded confidence models

The bounded confidence models, discussed in Section 3.2.2, can be easily extended to include some notion of stubbornness. Guillaume Deffuant proposed such an extension where stubbornness is correlated to extremism [26]. The model he proposed goes as follows. In bounded confidence models, the agents have an opinion x_i (which is a real number between $[-1, 1]$) and a threshold ϵ_i , which determines the range of opinions that can influence agent i (agents with opinions between $[x_i - \epsilon_i, x_i + \epsilon_i]$ are capable of influencing agent i). Guillaume Deffuant then introduced a fraction of extremists, f_e , which can have either the extreme opinion -1 or the extreme opinion 1 [26]. These extremists are given a threshold equal to ϵ_e [26]. The other agents are considered to be moderate and can have opinions between -1 and 1 . The moderates are given a threshold ϵ , with $\epsilon > \epsilon_e$ [26]. This last condition implicitly denotes the resistance of the extremes towards other opinions in contrast to the more flexible nature of the moderates, which is based on the idea that people with extreme opinions will be more convinced of that opinion and will be less likely to change it.

Since this thesis is not concerned with bounded confidence models, we will not discuss the results of this model here. Interested readers can find them in [26].

Another example of introducing some kind of persistence towards the own opinion of the nodes is the “hardening of positions” that was briefly discussed at the end of Section 3.2.1. The model intro-

duced by Friedkin and Johnsen (Section 3.2.1) in which each agent adheres to its initial opinion to a certain degree can also be seen as introducing a notion of stubbornness [63].

3.5.2 Stubbornness in binary models

Playing around with the threshold ϵ_i of the agents to include a notion of stubbornness, such as one can do for the bounded confidence models, is not possible for binary/discrete models. There are, however, many other ways to include some kind of stubborn actors in these models. In the following, two different possibilities will be discussed.

One small remark must be made here: previously, the link between stubbornness and extremism was often made and it was often assumed that the more extreme somebodies opinions are, the more persistent that somebody is towards those opinions. In binary models, however, there are only two possible opinions and in that sense it is less useful to talk about extreme and moderate opinions. However, we can still have people that rather keep their own opinion than be convinced by friends to switch to the other opinion.

Including a stubbornness parameter

One way of creating stubborn actors in the binary model is by giving each node i a stubbornness/resistance parameter r_i . This resistance parameter can have values between 0 and 1. If $r_i = 0$, the node is not stubborn and can be easily convinced of the value of the other opinion (according to which opinion dynamics model that is implemented: majority, probabilistic majority,...). If $r_i = 1$, the node is completely stubborn and there is no chance of convincing him/her of the other idea. If $0 < r_i < 1$, the node has some resistance but can still be convinced to switch to the other opinion, even though he/she will be less likely to do so. An uniform random number f between 0 and 1 is drawn. If $f > r_i$, the node will update his/her opinion; if $f \leq r_i$, the node is not convinced and keeps his/her own opinion.

The resistance parameter r_i can be different or the same for all nodes. One can also play around with the fraction of nodes that is stubborn, for example, there can be a fraction of nodes that is completely stubborn ($r = 1$) and a remaining fraction that is not stubborn at all ($r = 0$). Many other possibilities can be found according to how the stubborn actors are distributed and according to how stubborn they are made. This makes the model very flexible.

The threshold model

In the threshold model one introduces a notion of stubbornness by introducing a threshold parameter T . This parameter can be either the same for all the nodes (T) or can be made individual (T_i). The main idea is that nodes can only change their opinion to the other opinion if the fraction of friends with that opinion (p) is bigger than T ($p > T$). The idea behind this threshold model is that people are a bit hesitant to change their opinion, but if they have enough friends with the other opinion, they might get convinced of that opinion as well. The more persistent you are, the more friends you need in order to be convinced of the other idea.

There are different possibilities of implementing this model. One way, which makes use of the majority model, is as follows. First the fraction of friends with opinion A and opinion B, p_A and p_B respectively, are determined; then the following rules are used to update the opinion: if $p_A > p_B$ and $p_A > T$, opinion A is adopted; if $p_B > p_A$ and $p_B > T$, opinion B is adopted; in all other cases, the current opinion of the node is not changed.

If $T = 0$, this model reduces to the pure majority model described in Section 3.1.1. If $T = 1$, the nodes do not change their opinion. For $0 < T < 1$, the model is a majority model, but the nodes are more persistent towards their own opinion and need a larger fraction of friends to convince them to switch to the other viewpoint.

The above examples are only a handful of the possible ways to include some notion of stubbornness in the model, many more exist or can be invented.

Chapter 4

Materials and methods in this thesis

The previous two chapters, Chapter 2 and 3, gave a broad introduction/overview of networks and opinion dynamics models respectively. In this chapter we will summarize the specific networks and opinion dynamics models that are used in this thesis.

Section 4.1 gives an overview of the network models that are used. In chapter 2, Section 2.2 we discussed their main properties; here we will discuss why we use these networks. Which of their properties are of interest in this thesis? What are their benefits and possible shortcomings regarding to our goals?

In section 4.2, we will discuss the used real-world networks. The reasons of choosing these specific networks will be explained, together with their possible strengths and weaknesses.

Finally, Section 4.3 summarizes and discusses the opinion dynamics model that is implemented. We will focus on possible advantages and disadvantages of the model.

4.1 Network models

This thesis uses three network models: (i) the Erdős-Rényi model (ER); (ii) the Watts-Strogatz model (WS); and (iii) the stochastic block model, of which two types are implemented: the regular stochastic block model (SBM) and the stochastic Watts-Strogatz block model (SBM-WS).

Each of these networks serve specific goals which will be shortly discussed in the following paragraphs.

The Erdős-Rényi model

The Erdős-Rényi model is used as a benchmark model. In this thesis we focus intensively on two network topologies that may impact the formation of echo chambers: a high clustering coefficient and community structure. It is therefore necessary to have a model that lacks both of these features to compare the results with. The Erdős-Rényi model is one of the most simple random network models that does not display both of these features and is hence the perfect comparison model.

It is expected that the random nature of the model and the lack of high clustering and community structure will result in the absence of echo chambers.

The Erdős-Rényi model is also used in the regular stochastic block model to construct the constituent communities.

The Watts-Strogatz model

The Watts-Strogatz model is used as a general model to investigate the effect of high clustering on the evolution of opinions and the formation of echo chambers.

Perra and Rocha showed that a high clustering coefficient enhances the formation of echo chambers [66]. Here, we will use the Watts-Strogatz model to investigate the interplay between high clustering and the presence of stubborn actors and we will use it as a comparison for networks that posses a community structure without having a high clustering coefficient. We will investigate whether community structure behaves similar to high clustering regarding the appearance of echo chambers.

Beside the above, the Watts-Strogatz model is also used to build the constituent communities in the stochastic Watts-Strogatz block model.

The stochastic block model

One of the main features of the stochastic block model is the ability to generate networks with community structure. We will therefore use this model to investigate the impact of community structure/-modularity on the evolution of opinions and the formation of echo chambers.

It is expected that community structure will enhance the formation of echo chambers compared to the random network case. The question remains, however, whether the influence of community structure on the formation of echo chambers is of the same caliber as that of high clustering. It is also of interest to study the possible relation between the appearance of echo chambers and the modularity of the network.

The stochastic Watts-Strogatz block model is used as a model that has both high clustering and community structure. We will check if the combination of both features displays any difference in the formation of echo chambers compared to having only a single feature (either community structure or high clustering).

All the above models have a homogeneous degree distribution. We did not focus on network models which generate networks with a heterogeneous degree distribution such as the Barabási-Albert model. It might, however, be an interesting extension to investigate such types of models as well.

The above models obviously have their added value and benefits. One of their most important plus points is their simplicity. They are the most simple network models that one can create and each of

them have characteristics and topologies that can be easily tuned (clustering for WS, community structure for SBM). This makes it really easy to investigate the effect of these different network topologies without the need to take the interplay with other possible complex network features and topologies into account. This plus side is, however, also one of the possible downsides. Real networks are not simple networks with single, isolated characteristics, but are instead complex networks where many different characteristics and topologies may each play a role. In other words, network models may lack many features of real-world networks. It is thus always a bit tricky, and sometimes even incorrect, to extrapolate the results that are obtained by using network models to real-world situations.

The fact that all the above models have a homogeneous degree distribution may also be a drawback, since most real-world networks have a heterogeneous degree distribution.

4.2 Real-world networks

Ideally, we would test the opinion dynamics model that was used throughout this thesis on network data directly obtained from social network companies. However, most of these companies are not too keen on sharing any form of data. This makes it hard to find accurate and complete social media network data. Hence, we chose to test the model on other types of social networks, either on-line or off-line. Some possibilities are any form of friendship networks, e-mail networks, collaboration networks, etc.

One of the decisive properties of the real-world networks that were eventually used, was their size. The main, and actually only, reason for this was the computation time. If the networks are too big, it would take weeks, sometimes even months before there would be results.

The size of the network models that were used, was around a thousand nodes. For the real-world networks, we also used networks with a size of magnitude of thousand to ten-thousand. This benefits the computation time; it is, however, unknown how the network size affects the results. It is therefore recommended to test the model on larger network models and on larger real-world networks in future researches on this topic.

We used two real-world networks. The data was obtained from *The index of Complex networks* (ICON) [20]. The first real-world network is an on-line friendship network among Finnish users of the social music listening and sharing website Last.fm (data from 2006). Only the largest connected component of this on-line social network is included [20]. This data set was originally used in [74], which describes the data set. This on-line social network has the following properties: $N = 8003$; number of edges: 16824; $Q = 0.79$; $\langle cc \rangle = 0.31$; $\langle k \rangle = 4.2$. The degree distribution is heterogeneous and is best fitted by a log-normal

$$f(k) = \frac{1}{k\sigma\sqrt{2\pi}} \exp\left(-\frac{(\ln(k) - \mu)^2}{2\sigma^2}\right), \quad (4.1)$$

with $\mu = 1.0078272$ and $\sigma = 0.95173779$. The degree distribution of the Last.fm social network, together with the log-normal fit, is shown in Fig. 4.1a.

The second real-world network that was used is the giant component of the on-line, social network of users of the Pretty-Good-Privacy (PGP) algorithm for secure information interchange (data from 2004) [20]. This network was originally used in [13], which gives a detailed description of the network data. The main properties of this network are: $N = 10680$; number of edges: 24340; $Q = 0.85$; $\langle cc \rangle = 0.27$; $\langle k \rangle = 4.56$. The network has a heterogeneous degree distribution, which is best fitted by two power-laws

$$f(k) = ak^{-\gamma}, \quad (4.2)$$

with $a = 0.39604951$, $\gamma = 1.53568449$ for $k < 20$ and $a = 5.59021251$, $\gamma = 2.4944057$ for $k \geq 20$. The degree distribution for the PGP trust network, together with the power-law fits, is shown in Fig. 4.1b.

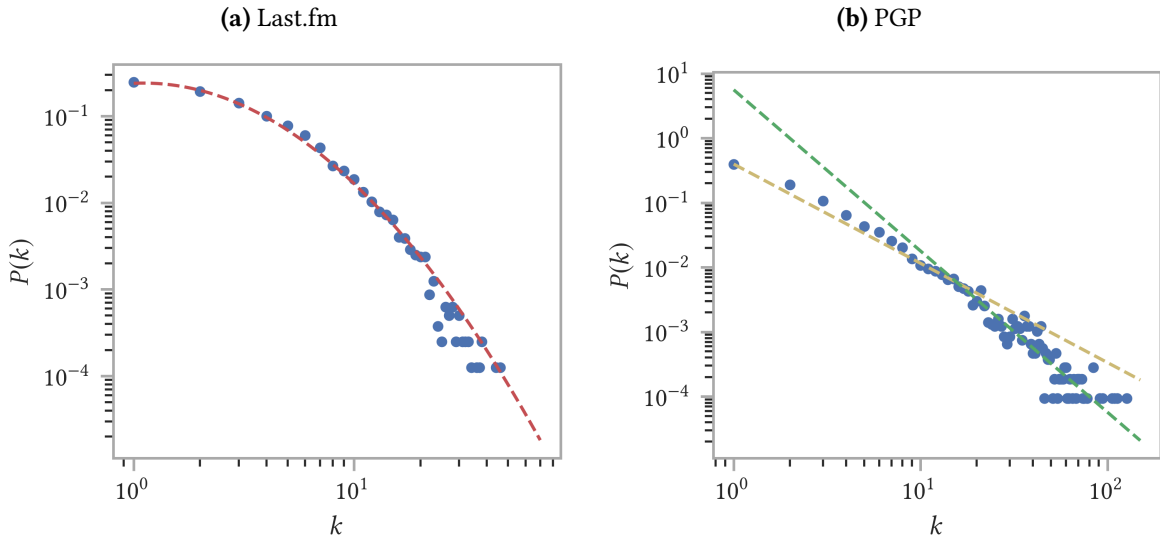


Figure 4.1: Degree distribution $P(k)$ of the two real-world networks used in this thesis. (a) Last.fm on-line social network with a log-normal fit ($\mu = 1.0078272$, $\sigma = 0.95173779$); (b) PGP on-line trust network with two power-law fits ($a = 0.39604951$, $\gamma = 1.53568449$ for $k < 20$ and $a = 5.59021251$, $\gamma = 2.4944057$ for $k \geq 20$).

4.3 Opinion dynamics model

In Chapter 3 we discussed opinion dynamics models and related topics such as algorithmic personalization, activation mechanisms and stubbornness. The goal of this section is to put everything together and summarize the opinion dynamics model of this thesis.

This thesis follows the opinion dynamics model that was designed by Perra and Rocha in [66]. We start with a network with $N = 10^3$ users. Initially, each user is given one of the two opinions A or B. Each time step a random fraction equal to $p = 0.1$ of these users becomes active, where p is the activation probability. As discussed in Chapter 3, Section 3.4, this thesis makes use of a constant activation probability. Every time step, all active users update their opinion synchronously. This updating

is done as follows. First, the active user sends his current opinion to all his neighbors (active or not). Then, he updates his own opinion according to the opinions on his time-line. This updating follows the probabilistic majority model, as explained in Chapter 3, Section 3.1.2. If another model is used, eg. the majority model, this will be explicitly stated. If not, one can assume that the probabilistic majority model is implemented. It is important to realize that what an active user sees on his/her time-line is only a selection of all the posts that his/her friends have posted. Each user has a hidden time-line $L_i(t)$. This hidden time-line contains the time-line of the user at the last time he/she was active (t_{last}) plus all the post that his/her friends posted from t_{last} until the user becomes active again at time t . If a user becomes active, the filtering algorithm (REF, REC or PR), discussed in Chapter 3, Section 3.3, selects S items from this hidden time-line and shows them on the actual time-line of the user. We will usually set $S = 20$, which quantifies the maximum length of the actual time-line.

Algorithm 1 Updating the opinions of the active nodes at time t

```

1:  $L \leftarrow$  hidden time-line
2:  $T \leftarrow$  actual time-line
3:  $S \leftarrow 20$                                       $\triangleright$  Maximum length of time-line  $T$ 
4:  $r$                                                $\triangleright$  Stubbornness parameter of each node, takes values between 0 and 1
5: for all active user do
6:   op  $\leftarrow$  current opinion
7:   for all neighbor do       $\triangleright$  Add opinion of active user to hidden time-line of each neighbor
8:     L.ADD(op)
9:   f  $\leftarrow$  rand(0, 1)           $\triangleright$  Draw random number between 0 and 1
10:  if  $f > r$  then
11:    op  $\leftarrow$  UPDATE OPINION( $L$ )           $\triangleright$  Update opinion of active user
12:  else
13:    op  $\leftarrow$  current opinion            $\triangleright$  Do not update opinion of active user
14: function UPDATE OPINION( $L$ )
15:   ORDER( $L$ )                       $\triangleright$  Order hidden time-line according to REF, REC or PR filtering
16:   if len( $L$ )  $> S$  then
17:     T  $\leftarrow$  L.RESIZE( $S$ )           $\triangleright$  Time-line  $T = S$  first elements of ordered hidden time-line
18:   op  $\leftarrow$  PROBMAJ( $T$ )           $\triangleright$  Update opinion according to probabilistic majority model
19:   return op                       $\triangleright$  Return updated opinion

```

If we want to introduce some kind of stubbornness in the model we will mainly use the stubbornness parameter, as was explained in Chapter 3, Section 3.5.2. Lets briefly summarize this concept of stubbornness. Each node is given a stubbornness parameter r_i , with $0 \leq r_i \leq 1$; $r_i = 0$ means not stubborn and $r_i = 1$ means completely stubborn. For all intermediate values of r_i , a random number f between zero and one is drawn; if $f > r_i$, the node can update his opinion, if $f \leq r_i$, the node will keep his current opinion.

Some results for the majority threshold model, also explained in Chapter 3, Section 3.5.2, will be shared as well. This is, however, not the main stubbornness model that we will focus on. If this model is used, this will be explicitly stated. Otherwise one can assume that we are making use of the stubbornness parameter.

In Algorithm 1, the pseudo-code for updating the opinions of the active nodes in case of using a stubbornness parameter r at time step t is displayed.

This model is a simple one, since it only allows for two different opinions in the system. The designed filtering algorithms are simple and intuitive as well. Some randomness is introduced by using the probabilistic majority model instead of the classic majority model. This might make the model more realistic. This simpleness combined with the touch of randomness to give the model a more realistic vibe are definitely some strong points of using this model compared to other, more complex models. A simple model is more tractable and allows for a better understanding of what is going on in the dynamics [49]. However, this might be a downside as well. Real-world opinion dynamics are, probably, far from simple. People do not update their opinion according to a simple probabilistic opinion dynamics model. Beside that, the cases where people have to choose between only two opinions are rather limited. Filtering algorithms, used by real social media companies, are unfortunately not publicly shared. We can however assume that they are not as simple as the ones we used in this thesis. Trying to model these far more complex systems by our simple model, might lead to the fact that a lot of the dynamics might be missed or not well captured by our model. This downside of trying to model real-world social behavior with simple, tractable models is really a call for the urgent need for more real-world data to which the results obtained from simple models can be compared and which can help make the models capable of generating more realistic results [16][69].

This does not mean that simple models should be thrown away. They might still be capable of capturing a lot of the dynamics that are seen in the real world [41]. Not because a system appears complex, that it cannot be modeled by something more simple [49]. This has been proven by physics research over and over again [41]. Beside that, if you do not know the dynamics/underlying processes of complex phenomena yet, the best thing you can do is try to model it with the most simple model that comes to mind. There is no need to make things too complex if simple works too. There is however a need to compare data from (computational) models to empirical, real-world data. A need for critical thinking and careful analyzing of results can also not be denied [69].

Chapter 5

Results

This chapter is subdivided into four main sections. We first discuss the impact of the network structure on the evolution of the prevalence of the opinions and the formation of echo chambers. Then, we introduce some kind of stubbornness in the system. The impact of how the opinions are initially distributed in a network with community structure (SBM) will be discussed afterwards. Finally, we will run the opinion dynamics model of this thesis on some real-world networks. We will discuss the results and compare them to results obtained from network models with a similar average degree, clustering coefficient and/or modularity.

5.1 Network structure

In this section we will discuss the results related to the network topologies of the different network models that are used in this thesis. We will focus on the effect of a high clustering coefficient and community structure. Two different opinion distributions are investigated, balanced starting conditions and unbalanced starting conditions. For both starting conditions we investigate the evolution of the prevalence of the opinions with time and the formation of echo chambers. Two filtering algorithms will be compared to each other, the REC and the PR filtering algorithms, in order to investigate the possible interplay between those filtering algorithms and the network structures.

5.1.1 Balanced starting conditions

In this configuration 50% of the nodes start with opinion A ($P_A(0) = 0.5$) and 50% of the nodes start with opinion B ($P_B(0) = 0.5$). The opinions are randomly distributed over the network. The opinion dynamics model discussed in Chapter 4, Section 4.3 is used. We set the activation probability equal to $p_{act} = 0.1$ and the actual time-line of each user has a maximum length equal to $S = 20$.

Four different network models are implemented, each with a total number of nodes $N = 10^3$ and average degree $\langle k \rangle \sim 10$. The baseline model is the Erdős-Rényi model (ER) with an edge probability $p = 0.01$. To investigate the effect of clustering on the dynamics, we use the Watts-Strogatz model (WS). Two different values of the rewire probability β are used, each with a slightly different value of the clustering coefficient: $\beta = 0.01$ with $\langle cc \rangle = 0.648 \pm 0.003$ and $\beta = 0.06$ with

$\langle cc \rangle = 0.557 \pm 0.007$. The impact of community structure on the dynamics is studied with the stochastic block model (SBM) with 10 communities of size 100. Two different modularities are investigated: a high modularity, $Q = 0.908 \pm 0.005$, with an edge probability inside the communities $p_{\text{cl}} = 0.1$ and an edge probability between communities $p_{\text{add}} = 0.001$; and a low modularity, $Q = 0.220 \pm 0.007$, with $p_{\text{cl}} = 0.03$ and $p_{\text{add}} = 0.008$. Finally, the impact of both clustering and community structure is investigated with the stochastic Watts-Strogatz block model (SBM-WS) with 10 communities of size 100. Each community has the following Watts-Strogatz parameters: mean degree $\langle k \rangle = 10$ and rewire probability $\beta = 0.01$. Edges are added between communities with a probability $p_{\text{add}} = 0.001$. This is a network with both high clustering ($\langle cc \rangle = 0.553 \pm 0.004$) and high modularity ($Q = 0.909 \pm 0.004$).

Evolution of the prevalence of the opinions

We start with the results for the evolution of the prevalence of the opinions in case of an initial 50/50 opinion distribution. Perra and Rocha showed that, for the case of balanced starting conditions, the prevalence of the opinions do not change over time for neither the random network, nor the Watts-Strogatz network and for none of the filtering algorithms [66].

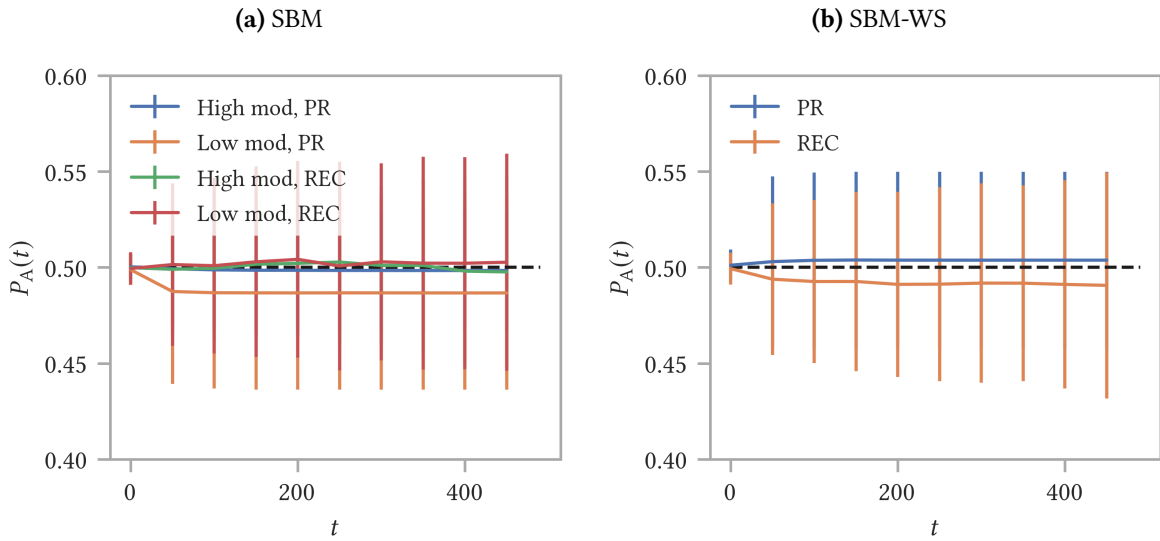


Figure 5.1: Evolution of the prevalence of opinion A ($P_A(t)$) over time for an initial 50/50 distribution. Two different network models with community structure are represented, each with average degree $\langle k \rangle \sim 10$ and $N = 10^3$: **(a)** SBM with 10 communities of size 100, a high modularity case ($p_{\text{cl}} = 0.1$, $p_{\text{add}} = 0.001$, $Q = 0.908 \pm 0.005$) and a low modularity case ($p_{\text{cl}} = 0.03$, $p_{\text{add}} = 0.008$, $Q = 0.220 \pm 0.007$) are depicted; **(b)** SBM-WS with 10 communities of size 100, each community has the following WS parameters: $\langle k \rangle = 10$, $\beta = 0.01$ and $p_{\text{add}} = 0.001$, $\langle cc \rangle = 0.553 \pm 0.004$ and $Q = 0.909 \pm 0.004$. For each model the REC and the PR filtering algorithms are compared. Each curve is the average of 10^2 independent simulations and data points are shown for every 50 time steps to improve visualization. Bars represent the standard deviation σ .

The results for the network model with community structure (SBM, Fig. 5.1a) and the network model with both community structure and high clustering (SBM-WS, Fig. 5.1b) are shown for both the REC

and the PR filtering algorithms. A community structure is also not able to break the status quo for both of the filtering algorithms. The initial prevalence of the opinions is maintained over time.

Echo chambers

Fig. 5.2 shows the distribution of the fraction of friends (nearest neighbors, nn) of node i with the same opinion B at $t = 500$, $\langle P_B^{\text{nn}} \rangle$. The value shown on the y -axis, $F_N(\langle P_B^{\text{nn}} \rangle)$, is the result of dividing the average distribution of opinions in each neighborhood at $t = 500$ by its corresponding value at $t = 0$. The region on the x -axis close to zero describes neighborhoods in which none, or very few users, adopt opinion B (these are thus neighborhoods in which most users adopt opinion A). Conversely, the region on the x -axis close to one describes neighborhoods in which a majority of the users adopt opinion B. The distribution is obtained by imposing ten equispaced bins, $\Delta x = 0.1$ [66].

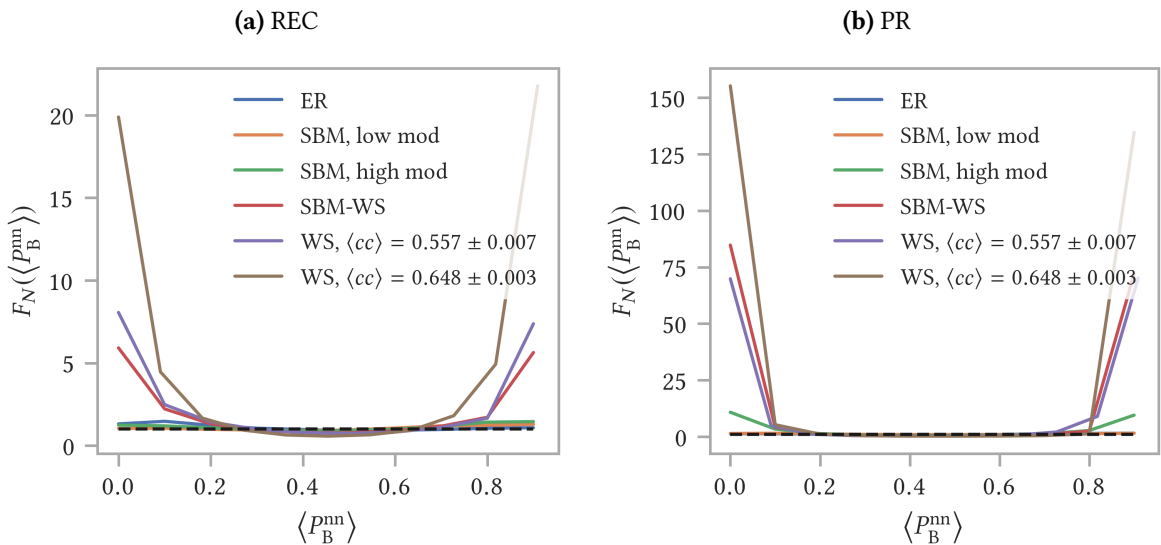


Figure 5.2: Distribution of the fraction of friends (nearest neighbors, nn) of node i with the same opinion B at $t = 500$. The distribution is normalized by dividing for the same quantity computed at $t = 0$. **(a)** REC filtering algorithm; **(b)** PR filtering algorithm. Four different network models are used, each with $N = 10^3$ and average degree $\langle k \rangle \sim 10$: ER with $p = 0.01$; SBM with 10 communities of size 100, a high modularity case ($p_{\text{cl}} = 0.1$, $p_{\text{add}} = 0.001$, $Q = 0.908 \pm 0.005$) and a low modularity case ($p_{\text{cl}} = 0.03$, $p_{\text{add}} = 0.008$, $Q = 0.220 \pm 0.007$) are depicted; SBM-WS with 10 communities of size 100, each community has the following WS parameters: $\langle k \rangle = 10$, $\beta = 0.01$ and $p_{\text{add}} = 0.001$, $\langle cc \rangle = 0.553 \pm 0.004$ and $Q = 0.909 \pm 0.004$; WS with $\langle k \rangle = 10$, two slightly different values of the clustering coefficient are used ($\langle cc \rangle = 0.557 \pm 0.007$ and $\langle cc \rangle = 0.648 \pm 0.003$). The starting conditions are $P_A(0) = 0.5$ and $P_B(0) = 0.5$. Each curve is the average of 10^2 independent simulations. Error bars are omitted for an improved visualization.

In Fig. 5.2 two different filtering algorithms are compared, the REC and the PR filtering algorithms. The results for both filtering algorithms are qualitatively the same. The main difference is that the formation of echo chambers, using the PR filtering algorithm, is about ten times as big compared to the formation of echo chambers using the REC filtering algorithm.

The Erdős-Rényi model (ER) shows no, or a very limited, sign of echo chambers, for both the REC filtering algorithm and the PR filtering algorithm. Networks with high clustering (WS and SBM-WS), on the other hand, show a clear sign of polarization and formation of echo chambers (visible in the two spikes, one around zero and one around one). Going to slightly higher values of the clustering coefficient ($\langle cc \rangle = 0.557 \pm 0.007$ to $\langle cc \rangle = 0.648 \pm 0.003$) in the Watts-Strogatz model results in significantly larger echo chambers. This suggests that the formation of echo chambers is really sensitive to changes in the clustering coefficient. The stochastic block model (SBM) with a high modularity, a clear community structure, does show an appearance of polarization (mainly when using the PR filtering algorithm), however, the formation of echo chambers is significantly smaller compared to networks with high clustering. The stochastic block model with a low modularity has no, or very limited, echo chambers, similar as for the Erdős-Rényi model. This is to be expected, since a stochastic block model with a low modularity, and hence a blurred, almost non-existing community structure, strongly resembles an Erdős-Rényi network. The stochastic Watts-Strogatz block model (SBM-WS) has both community structure and high average clustering. The formation of echo chambers when using this model is approximately of the same size as the formation of echo chambers in a Watts-Strogatz model with a similar average clustering. This suggests that it is mainly the high clustering that drives the system to form echo chambers, while the community structure plays a less important role. However, as said before, the stochastic block model with a high modularity also has a (smaller) formation of echo chambers, so having a clear and strong community structure definitely plays some role in phenomena such as polarization and the formation of opinion clusters.

For balanced starting conditions, none of the network models, nor the filtering algorithms could break the status quo (Fig. 5.1 and related results in [66]). Despite this preserving of the balanced opinion distribution, the interplay of filtering algorithms and network structure can potentially shift the initial randomly distributed opinions to a more clustered opinion distribution and thus lead to polarization and formation of echo chambers.

5.1.2 Unbalanced starting conditions

We will now investigate the effect of unbalanced starting conditions, that is one opinion is initially more prevalent than the other. The initial prevalence of opinion A is $P_A(0) = 0.2$, opinion A thus becomes the minority opinion. The initial prevalence of opinion B is $P_B(0) = 0.8$, hence this is the majority opinion. The opinions are, initially, randomly distributed over the system.

We study four different network models each with a total number of nodes $N = 10^3$ and average degree $\langle k \rangle \sim 10$. The baseline model is the Erdős-Rényi model (ER) with an edge probability $p = 0.01$. To investigate the effect of clustering on the dynamics, we use the Watts-Strogatz model (WS). The rewire probability is $\beta = 0.06$, which gives a clustering coefficient equal to $\langle cc \rangle = 0.557 \pm 0.007$. The impact of community structure on the dynamics is studied with the stochastic block model (SBM) with 10 communities of size 100. Two different modularities are investigated: a high modularity, $Q = 0.908 \pm 0.005$, with an edge probability inside the communities $p_{cl} = 0.1$ and an edge probability between communities $p_{add} = 0.001$; and a low modularity, $Q = 0.220 \pm 0.007$, with $p_{cl} = 0.03$ and $p_{add} = 0.008$. Finally, the impact of both clustering and community structure is investigated with the stochastic Watts-

Strogatz block model (SBM-WS) with 10 communities of size 100. Each community has the following Watts-Strogatz parameters: mean degree $\langle k \rangle = 10$ and rewire probability $\beta = 0.01$. Edges are added between communities with a probability $p_{\text{add}} = 0.001$. This is a network with both high clustering ($\langle cc \rangle = 0.553 \pm 0.004$) and high modularity ($Q = 0.909 \pm 0.004$).

Evolution of the prevalence of the opinions

Fig. 5.3 shows the results for the evolution of the prevalence of opinion A, which is the minority opinion, over time. For each network model two filtering algorithms are compared, the REC filtering algorithm and the PR filtering algorithm.

The REC filtering algorithm maintains the status quo; the prevalence of opinion A remains stable over time for the four different network models. When using the PR filtering algorithm, the results are different. The prevalence of the minority opinion, $P_A(t)$, decreases over time. This decrease is a consequence of the PR filtering algorithm. Since the PR filtering algorithm orders the posts according to the users' preferences, nodes with the majority opinion B will mainly see posts with the same opinion B on their time-line, which limits the chance of changing their opinion to the minority opinion. Nodes with the minority opinion A, on the other hand, will see posts with opinion A on their time-line when using the PR filtering algorithm. However, since there are more nodes with opinion B than nodes with opinion A, the nodes with the minority opinion A will also see a significant number of posts with the majority opinion B on their time-line. When using the PR filtering algorithm, there is an imbalance in the sense that nodes with the minority opinion A have a chance of switching to the majority opinion B, whereas nodes with the majority opinion B have (almost) no chance of switching to the minority opinion A. This imbalance leads to the decrease of the minority opinion A.

Fig. 5.3 shows that the minority opinion A eventually vanishes. This is the case for the low clustering networks, with $P_A(500) = 0.001 \pm 0.003$ for the ER network, $P_A(500) = 0.002 \pm 0.003$ for the SBM with a low modularity and $P_A(500) = 0.003 \pm 0.006$ for the SBM with a high modularity. The high clustering coefficient in the WS and SBM-WS networks seems to slightly hamper this vanishing of the minority opinion with an average value of $P_A(500) = 0.007 \pm 0.014$ for the SBM-WS network (Fig. 5.3d) and an average value of $P_A(500) = 0.009 \pm 0.015$ for the WS network (Fig. 5.3b).

This result differs from results in [66], where the minority opinion was able to survive over time for all the network models, even for the PR filtering algorithm, and where a minority opinion prevalence at $t = 500$ between $P_A(500) = 0.06$ and $P_A(500) = 0.09$ was reported [66]. The results that were obtained in [66] are, however, for networks with a total number of nodes $N = 10^5$ and average degree $\langle k \rangle \sim 6$. In this thesis results are obtained for $N = 10^3$ and average degree $\langle k \rangle \sim 10$. In both cases the maximum length of the actual time-line is set equal to $S = 20$. The difference in the results is most likely due to an interplay between the network size N , the average degree $\langle k \rangle$ and the maximum length of the actual time-line S . This can for example be seen in Fig. 5.4, which shows the results for the evolution of the prevalence of opinion A for an initial 20/80 opinion distribution and using the PR filtering algorithm; Fig. 5.4a displays the results for a WS model with $N = 10^3$, $\langle k \rangle = 6$ and $\beta = 0.01$; Fig. 5.4b shows the results for a WS model with $N = 10^4$, $\langle k \rangle = 6$ and $\beta = 0.01$. In both cases the

average clustering coefficient is $\langle cc \rangle = 0.584 \pm 0.003$ and the maximum length of the actual time-line is $S = 20$. In this figure we can see that the minority opinion A reaches higher final values of $P_0(500)$ compared to the case depicted in Fig. 5.3b, with a value of $P_A(500) = 0.027 \pm 0.023$ in Fig. 5.4a and a value of $P_A(500) = 0.030 \pm 0.018$ in Fig. 5.4b.

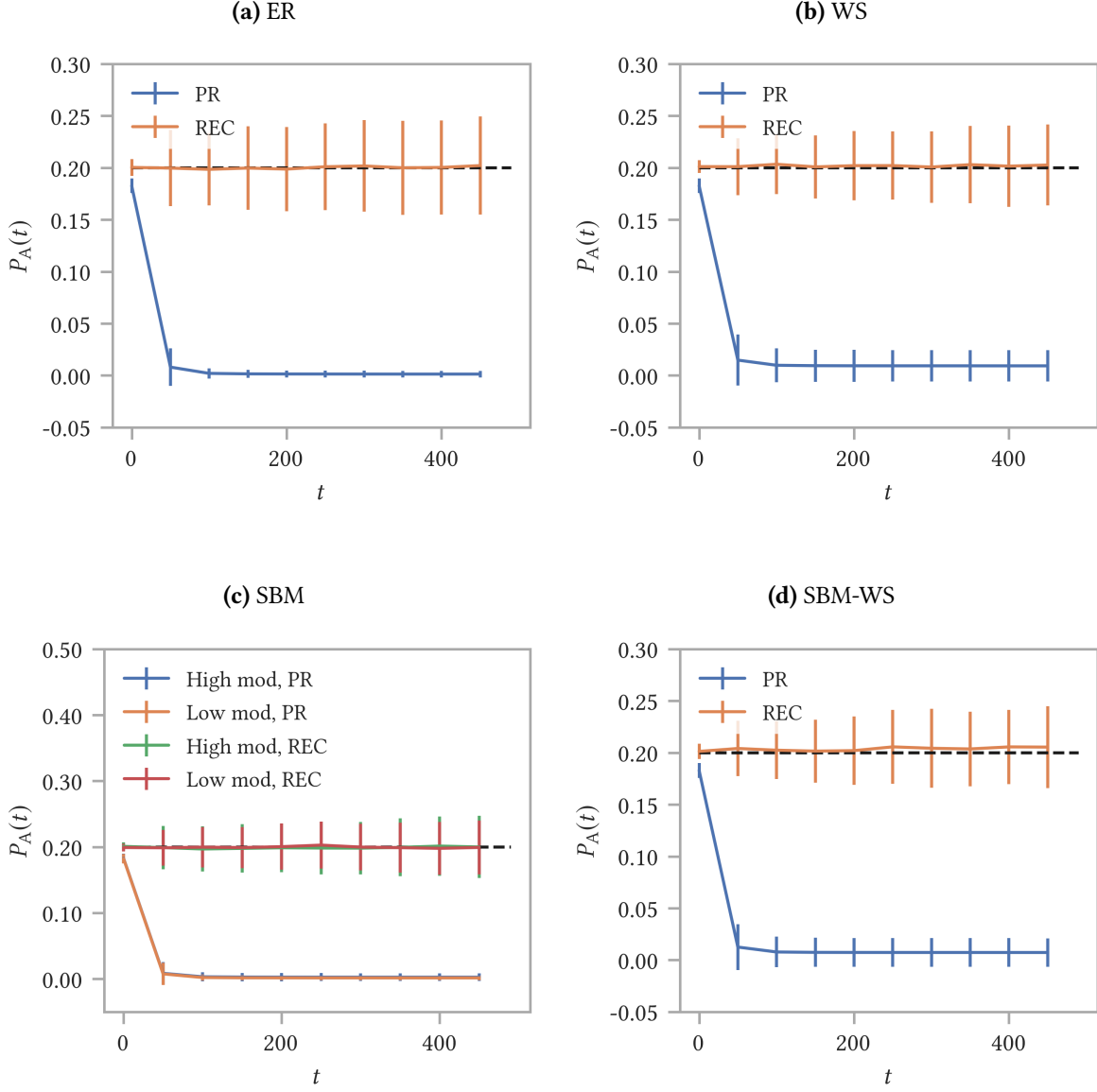


Figure 5.3: Evolution of the prevalence of opinion A ($P_A(t)$) over time for an initial 20/80 distribution. Four different network models are used, each with average degree $\langle k \rangle \sim 10$ and $N = 10^3$: (a) ER, $p = 0.01$; (b) WS with $\langle k \rangle = 10$, $\beta = 0.06$ and $\langle cc \rangle = 0.557 \pm 0.007$; (c) SBM with 10 communities of size 100, a high modularity case ($p_{cl} = 0.1$, $p_{add} = 0.001$, $Q = 0.908 \pm 0.005$) and a low modularity case ($p_{cl} = 0.03$, $p_{add} = 0.008$, $Q = 0.220 \pm 0.007$) are depicted; (d) SBM-WS with 10 communities of size 100, each community has the following WS parameters: $\langle k \rangle = 10$, $\beta = 0.01$ and $p_{add} = 0.001$, $\langle cc \rangle = 0.553 \pm 0.004$ and $Q = 0.909 \pm 0.004$. For each model the REC and the PR filtering algorithms are compared. Each curve is the average of 10^2 independent simulations and data points are shown for every 50 time steps to improve visualization. Bars represent the standard deviation σ .

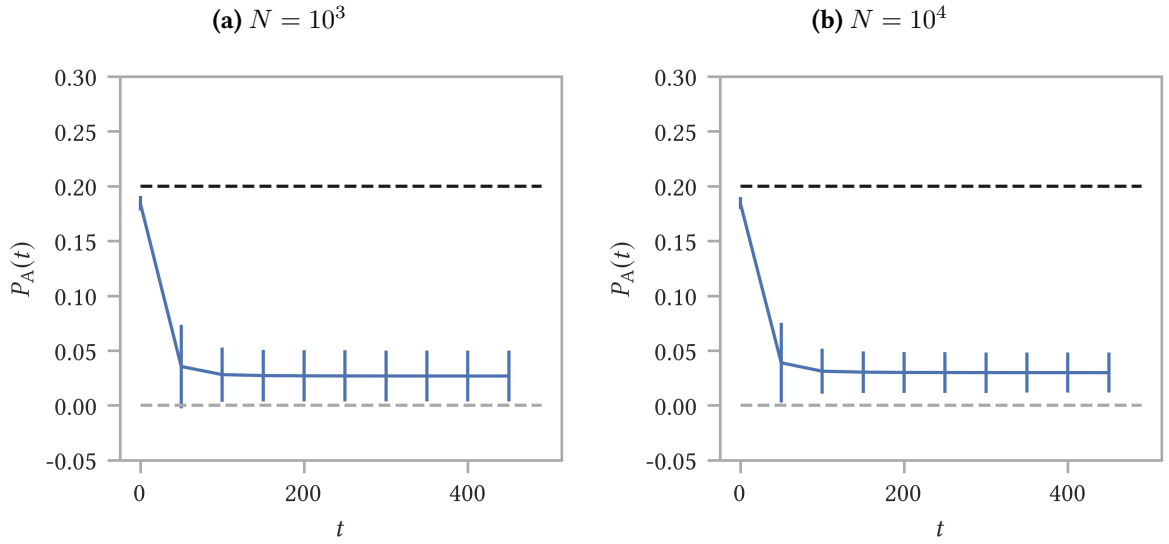


Figure 5.4: Evolution of the prevalence of opinion A ($P_A(t)$) over time for an initial 20/80 distribution. The Watts-Strogatz network with $\langle k \rangle = 6$ and $\beta = 0.01$ is depicted with (a) $N = 10^3$; (b) $N = 10^4$. In both cases the average clustering coefficient is $\langle cc \rangle = 0.584 \pm 0.003$ and the PR filtering filtering algorithm is used. Each curve is the average of 10^2 independent simulations and data points are shown for every 50 time steps to improve visualization. Bars represent the standard deviation σ .

Echo chambers

Fig. 5.5 shows the distribution of the fraction of friends of node i with the same opinion B at $t = 500$ for the four network models: Erdős-Rényi model (ER), Watts-Strogatz model (WS), stochastic block model (SBM) and stochastic Watts-Strogatz block model (SBM-WS). For each network, the REC and PR filtering algorithm are compared. The interpretation of the figure is the same as was described in Subsection 5.1.1 in the “Echo chambers” paragraph.

The results for the Erdős-Rényi model and the stochastic block model (both the high and low modularity case) look qualitatively the same. Similarly, the results for the Watts-Strogatz model and the stochastic Watts-Strogatz block model agree with each other as well. This difference in results between ER/SBM (negligible clustering) and WS/SBM-WS (high clustering) suggests that it is mainly the clustering that drives these differences.

There are no visible effects of having a clear community structure. Fig. 5.5c shows the results for a stochastic block model with a high modularity (clear community structure) and a low modularity (negligible community structure). There is (almost) no difference in the results for a high and a low modularity.

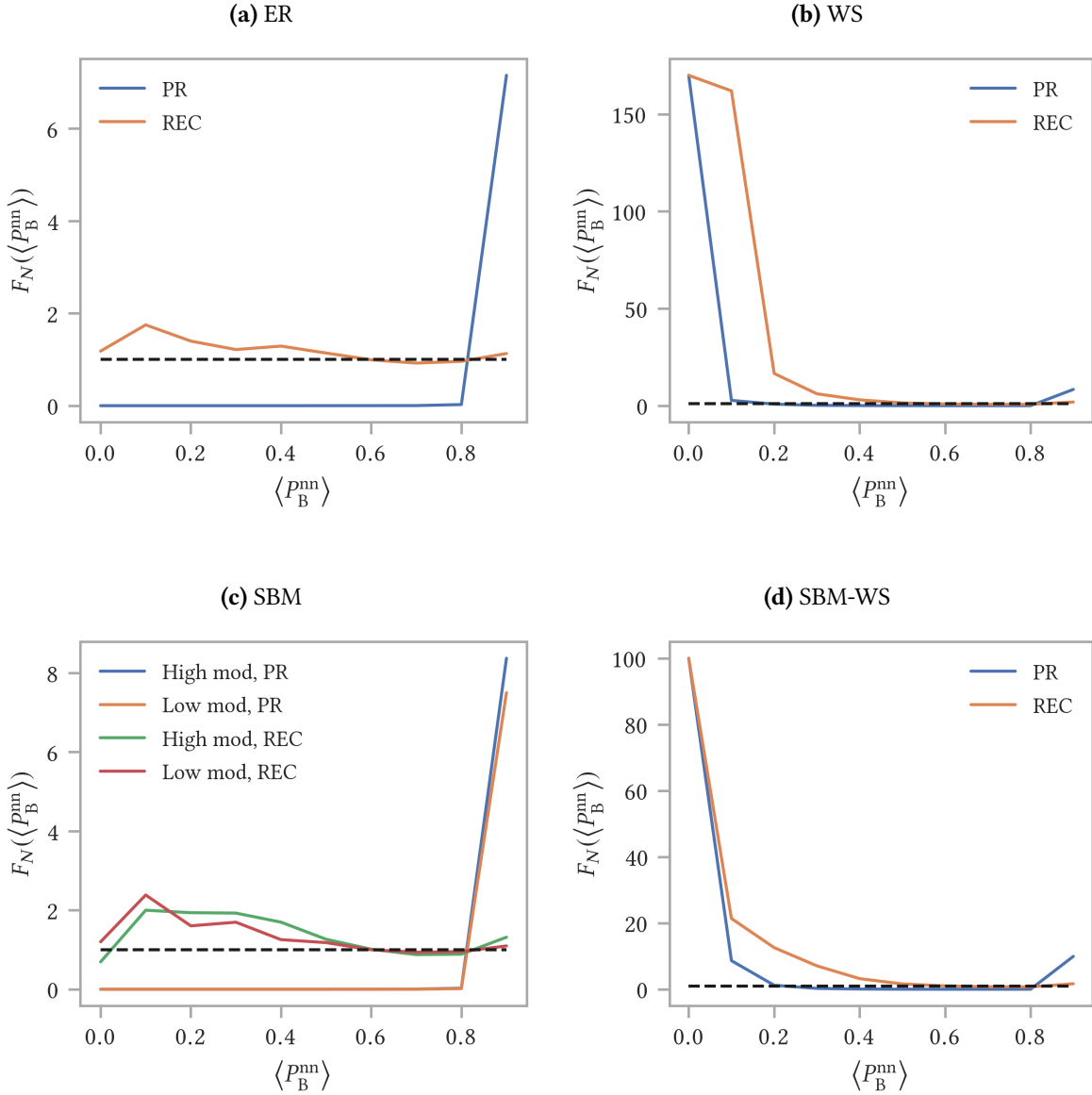


Figure 5.5: Distribution of the fraction of friends (nearest neighbors, nn) of node i with the same opinion B at $t = 500$. The distribution is normalized by dividing for the same quantity computed at $t = 0$. Four different network models are used, each with $N = 10^3$ and average degree $\langle k \rangle \sim 10$: **(a)** ER, $p = 0.01$; **(b)** WS with $\langle k \rangle = 10$, $\beta = 0.06$ and $\langle cc \rangle = 0.557 \pm 0.007$; **(c)** SBM with 10 communities of size 100, a high modularity case ($p_{cl} = 0.1$, $p_{add} = 0.001$, $Q = 0.908 \pm 0.005$) and a low modularity case ($p_{cl} = 0.03$, $p_{add} = 0.008$, $Q = 0.220 \pm 0.007$) are depicted; **(d)** SBM-WS with 10 communities of size 100, each community has the following WS parameters: $\langle k \rangle = 10$, $\beta = 0.01$ and $p_{add} = 0.001$, $\langle cc \rangle = 0.553 \pm 0.004$ and $Q = 0.909 \pm 0.004$. For each model the REC and the PR filtering algorithms are compared. The starting conditions are $P_A(0) = 0.2$ and $P_B(0) = 0.8$. Each curve is the average of 10^2 independent simulations. Error bars are omitted for an improved visualization.

Lets first discuss the results for the Erdős-Rényi model and the stochastic block model (Fig. 5.5a and Fig. 5.5c). When using the REC filtering algorithm, the formation of echo chambers around the majority opinion B is hampered. This is probably a consequence of the absence of clustering and the presence

of short average path lengths in these models. There is even a little spike around $\langle P_1^{\text{nn}} \rangle = 0.1$, which indicates a small increase in the fraction of nodes with the majority of their neighbors carrying the minority opinion A. From Fig. 5.3 it was concluded that the REC filtering algorithm does not break the prevalence of the opinions. The opinion distribution is however slightly shifted from the case where the minority opinion A is more or less randomly distributed over the network to the case where the minority opinion A groups together in opinion clusters.

The PR filtering algorithm shows a different tendency. There is an increase in the fraction of nodes with (almost) all their neighbors carrying the majority opinion B. This is a consequence from the fact that the PR filtering algorithm reduces the visibility of the minority opinion A in the neighborhood of nodes with the majority opinion B. This reduced visibility of the minority opinion A in these neighborhoods drives them eventually to adopt opinion B, with an increase in the number of echo chambers around the majority opinion B as a consequence. Remember from Fig. 5.3, that the PR filtering algorithm strongly reduces the prevalence of the minority opinion. Hence, the increase in the formation of echo chambers around the majority opinion B is not only a consequence of a reorganization of the system from a random opinion distribution to a clustered opinion distribution, but also from a shift in the initial 20/80 opinion distribution to a final (close to) 0/100 opinion distribution. This can also be seen in the fact that, across the x -axis, the average number of neighborhoods with some fraction of the nodes carrying the minority opinion A becomes equal to zero.

Networks with a high clustering coefficient (WS and SBM-WS) behave completely different. For both the REC and PR filtering algorithms the high clustering enhances the formation of echo chambers around the minority opinion A (clearly visible in the spike around $\langle P_1^{\text{nn}} \rangle = 0$ in Fig. 5.5b and Fig. 5.5d). An important note must be made here: the absolute value of neighborhoods with all the nodes carrying the minority opinion A at $t = 0$ is equal to zero in the case of a WS network in Fig. 5.5b and in the case of a SBM-WS network in Fig. 5.5d. This leads to a normalized average value of the echo chambers, which is obtained by dividing the value at $t = 500$ by the corresponding value at $t = 0$, equal to infinity. In Fig. 5.5b and Fig. 5.5d, the spikes around zero are not actually reaching infinity, but are cut off around values equal to 100/180. These large spikes, indicating a large increase of echo chambers around the minority opinion, do not necessarily mean that we have a huge absolute number of echo chambers around the minority opinion A at $t = 500$. They merely indicate that, compared to the beginning at $t = 0$, the increase is large (and if there are zero echo chambers around the minority opinion A at $t = 0$, the increase would be infinite even if there is only one echo chamber around the minority opinion A at $t = 500$). If we would look at the absolute values of the number of echo chambers at $t = 500$, we would still find that the vast majority of the like-minded neighborhoods carry the majority opinion B and that only a minor fraction carries the minority opinion A.

This enhancing of the formation of echo chambers around the minority opinion in case of networks with a high clustering coefficient is remarkable, especially in the case of the PR filtering algorithm. Remember from Fig. 5.3 that in case of the PR filtering algorithm the minority opinion A decreases to less than 1% of the entire population for the high clustering networks. Even though the total fraction of the minority opinion strongly decreases, the high clustering forces the remaining nodes with this minority opinion to group together and form opinion clusters. The normalized value of the formation of echo

chambers around the majority opinion reaches values approximately equal to $F_N(\langle P_1^{\text{nn}} \rangle = 1) = 1$ when using the REC filtering algorithm. This means that the average fraction of nodes with all their neighbors carrying the majority opinion B remains the same before and after the time evolution. In case of the PR filtering algorithm this value is slightly higher than 1, indicating a small increase in the number of majority opinion echo chambers after the time evolution.

5.1.3 Formation of echo chambers versus community structure

In Fig. 5.6, the size of the echo chambers versus the modularity is depicted. The y -axis represents the average of the normalized fraction of nodes with all neighbors carrying opinion A and the normalized fraction of nodes with all neighbors carrying opinion B (with normalized we mean that the computed value for the fraction of nodes with all neighbors having opinion A or all neighbors having opinion B at $t = 500$ is divided by the corresponding value at $t = 0$). This is a measure for the formation of echo chambers (opinion clusters) in the system. The data points represent the value of the echo chamber size in networks with a different modularity. The initial opinion distribution was 50/50 and was randomly distributed over the network.

The data points are shown together with the standard error $SE = \sigma/\sqrt{N}$. The standard error SE is chosen here instead of the standard deviation σ . This is because the standard deviation is quite large. Each data point is the average of 10^2 independent simulations. The dispersion/variation, which is measured by the standard deviation, in the set of the 10^2 obtained values is quite large. However, if we run the 10^2 simulations over and over again, each time calculating the average, the obtained value of the average is always more or less the same. This suggests that the value of the calculated average lies close to the real average. Since we are mostly interested in the correctness of the value of the average, which is quantified by the standard error, we chose to depict the results together with this standard error.

Table 5.1 displays the network models that are used in Fig. 5.6 (all with $N = 10^3$ and average degree $\langle k \rangle \sim 10$).

Q	Network Model
0	Erdős-Rényi model; $p = 0.01$
0.220 ± 0.007	SBM with 10 communities of size 100; $p_{\text{cl}} = 0.03$ and $p_{\text{add}} = 0.008$
0.476 ± 0.009	SBM with 10 communities of size 100; $p_{\text{cl}} = 0.05$ and $p_{\text{add}} = 0.005$
0.624 ± 0.008	SBM with 10 communities of size 100; $p_{\text{cl}} = 0.07$ and $p_{\text{add}} = 0.004$
0.908 ± 0.005	SBM with 10 communities of size 100; $p_{\text{cl}} = 0.1$ and $p_{\text{add}} = 0.001$

Table 5.1: Network models used in Fig. 5.6.

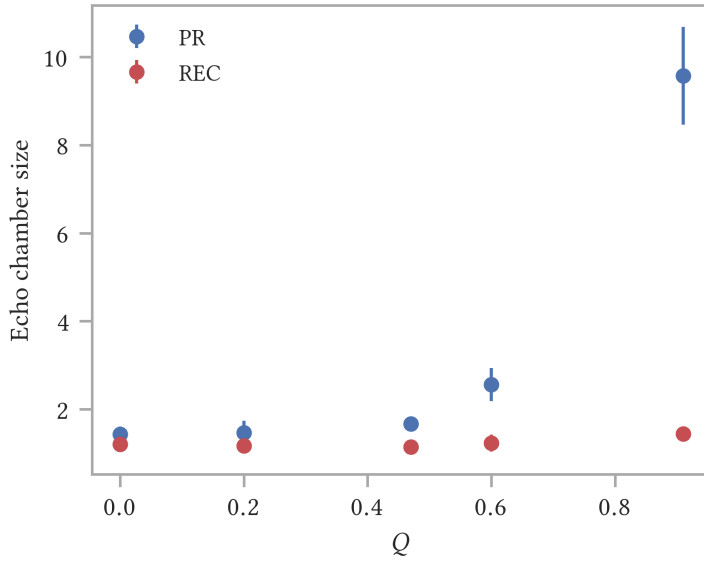


Figure 5.6: The relation between the formation of echo chambers and the community structure, represented by the modularity Q , for both the PR and REC filtering algorithms. The y -axis shows the average of the normalized fraction of nodes with all neighbors having opinion A and the normalized fraction of nodes with all neighbors having opinion B. This value represents the formation of echo chambers in the system (denoted with echo chamber size in the figure). The initial opinion distribution is 50/50. The data point with $Q = 0$ is the result for an ER network with $N = 10^3$, $p = 0.01$ and average degree around 10. The other four data points are the results for SBM's with 10 communities of size 100 ($N = 10^3$), each with a different modularity (the modularity is changed by changing the edge probabilities) and average degree $\langle k \rangle \sim 10$. Each data point is the average of 10^2 independent simulations. Bars represent the standard error SE .

The PR and REC filtering algorithms are compared. For most values of the modularity, the REC filtering algorithm produces almost no echo chambers. If the modularity becomes high enough we see a small increase in the formation of echo chambers, however even for $Q = 0.908 \pm 0.005$, the size of the echo chambers remains smaller than two. This means that after 500 time steps there are less than twice as much echo chambers than in the beginning at $t = 0$.

For the PR filtering algorithm, the increase in the size of the echo chambers with increasing modularity is more significant. From a modularity equal to $Q = 0.476 \pm 0.009$, we see a sharp increase in the formation of echo chambers. For $Q < 0.476$, the formation of echo chambers remains small, even when using the PR filtering algorithm.

These results suggest that the community structure enhances the formation of echo chambers, mostly when using the PR filtering algorithm. A strong community structure, high modularity, is however required to see the effect of community structure on the formation of opinion clusters.

5.2 Stubborn actors

In this section, we will study the effect of stubborn actors on the opinion dynamics. We focus on two different stubbornness models, both are thoroughly discussed in Chapter 3, Section 3.5.2. The results of the first model, including a stubbornness parameter, are given in Section 5.2.1. The results of the second model, the majority threshold model, are presented in Section 5.2.2.

We will implement four different network models in order to investigate the possible interplay between network structure and stubbornness. Each of the network models have a total number of nodes $N = 10^3$ and average degree $\langle k \rangle \sim 10$. The baseline model is the Erdős-Rényi model (ER) with edge probability $p = 0.01$. The interplay between stubbornness and clustering is studied with the Watts-Strogatz model (WS) with mean degree $\langle k \rangle = 10$, rewire probability $\beta = 0.06$ and clustering coefficient $\langle cc \rangle = 0.557 \pm 0.007$. The effect of community structure is investigated with the stochastic block model (SBM) with 10 communities of size 100. Two different modularities are implemented: a high modularity, $Q = 0.908 \pm 0.005$, with $p_{cl} = 0.1$ and $p_{add} = 0.001$) and a low modularity, $Q = 0.220 \pm 0.007$, with $p_{cl} = 0.03$ and $p_{add} = 0.008$. Finally, the interplay between stubbornness and both clustering and community structure is studied with the stochastic Watts-Strogatz block model (SBM-WS) with 10 communities of size 100. Each community has the following Watts-Strogatz parameters: mean degree $\langle k \rangle = 10$ and rewire probability $\beta = 0.01$. Edges are added between communities with a probability $p_{add} = 0.001$. The clustering coefficient of this network is $\langle cc \rangle = 0.553 \pm 0.004$ and the modularity is $Q = 0.909 \pm 0.004$.

For each network model, we compare the REF, REC and PR filtering algorithms to analyze the possible interplay between stubbornness and filtering algorithm.

5.2.1 Including a stubbornness parameter

In this section, we study the effect of a stubbornness parameter r_i on two configurations: (i) fraction of nodes completely stubborn, (ii) all nodes partly stubborn.

In both cases we study both the evolution of the prevalence of the opinions and the formation of echo chambers. This is done for two different starting conditions: balanced starting conditions and unbalanced starting conditions.

The opinion dynamics model described in Chapter 4, Section 4.3 is implemented with an activation probability $p_{act} = 0.1$ and a maximum length of the actual time-line $S = 20$.

Completely stubborn actors

We make a fraction of the nodes (fracRes) completely stubborn ($r_i = 1$). We go from no stubborn nodes, $fracRes = 0$, to all the nodes are stubborn, $fracRes = 1$. In all cases, the stubborn nodes are randomly distributed over the network.

We will first discuss the formation of echo chambers for an initial 50/50 opinion distribution, after

which the results for the opinion evolution will be shared. Then we will discuss the formation of echo chambers and the evolution of the prevalence of the opinions for an initial 20/80 opinion distribution.

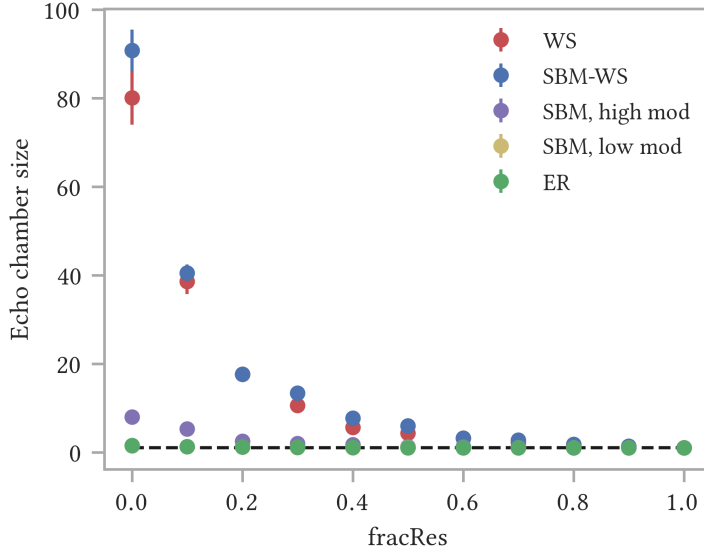


Figure 5.7: Formation of echo chambers versus the fraction of completely stubborn actors, fracRes , for an initial 50/50 opinion distribution and using the PR filtering algorithm. The y -axis shows the average of the normalized fraction of nodes with all neighbors having opinion A and the normalized fraction of nodes with all neighbors having opinion B. This value represents the formation of echo chambers in the system (denoted with echo chamber size in the figure). Results are shown for four different network models, each with $N = 10^3$ and average degree $\langle k \rangle \sim 10$: WS with $\langle k \rangle = 10$, $\beta = 0.06$ and $\langle cc \rangle = 0.557 \pm 0.007$; SBM-WS with 10 communities of size 100, each community has the following WS parameters: $\langle k \rangle = 10$, $\beta = 0.01$ and $p_{\text{add}} = 0.001$, $\langle cc \rangle = 0.553 \pm 0.004$ and $Q = 0.909 \pm 0.004$; SBM with 10 communities of size 100, a high modularity case ($p_{\text{cl}} = 0.1$, $p_{\text{add}} = 0.001$, $Q = 0.908 \pm 0.005$) and a low modularity case ($p_{\text{cl}} = 0.03$, $p_{\text{add}} = 0.008$, $Q = 0.220 \pm 0.007$) are depicted; ER with $p = 0.01$. Each data point is the average of 10^2 independent simulations. Bars represent the standard error SE .

Fig. 5.7 shows the formation of echo chambers in the system versus the fraction of completely stubborn actors, fracRes , when using the PR filtering algorithm for balanced starting conditions. The y -axis represents the formation of echo chambers in the same way as was explained for Fig. 5.6 in Subsection 5.1.3. The dotted black line represents an echo chamber size equal to one. This means that the number of echo chambers remains constant over time.

The Erdős-Rényi model (ER) shows no appearance of echo chambers. Introducing a fraction of completely stubborn actors does not change this behavior. The stochastic block model with a low modularity behaves similar as the Erdős-Rényi model (no formation of echo chambers). The data points for the SBM with a low modularity are not visible in Fig. 5.7, since they lie behind the ER data points.

The other three networks (WS, SBM-WS and SBM with a high modularity) all show qualitatively the same behavior. If an increasing fraction of completely stubborn actors is introduced, the formation of echo chambers decreases with this increasing fraction of stubborn actors.

The WS and SBM-WS networks are the high clustering networks. For a small fraction of stubborn actors they show the largest echo chambers. The stochastic block model with a high modularity has smaller echo chambers than the high clustering networks, but still has some formation of echo chambers for $\text{fracRes} \leq 0.1$. This leads us to make the same conclusion as before: a community structure enhances the formation of echo chambers compared to a random network, however not as significant as networks with a high clustering coefficient.

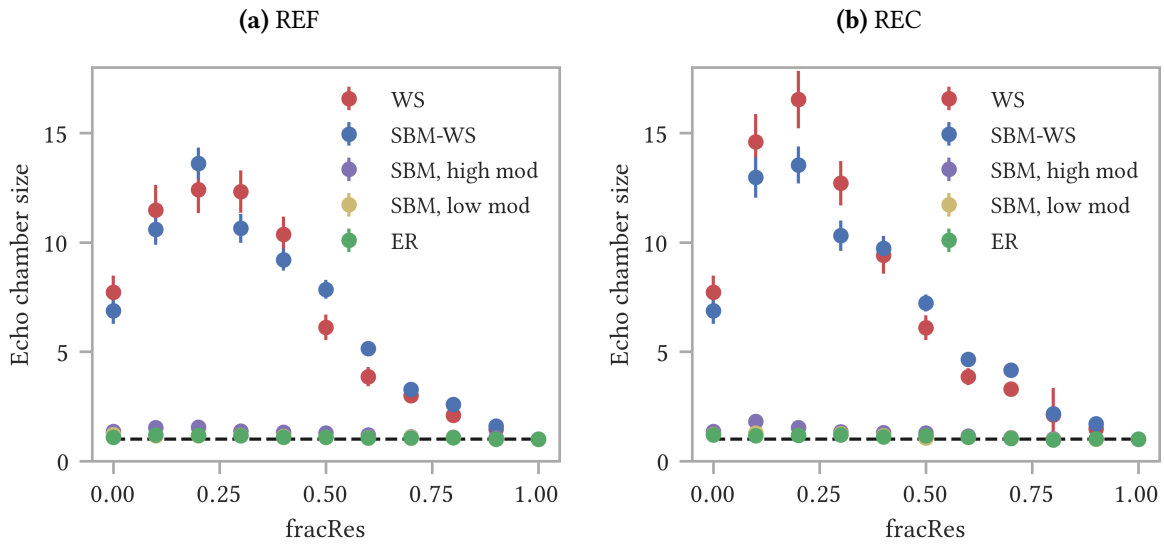


Figure 5.8: Formation of echo chambers versus the fraction of completely stubborn actors, fracRes , for an initial 50/50 opinion distribution. **(a)** REF filtering algorithm; **(b)** REC filtering algorithm. The y -axis shows the average of the normalized fraction of nodes with all neighbors having opinion A and the normalized fraction of nodes with all neighbors having opinion B. This value represents the formation of echo chambers in the system (denoted with echo chamber size in the figure). Results are shown for four different network models, each with $N = 10^3$ and average degree $\langle k \rangle \sim 10$: WS with $\langle k \rangle = 10$, $\beta = 0.06$ and $\langle cc \rangle = 0.557 \pm 0.007$; SBM-WS with 10 communities of size 100, each community has the following WS parameters: $\langle k \rangle = 10$, $\beta = 0.01$ and $p_{\text{add}} = 0.001$, $\langle cc \rangle = 0.553 \pm 0.004$ and $Q = 0.909 \pm 0.004$; SBM with 10 communities of size 100, a high modularity case ($p_{\text{cl}} = 0.1$, $p_{\text{add}} = 0.001$, $Q = 0.908 \pm 0.005$) and a low modularity case ($p_{\text{cl}} = 0.03$, $p_{\text{add}} = 0.008$, $Q = 0.220 \pm 0.007$) are depicted; ER with $p = 0.01$. Each data point is the average of 10^2 independent simulations. Bars represent the standard error SE .

Fig. 5.8 shows the formation of echo chambers in the system versus the fraction of completely stubborn actors, fracRes , when using the REF and REC filtering algorithms. The results are obtained for an initial 50/50 opinion distribution. The results for the REF and REC filtering algorithms behave qualitatively the same, but are different from those obtained with the PR filtering algorithm (Fig. 5.7). Instead of a decrease in the formation of echo chambers with an increasing fraction of completely stubborn actors, we first observe an increase in the formation of echo chambers, followed by a decrease. This is especially clear for the high clustering networks (WS and SBM-WS). The SBM with a high modularity displays a tiny bump. The ER and the SBM with a low modularity (data points for this model lie behind

the ER data points) do not seem to have a significant bump.

These results suggest that the interplay between the REF or REC filtering algorithm and the presence of a (small) fraction of stubborn actors enhances the formation of echo chambers (mainly for networks with a high clustering and/or a clear community structure). If $\text{fracRes} \geq 0.25$, the formation of echo chambers starts to decrease. This is probably due to the fact that too many nodes become stubborn, so there are more and more nodes that will not change opinions. This in turn increases the chance of having stubborn neighbors, each with different opinions, who cannot change opinions, which disables the formation of echo chambers.

This discrepancy between the results for the PR filtering algorithm and those for the REF/REC filtering algorithms in combination with a small fraction of stubborn actors can be potentially explained with the help of the following simple example. Assume we have three nodes that form a triangle. Two nodes initially carry opinion A and one node carries opinion B. Let's first discuss the PR filtering algorithm and assume that none of the nodes are stubborn. In case of the PR filtering algorithm this triangle has a high chance of forming an echo chamber (which is obtained if all the nodes adopt the same opinion). This can be easily seen: the one node with opinion B is likely to switch to opinion A, since all his friends carry this opinion and hence, this opinion will be strongly pushed on his time-line (the fact that the PR filtering algorithm wants to promote posts with opinion B does not matter here, since there are no neighbors with opinion B). The two nodes with opinion A will have more chance of keeping that opinion than switching to opinion B in case of the PR filtering algorithm. This is because the PR filtering algorithm will promote the posts of the friend with the same opinion A over the posts of the friend with opinion B. The end result will be that there is a high chance that all the three nodes will adopt opinion A and hence, form an echo chamber. Now assume that we make the node with opinion B stubborn. This node is no longer capable of switching to opinion A. However, the two nodes with opinion A still have more chance of keeping this opinion in case of the PR filtering algorithm, because this filtering algorithm keeps on promoting the posts of the neighbor with the same opinion A, and hence reduces the visibility of the posts of the stubborn friend with opinion B. The system will not form an echo chamber, since the stubborn node with opinion B cannot switch to opinion A and the PR filtering algorithm reduces the chance of changing the opinion of the nodes with opinion A to opinion B. The conclusion is that, in case of the PR filtering algorithm, making a fraction of the nodes stubborn reduces the ability of the system to form echo chambers compared to the case where there are no stubborn actors. What happens if we use the REF/REC filtering algorithms? Again we have one node with opinion B and two nodes with opinion A in the triangle. Assume first that none of the nodes are stubborn. For the PR filtering algorithm, we argued that in this case, the triangle has a high chance of evolving towards an echo chamber. For the REF/REC filtering algorithms this chance is however smaller, which can be seen as follows. The node with opinion B still has a high chance of switching to opinion A, because all his friends (which are the two other nodes in the triangle) carry this opinion. However, the two nodes with opinion A will now not have a higher chance of keeping this opinion than to switch to opinion B, as was the case for the PR filtering algorithm. Instead, they have an equal chance of keeping their opinion as to change to the other opinion. This is because both the REF and REC filtering algorithms do not discriminate between the two different opinions of the friends of the nodes with opinion A. Both opinion A and opinion B have an equal chance of being promoted on

the time-line of the nodes with opinion A. This reduced tendency of the nodes with opinion A to not change their opinion (compared to using the PR filtering algorithm) hampers the ability of the triangle to form an echo chamber. This would explain why, in case of no stubborn actors, the REC/REF filtering algorithms show a lower formation of echo chambers compared to the PR filtering algorithm. Now, let's again assume that we make the node with opinion B stubborn. In case of the PR filtering algorithm this reduced the formation of echo chambers in the triangle. For the REC/REF filtering algorithms, things are different. The stubborn node with opinion B will not change opinion. The two nodes with opinion A, on the other hand, will now have a higher chance of switching to opinion B (which was not the case when using the PR filtering algorithm). This can be seen as follows. The REF/REC filtering algorithms do not discriminate between the two different opinions of the two friends of the nodes with opinion A. If the node with opinion B is, however, stubborn it will keep on pushing that opinion on the time-lines of the two nodes with opinion A. This will eventually lead to an increase of posts with opinion B, compared to posts with opinion A, on the time-lines of the two nodes with opinion A. The result will then be that the nodes with opinion A will have a higher chance of switching to opinion B, which enhances the formation of echo chambers in the triangle. This would explain the increase in the formation of echo chambers for a small fraction of stubborn actors when using the REF or REC filtering algorithms. If too many nodes become stubborn, this increased ability of the system to form echo chambers, in case of using the REC/REF filtering algorithms, starts to decrease which can also be easily seen with the help of the triangle example. If the fraction of stubborn actors becomes too high, we might end up with the case where both the node with opinion B and one of the nodes with opinion A are stubborn. This strongly reduces the ability to form echo chambers in the triangle since we can no longer have a final situation in which all the three nodes in the triangle carry the same opinion.

So far the results for the formation of echo chambers in the system for balanced starting conditions and introducing a fraction of completely stubborn actors. But what about the evolution of the prevalence of the opinions over time? Are these affected by introducing stubborn actors in the system? The short answer is no. Introducing stubborn actors in the system does not affect the evolution of the prevalence of the opinions over time for neither the REC, nor the PR filtering algorithm. The balanced opinion distribution is maintained over time. This result is valid for all the four implemented network models (ER, WS, SBM and SBM-WS). Network topologies such as a high clustering coefficient and/or a community structure do not change this result.

Lets now study the situation for unbalanced starting conditions, combined with a fraction of stubborn actors. The initial prevalence of opinion A is $P_A(0) = 0.2$ and the initial prevalence of opinion B is $P_B(0) = 0.8$.

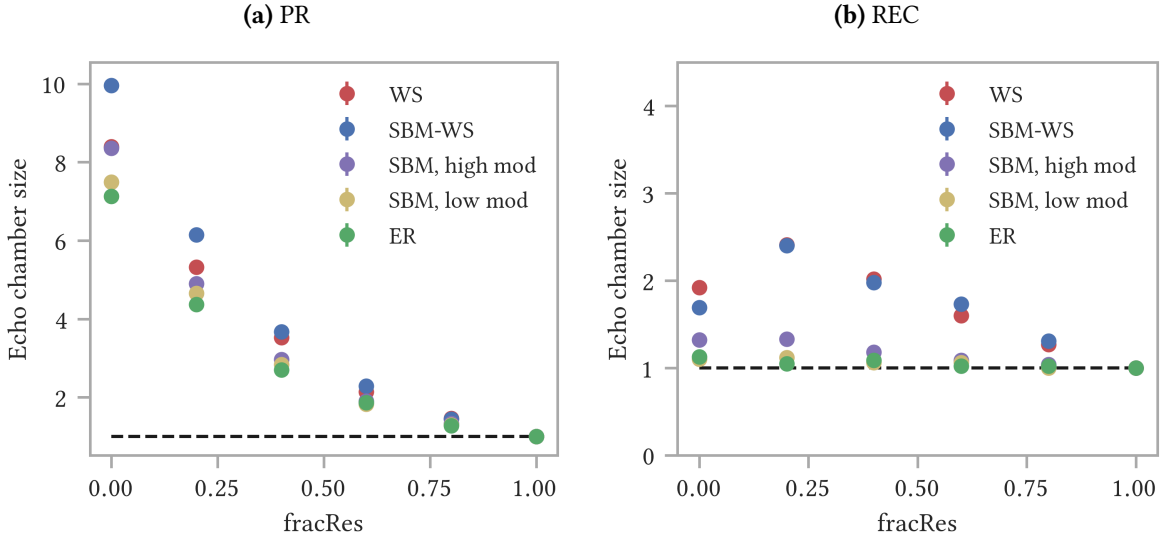


Figure 5.9: Formation of echo chambers versus the fraction of completely stubborn actors, fracRes , for an initial 20/80 opinion distribution. **(a)** PR filtering algorithm; **(b)** REC filtering algorithm. The y -axis shows the total number of like-minded neighborhoods (sum of the number of echo chambers around opinion A and the number of echo chambers around opinion B) at $t = 500$ divided by the total number of like-minded neighborhoods at $t = 0$. This value represents the formation of echo chambers in the system (denoted with echo chamber size in the figure). Results are shown for four different network models, each with $N = 10^3$ and average degree $\langle k \rangle \sim 10$: WS with $\langle k \rangle = 10$, $\beta = 0.06$ and $\langle cc \rangle = 0.557 \pm 0.007$; SBM-WS with 10 communities of size 100, each community has the following WS parameters: $\langle k \rangle = 10$, $\beta = 0.01$ and $p_{\text{add}} = 0.001$, $\langle cc \rangle = 0.553 \pm 0.004$ and $Q = 0.909 \pm 0.004$; SBM with 10 communities of size 100, a high modularity case ($p_{\text{cl}} = 0.1$, $p_{\text{add}} = 0.001$, $Q = 0.908 \pm 0.005$) and a low modularity case ($p_{\text{cl}} = 0.03$, $p_{\text{add}} = 0.008$, $Q = 0.220 \pm 0.007$) are depicted; ER with $p = 0.01$. Each data point is the average of 10^2 independent simulations. Bars represent the standard error SE .

Fig. 5.9 shows the formation of echo chambers versus the fraction of completely stubborn actors, fracRes , for an initial 20/80 opinion distribution (opinion A is the minority opinion, opinion B is the majority opinion). The PR and the REC filtering algorithms are compared. The standard errors SE are small and not visible in the figure. The dotted black line represent the situation in which the number of echo chambers remains constant over time. The interpretation of the y -axis is slightly different than before. In previous figures, the echo chamber size was interpreted as the average of the normalized fraction of nodes with all neighbors having opinion A and the normalized fraction of nodes with all neighbors having opinion B. Thus we first normalized the echo chambers around opinion A and those around opinion B and then took the average of both. In case of a 20/80 distribution we have a skewed echo chamber distribution, as can be seen in Fig. 5.5, with normalized values going to infinity. We still want to have some average of the echo chambers around opinion A and those around opinion B to quantify the total formation of echo chambers in the system, but we want to avoid problems with those infinities. Hence, we opted for a different average: first we calculate the total number of like-minded neighborhoods at $t = 500$ (thus the sum of the number of echo chambers around opinion A and the number of echo chambers around opinion B), then we divide that quantity by the total number

of like-minded neighborhoods at $t = 0$ (hence, we first take the average and then normalize it, instead of normalizing first and then taking the average, as was done before). By taking the average, we neglect the skewed echo chamber distribution. This is, however, not a problem. We want a sense of the total number of echo chambers in the system and how this total number is impacted by the presence of stubborn actors and are less interested in the distribution of those echo chambers.

When using the PR filtering algorithm (Fig. 5.9a) we observe a decrease in the formation of echo chambers with an increasing fraction of stubborn actors. This behavior is similar to the case of balanced starting conditions in combination with the PR filtering algorithm (Fig. 5.7). For unbalanced starting conditions, in combination with the PR filtering algorithm, the formation of echo chambers in the Erdős-Rényi network and the stochastic block model with a low modularity is non-zero (for $\text{fracRes} = 0$), as can be observed in Fig. 5.5. This behavior is a consequence of the fact that for an initial 20/80 opinion distribution, in combination with the PR filtering algorithm, the prevalence of the majority opinion strongly increases, as was explained for Fig. 5.5.

The formation of echo chambers for networks with a high clustering and/or a high modularity is slightly higher. It is however not recommended to (quantitatively) compare the formation of echo chambers between the different network models when depicting the results as the average of the echo chambers around opinion A and those around opinion B in case of unbalanced starting conditions. The reason is that this average neglects the skewed echo chamber distributions as depicted in Fig. 5.5. When comparing the different network models, these skewed distributions should not be overlooked. The goal of this figure is to show the dependency of the formation of echo chambers in the network models on the presence of a fraction of stubborn actors and not to (quantitatively) compare the different models against each other.

The results for the REC filtering algorithm (Fig. 5.9b) are different than those for the PR filtering algorithm. The high clustering networks (WS and SBM-WS) show an increase in the formation of echo chambers with an increasing fraction of completely stubborn actors, followed by a decrease. This result is similar to the results for balanced starting conditions in combination with the REC filtering algorithm (Fig. 5.8b). The stochastic block model with a high modularity does not show an increase in the formation of echo chambers but remains flat for $\text{fracRes} \leq 0.2$; if the fraction of stubborn actors increases further, we see a decrease in the formation of echo chambers. The Erdős-Rényi network and the stochastic block model with a low modularity show no significant formation of echo chambers. For an increasing fraction of the completely stubborn actors, the echo chambers eventually converge to one (for all the network models), indicating a constant amount of echo chambers over time (represented by the black dotted line).

We can conclude that the formation of echo chambers versus the fraction of completely stubborn actors, for unbalanced starting conditions, qualitatively resembles the results for balanced starting conditions (decrease in formation of echo chambers with an increasing fraction of stubborn actors for the PR filtering algorithm versus an increase in the formation of echo chambers with an increasing fraction of stubborn actors, followed by a decrease for the REC filtering algorithm).

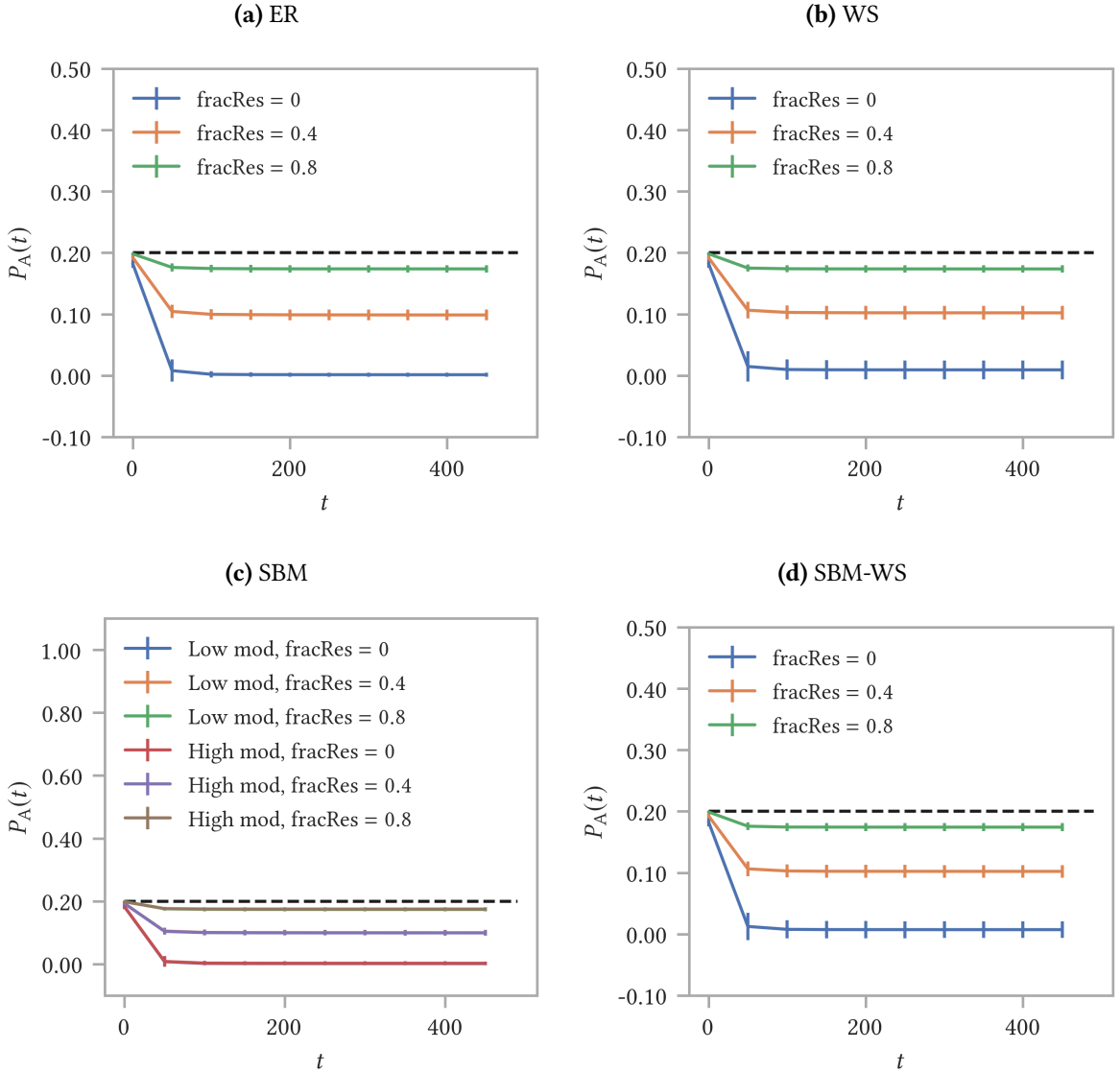


Figure 5.10: Evolution of the prevalence of opinion A ($P_A(t)$) over time for an initial 20/80 distribution, using the PR filtering algorithm and comparing three different fractions of completely stubborn actors ($\text{fracRes} = 0$, $\text{fracRes} = 0.4$ and $\text{fracRes} = 0.8$). Four different network models are used, each with average degree $\langle k \rangle \sim 10$ and $N = 10^3$: (a) ER, $p = 0.01$; (b) WS with $\langle k \rangle = 10$, $\beta = 0.06$ and $\langle cc \rangle = 0.557 \pm 0.007$; (c) SBM with 10 communities of size 100, a high modularity case ($p_{\text{cl}} = 0.1$, $p_{\text{add}} = 0.001$, $Q = 0.908 \pm 0.005$) and a low modularity case ($p_{\text{cl}} = 0.03$, $p_{\text{add}} = 0.008$, $Q = 0.220 \pm 0.007$) are depicted; (d) SBM-WS with 10 communities of size 100, each community has the following WS parameters: $\langle k \rangle = 10$, $\beta = 0.01$ and $p_{\text{add}} = 0.001$, $\langle cc \rangle = 0.553 \pm 0.004$ and $Q = 0.909 \pm 0.004$. Each curve is the average of 10^2 independent simulations and data points are shown for every 50 time steps to improve visualization. Bars represent the standard deviation σ .

Lets now discuss the evolution of the prevalence of the opinions. In Fig. 5.3, we saw that for a system with no stubborn actors the REC filtering algorithm does not break the prevalence of the initial opinions in case of unbalanced starting conditions. The PR filtering algorithm, on the other hand, resulted in a decrease of the prevalence of the minority opinion. Are these results affected by introducing stubborn actors? As for the balanced starting conditions, introducing stubborn actors does not break the

prevalence of the initial opinions for the REC filtering algorithm. The status quo is maintained over time. Introducing stubborn actors combined with the PR filtering algorithm, on the other hand, does have an impact in case of unbalanced starting conditions.

Fig. 5.10 shows the results for the prevalence of opinion A versus time in case of unbalanced starting conditions and using the PR filtering algorithm. We compare four different network models (ER, WS, SBM (high and low modularity) and SBM-WS). For each model we compare the results for three different fractions of stubborn actors ($\text{fracRes} = 0$, $\text{fracRes} = 0.4$ and $\text{fracRes} = 0.8$).

If there are no stubborn actors, the PR filtering algorithm leads to a significant decrease in the prevalence of the minority opinion in case of unbalanced starting conditions. Introducing a fraction of stubborn actors changes this scenario. For an increasing fraction of stubborn actors, the decrease of the minority opinion becomes less and less strong. This result is valid for all the different network topologies. If there are no stubborn actors, the PR filtering algorithm forces nodes with the minority opinion to switch to the majority opinion. If we introduce a fraction of stubborn actors in the system, we end up with stubborn actors that carry the minority opinion. These stubborn actors will not switch to the majority opinion, no matter how hard the PR filtering algorithm pushes them. The consequence is that these stubborn actors with the minority opinion hamper the decrease of that minority opinion.

All actors partly stubborn

In the second configuration, all the nodes are partly stubborn. They still have some chance of changing their opinion, they are however less eager to do so. All the nodes are given the same stubbornness parameter r and we let this stubbornness parameter vary from $r = 0$ (all the nodes are completely willing to change opinions) to $r = 1$ (all the nodes are completely stubborn).

We first study the formation of echo chambers and the evolution of the prevalence of the opinions for balanced starting conditions, where-after we investigate the results for unbalanced starting conditions.

Fig. 5.11 shows the formation of echo chambers versus the stubbornness parameter of all the nodes, r , for an initial 50/50 opinion distribution and using the PR filtering algorithm. The interpretation of the y -axis is again as explained in Subsection 5.1.3. The results are similar to the case where a fraction of the nodes is completely stubborn combined with the PR filtering algorithm (Fig. 5.7).

The Erdős-Rényi model has no appearance of echo chambers. This is not changed by making the nodes more and more stubborn. The same result is obtained for the stochastic block model with a low modularity (the data points lie behind those of the ER network).

The stochastic block model with a high modularity has a (small) formation of echo chambers for $r = 0$. If the nodes become more and more convinced of their own opinion (r increases), the formation of echo chambers decreases. This is especially visible for the high clustering networks (WS and SBM-WS), which have the highest formation of echo chambers for $r = 0$. If r increases and the nodes become

more and more convinced of their own beliefs, which makes them less and less willing to change that belief, the formation of echo chambers starts to decrease. If $r = 1$, the nodes retain their initial opinion and the number of echo chambers before and after the time evolution remains the same. This situation is represented by the black dotted line.

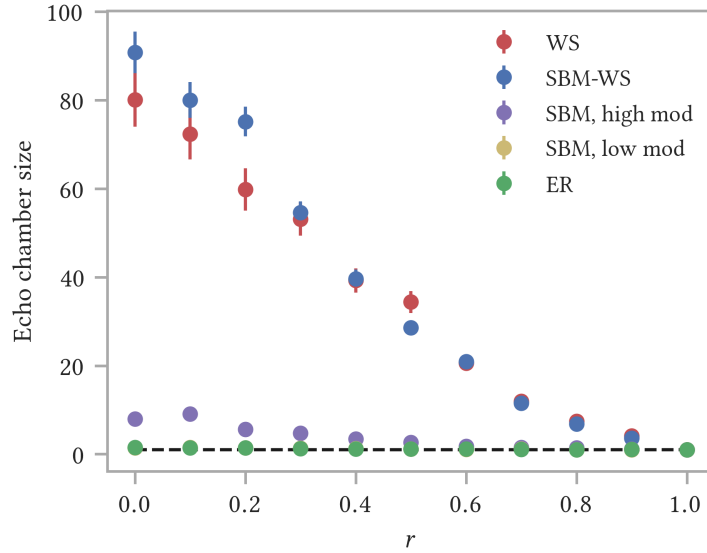


Figure 5.11: Formation of echo chambers versus the stubbornness parameter of all the nodes, r , for an initial 50/50 opinion distribution and using the PR filtering algorithm. The y -axis shows the average of the normalized fraction of nodes with all neighbors having opinion A and the normalized fraction of nodes with all neighbors having opinion B. This value represents the formation of echo chambers in the system (denoted with echo chamber size in the figure). Results are shown for four different network models, each with $N = 10^3$ and average degree $\langle k \rangle \sim 10$: WS with $\langle k \rangle = 10$, $\beta = 0.06$ and $\langle cc \rangle = 0.557 \pm 0.007$; SBM-WS with 10 communities of size 100, each community has the following WS parameters: $\langle k \rangle = 10$, $\beta = 0.01$ and $p_{\text{add}} = 0.001$, $\langle cc \rangle = 0.553 \pm 0.004$ and $Q = 0.909 \pm 0.004$; SBM with 10 communities of size 100, a high modularity case ($p_{\text{cl}} = 0.1$, $p_{\text{add}} = 0.001$, $Q = 0.908 \pm 0.005$) and a low modularity case ($p_{\text{cl}} = 0.03$, $p_{\text{add}} = 0.008$, $Q = 0.220 \pm 0.007$) are depicted; ER with $p = 0.01$. Each data point is the average of 10^2 independent simulations. Bars represent the standard error SE .

In Fig. 5.12 the formation of echo chambers versus the stubbornness parameter of all the nodes, r , is depicted for an initial 50/50 opinion distribution. Fig. 5.12a shows the results for the REF filtering algorithm and Fig. 5.12b shows those for the REC filtering algorithm.

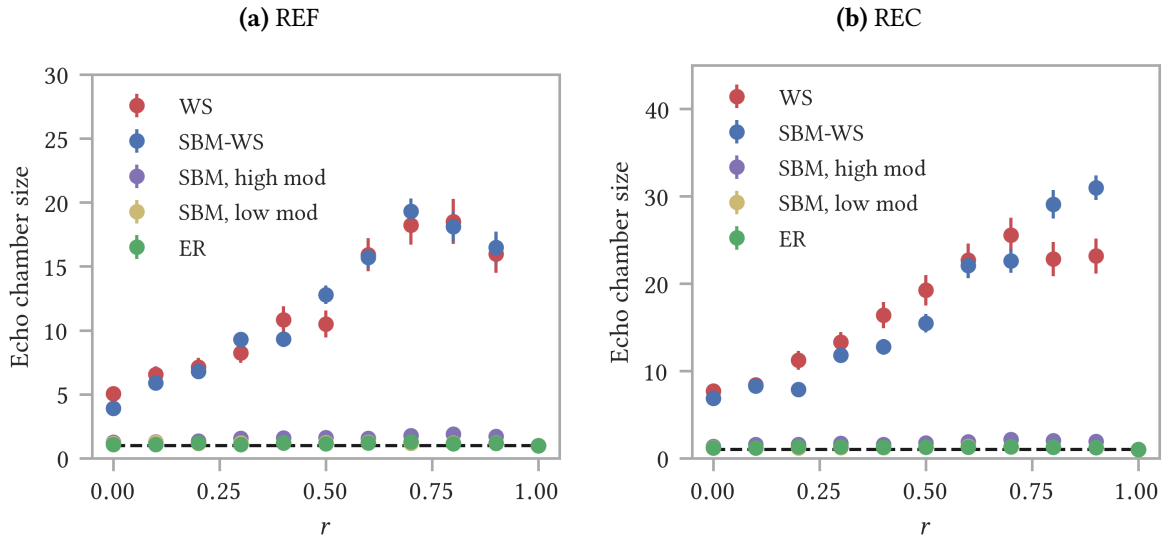


Figure 5.12: Formation of echo chambers versus the stubbornness parameter of all the nodes, r , for an initial 50/50 opinion distribution. **(a)** REF filtering algorithm; **(b)** REC filtering algorithm. The y -axis shows the average of the normalized fraction of nodes with all neighbors having opinion A and the normalized fraction of nodes with all neighbors having opinion B. This value represents the formation of echo chambers in the system (denoted with echo chamber size in the figure). Results are shown for four different network models, each with $N = 10^3$ and average degree $\langle k \rangle \sim 10$: WS with $\langle k \rangle = 10$, $\beta = 0.06$ and $\langle cc \rangle = 0.557 \pm 0.007$; SBM-WS with 10 communities of size 100, each community has the following WS parameters: $\langle k \rangle = 10$, $\beta = 0.01$ and $p_{\text{add}} = 0.001$, $\langle cc \rangle = 0.553 \pm 0.004$ and $Q = 0.909 \pm 0.004$; SBM with 10 communities of size 100, a high modularity case ($p_{\text{cl}} = 0.1$, $p_{\text{add}} = 0.001$, $Q = 0.908 \pm 0.005$) and a low modularity case ($p_{\text{cl}} = 0.03$, $p_{\text{add}} = 0.008$, $Q = 0.220 \pm 0.007$) are depicted; ER with $p = 0.01$. Each data point is the average of 10^2 independent simulations. Bars represent the standard error SE .

We can make similar observations as we did in the “Completely stubborn actors” paragraph. The results for the REF and REC filtering algorithms are qualitatively similar to each other and differ from the results obtained with the PR filtering algorithm (Fig. 5.11). The formation of echo chambers in the high clustering networks (WS and SBM-WS) increases if the stubbornness of the nodes r increases. For the REF filtering algorithm, this increases reaches a maximum around $r = 0.7$ and then starts to slowly decrease between $r = 0.7$ and $r = 0.9$. Between $r = 0.9$ and $r = 1$ there is a steep drop in the formation of echo chambers. The REC filtering algorithm also seems to have a maximum around $r = 0.7$ for the WS model. The SBM-WS model, on the other hand, displays a continuous increase until $r = 0.9$. In both cases we have a sharp drop from $r = 0.9$ to $r = 1$. If $r = 1$, the nodes are completely stubborn and thus keep their initial opinion. Hence, the number of like minded neighborhoods does not change over time, which gives a normalized number of echo chambers equal to one. This is represented by the black dotted line. It is remarkable that for high levels of the stubbornness of the nodes r , up to $r = 0.9$, the formation of echo chambers is large and even larger than if the nodes are not stubborn. We can conclude that making the nodes partly stubborn enhances the formation of echo chambers when using the REC/REF filtering algorithms in case of networks with a high clustering coefficient. This is the opposite of the case where the PR filtering algorithm is used (which shows a decrease in the formation of echo

chambers with an increasing stubbornness of the nodes). The reason for this discrepancy is probably of a similar nature as for this discrepancy in case of introducing a fraction of completely stubborn actors, see the “Completely stubborn actors” paragraph. If we zoom in on the stochastic block model with a high modularity, we see a slight increase in the formation of echo chambers. The increase is however not as strong as for the high clustering networks.

The Erdős-Rényi network and the stochastic block model with a low modularity (data points are hidden behind those of the ER network) do not have any dependency on the stubbornness level of the nodes. This seems to suggest that it is mainly the interplay between the high clustering, and to a lesser extent a clear community structure (high modularity), and the REF/REC filtering algorithms that drives this increase in the formation of echo chambers with increasing r .

What about the results for the evolution of the prevalence of the opinions in case of balanced starting conditions and making all the nodes partly stubborn? Making all the nodes partly stubborn does not disturb/change the evolution of the opinions. The balanced starting conditions remain balanced over time, as was the case for no stubbornness in the system. This result is valid for all the network models (ER, WS, SBM and SBM-WS) and for both the REC and PR filtering algorithm.

Lets now study the results for unbalanced starting conditions (20/80). Opinion A is the minority opinion, which makes opinion B the majority opinion. First, we discuss the formation of echo chambers. Then, we investigate the results for the evolution of the prevalence of the opinions.

Fig. 5.13 shows the results for the formation of echo chambers versus the stubbornness parameter r of all the nodes for an initial 20/80 distribution. The standard error SE is small and not visible in the figure. Fig. 5.13a gives the results for the PR filtering algorithm and Fig. 5.13b gives the results for the REC filtering algorithm. The y -axis is interpreted in the same way as explained for Fig. 5.9.

In case of the PR filtering algorithm (Fig. 5.13a), the formation of echo chambers remains more or less flat for all the network models if $r \leq 0.4$. If $r > 0.4$, the formation of echo chambers starts to decrease for all the network models. This behavior is slightly different than in case of balanced starting conditions, combined with the PR filtering algorithm (Fig. 5.11). In that case, we could already observe a decrease in the formation of echo chambers for $r > 0$ (except for the SBM with a high modularity which showed a decrease if $r > 0.1$). This difference is probably a consequence of the unbalanced starting conditions, which seems to make the system less sensitive to the stubbornness parameter r .

As was explained for Fig. 5.9, the formation of echo chambers in the ER network and the SBM with a low modularity in case of unbalanced starting conditions, combined with the PR filtering algorithm is non-zero. These figures are not suited to (quantitatively) compare the formation of echo chambers in the different network models in case of unbalanced starting conditions. In order to perform such a (quantitative) comparison, one should look at the complete distribution (see eg. Fig. 5.5), as was explained for Fig. 5.9.

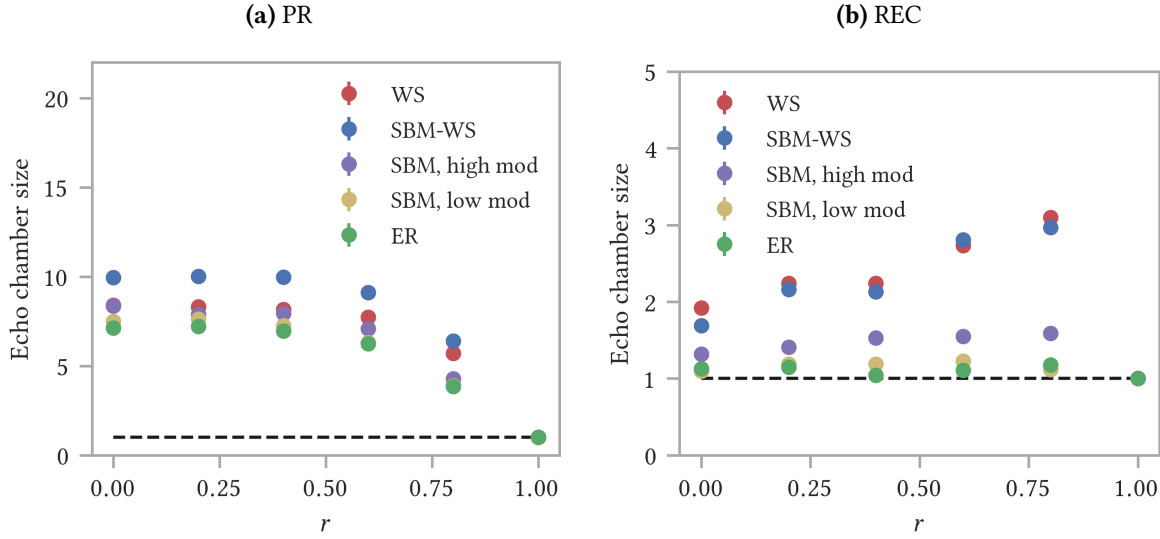


Figure 5.13: Formation of echo chambers versus the stubbornness parameter of all the nodes, r , for an initial 20/80 opinion distribution. **(a)** PR filtering algorithm; **(b)** REC filtering algorithm. The y -axis shows the total number of like-minded neighborhoods (sum of the number of echo chambers around opinion A and the number of echo chambers around opinion B) at $t = 500$ divided by the total number of like-minded neighborhoods at $t = 0$. This value represents the formation of echo chambers in the system (denoted with echo chamber size in the figure). Results are shown for four different network models, each with $N = 10^3$ and average degree $\langle k \rangle \sim 10$: WS with $\langle k \rangle = 10$, $\beta = 0.06$ and $\langle cc \rangle = 0.557 \pm 0.007$; SBM-WS with 10 communities of size 100, each community has the following WS parameters: $\langle k \rangle = 10$, $\beta = 0.01$ and $p_{\text{add}} = 0.001$, $\langle cc \rangle = 0.553 \pm 0.004$ and $Q = 0.909 \pm 0.004$; SBM with 10 communities of size 100, a high modularity case ($p_{\text{cl}} = 0.1$, $p_{\text{add}} = 0.001$, $Q = 0.908 \pm 0.005$) and a low modularity case ($p_{\text{cl}} = 0.03$, $p_{\text{add}} = 0.008$, $Q = 0.220 \pm 0.007$) are depicted; ER with $p = 0.01$. Each data point is the average of 10^2 independent simulations. Bars represent the standard error SE .

The results for the REC filtering algorithm (Fig. 5.13b) resemble those for balanced starting conditions (Fig. 5.12b). The high clustering networks (WS and SBM-WS) show an increase in the formation of echo chambers up to $r = 0.8$, after which a sharp drop to one, for $r = 1$, is observed. The increase seems less steep than the increase for balanced starting conditions, which we can observe in Fig. 5.12b. This again seems to suggest that the system is less sensitive to the stubbornness parameter r for unbalanced starting conditions than for balanced starting conditions.

The stochastic block model with a high modularity shows a slight increase in the formation of echo chambers up to $r = 0.8$. This increase can even be observed for the low modularity case, albeit less strong. The Erdős-Rényi network wiggles around a formation of echo chambers equal to one.

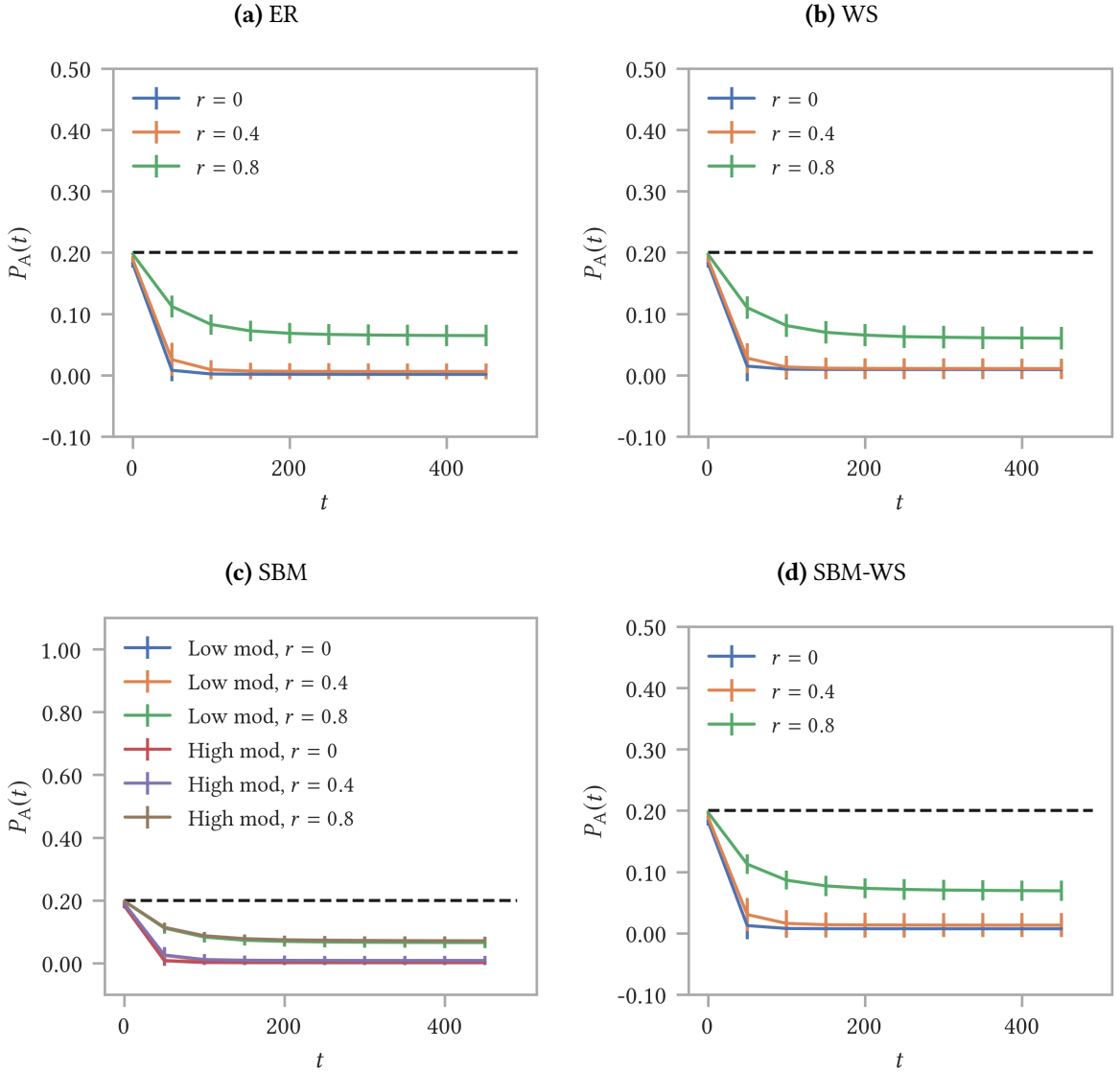


Figure 5.14: Evolution of the prevalence of opinion A ($P_A(t)$) over time for an initial 20/80 distribution, using the PR filtering algorithm and comparing three different values of the stubbornness parameter r of all the nodes ($r = 0$, $r = 0.4$ and $r = 0.8$). Four different network models are used, each with average degree $\langle k \rangle \sim 10$ and $N = 10^3$: **(a)** ER, $p = 0.01$; **(b)** WS with $\langle k \rangle = 10$, $\beta = 0.06$ and $\langle cc \rangle = 0.557 \pm 0.007$; **(c)** SBM with 10 communities of size 100, a high modularity case ($p_{cl} = 0.1$, $p_{add} = 0.001$, $Q = 0.908 \pm 0.005$) and a low modularity case ($p_{cl} = 0.03$, $p_{add} = 0.008$, $Q = 0.220 \pm 0.007$) are depicted; **(d)** SBM-WS with 10 communities of size 100, each community has the following WS parameters: $\langle k \rangle = 10$, $\beta = 0.01$ and $p_{add} = 0.001$, $\langle cc \rangle = 0.553 \pm 0.004$ and $Q = 0.909 \pm 0.004$. Each curve is the average of 10^2 independent simulations and data points are shown for every 50 time steps to improve visualization. Bars represent the standard deviation σ .

We will now discuss the results for the evolution of the prevalence of the opinions in case of unbalanced starting conditions and making all the nodes partly stubborn. We investigate four different network models. For each model the results for three different values of the stubbornness parameter r ($r = 0$, $r = 0.4$ and $r = 0.8$) are compared. Two filtering algorithms are investigated, the REC filtering algorithm and the PR filtering algorithm.

The prevalence of opinion A versus time in case of the REC filtering algorithm is not affected by making all the nodes more and more stubborn. The prevalence of the opinions is maintained and the status quo is not broken. The PR filtering algorithm gives us another story. The results for the prevalence of opinion A over time for an initial 20/80 opinion distribution in case of the PR filtering algorithm and making all the nodes partly stubborn are given in Fig. 5.14. If the nodes are not stubborn, the PR filtering algorithm reduces the prevalence of the minority opinion over time. Making the nodes more and more stubborn reduces this tendency. This result is more or less similar to the corresponding case in which a fraction of completely stubborn actors was introduced in the system (Fig. 5.10). The only difference is that making all the nodes partly stubborn seems to be less effective in reducing the decrease of the prevalence of the minority opinion compared to making a fraction of the nodes completely stubborn. For $r = 0.4$, the decrease of the prevalence of the minority opinion is almost not hampered, it is merely slowed down. All the nodes need to be really stubborn ($r = 0.8$) to see a hampering in the decrease of the prevalence of the minority opinion. Even then, the final prevalence of the minority opinion remains lower than for the case where a fraction of completely stubborn actors equal to $\text{fracRes} = 0.4$ was introduced ($P_A(500) = 0.064 \pm 0.017$ versus $P_A(500) = 0.099 \pm 0.009$, respectively).

5.2.2 The majority threshold model

In this subsection, the results of the majority threshold model are shared and discussed. This model is explained in Chapter 3, Section 3.5.2. We do not make use of a probabilistic majority model, but a classic majority model, as explained in Chapter 3, Section 3.1.1, is implemented. The rest of the model (filtering algorithms, activation mechanism,...) is unchanged and still follows the rules as stated in Chapter 4, Section 4.3. The activation probability is set equal to $p_{\text{act}} = 0.1$ and the maximum length of the actual time-line of the users is $S = 20$. The threshold parameter T is equal for all the nodes and varies between $T = 0$ and $T = 1$.

For this model we only investigate the case of balanced starting conditions. We focus on the formation of echo chambers versus the threshold parameter T and we compare three different filtering algorithms: the PR, REF and REC filtering algorithms.

Fig. 5.15 shows the formation of echo chambers versus the threshold parameter T for an initial 50/50 distribution. In this figure, the PR filtering algorithm is used. Data points are shown together with their standard deviation σ to emphasize on the spread in the data. The y -axis is interpreted in the same way as explained for Fig. 5.6 in Subsection 5.1.3.

The high clustering models (WS and SBM-WS) show a large formation of echo chambers, which remain more or less flat for $T \leq 0.5$. This makes sense, since for $T \leq 0.5$, the threshold has no effect. This is because the majority opinion of the neighbors of a node will always be larger than the threshold if $T \leq 0.5$ (the sum of the two opinion fractions is always equal to one, so the fraction of neighbors with the majority opinion will always take values between 0.5 and 1). If $T \geq 0.5$, it starts to have an effect. The nodes become more hesitant to change their opinion and the formation of echo chambers starts to decrease.

Similar observations can be made for the stochastic block model with a high modularity. The only difference is of a quantitative nature (the formation of echo chambers is not as large as for the high clustering networks).

The Erdős-Rényi network and the stochastic block model with a low modularity (data points lie behind those of the Erdős-Rényi network) do not enhance the formation of echo chambers in any way. Including a threshold T does not change this tendency.

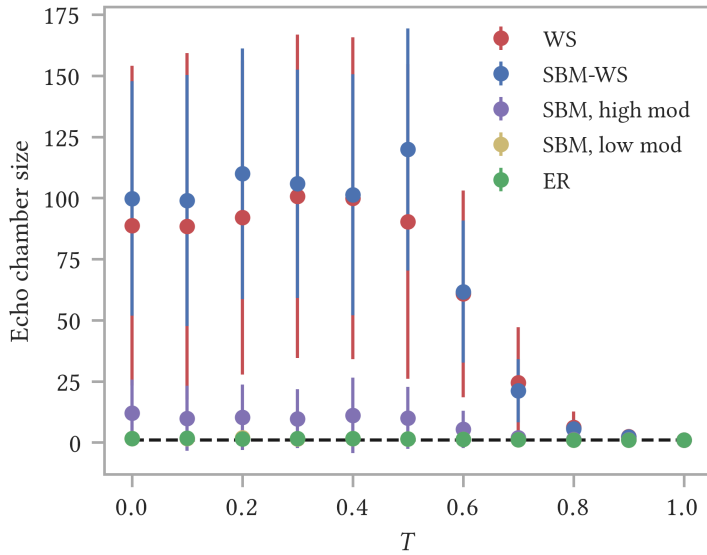


Figure 5.15: Formation of echo chambers versus the threshold parameter of all the nodes, T , for an initial 50/50 opinion distribution and using the PR filtering algorithm. The majority threshold model is implemented. The y -axis shows the average of the normalized fraction of nodes with all neighbors having opinion A and the normalized fraction of nodes with all neighbors having opinion B. This value represents the formation of echo chambers in the system (denoted with echo chamber size in the figure). Results are shown for four different network models, each with $N = 10^3$ and average degree $\langle k \rangle \sim 10$: WS with $\langle k \rangle = 10$, $\beta = 0.06$ and $\langle cc \rangle = 0.557 \pm 0.007$; SBM-WS with 10 communities of size 100, each community has the following WS parameters: $\langle k \rangle = 10$, $\beta = 0.01$ and $p_{\text{add}} = 0.001$, $\langle cc \rangle = 0.553 \pm 0.004$ and $Q = 0.909 \pm 0.004$; SBM with 10 communities of size 100, a high modularity case ($p_{\text{cl}} = 0.1$, $p_{\text{add}} = 0.001$, $Q = 0.908 \pm 0.005$) and a low modularity case ($p_{\text{cl}} = 0.03$, $p_{\text{add}} = 0.008$, $Q = 0.220 \pm 0.007$) are depicted; ER with $p = 0.01$. Each data point is the average of 10^2 independent simulations. Bars represent the standard deviation σ .

Fig. 5.16 shows the formation of echo chambers versus the threshold T for the REF (Fig. 5.16a) and REC (Fig. 5.16b) filtering algorithms. The initial opinion distribution is 50/50. The results for the REF and REC filtering algorithms resemble each other. Data points are again shown together with their standard deviation σ to emphasize the large spread in the data (the standard deviations are of the order $\sigma \sim 150$). These large errors are a result of the majority model. If we run the majority model once, the model forces the system to converge to a single opinion. To which of the two opinions the model converges is a matter of random fluctuations. On average, the opinion distribution will remain 50/50. However, each run the system converges to one of the two opinions, with the result that the number of echo

chambers around this opinion strongly increases. After the 10^2 independent simulations, the spread in the formation of echo chambers will be large, since there will have been simulations that converge to opinion B (and thus resulting in large echo chambers around opinion B) and there will have been simulations that converge to opinion A (resulting in almost no echo chambers around opinion B).

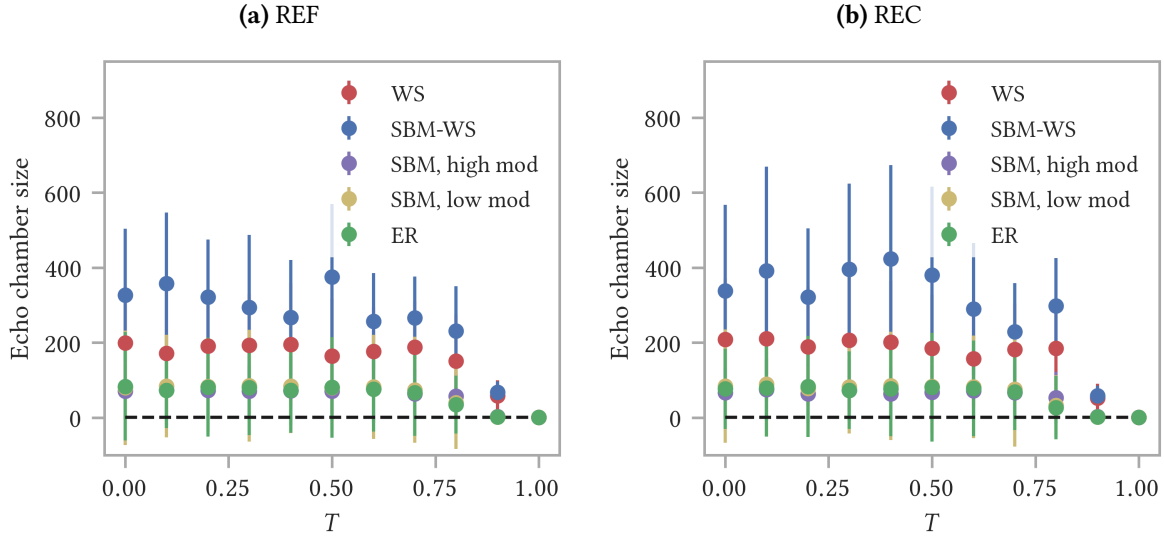


Figure 5.16: Formation of echo chambers versus the threshold parameter of all the nodes, T , for an initial 50/50 opinion distribution. The majority threshold model is implemented. **(a)** REF filtering algorithm; **(b)** REC filtering algorithm. The y -axis shows the average of the normalized fraction of nodes with all neighbors having opinion A and the normalized fraction of nodes with all neighbors having opinion B. This value represents the formation of echo chambers in the system (denoted with echo chamber size in the figure). Results are shown for four different network models, each with $N = 10^3$ and average degree $\langle k \rangle \sim 10$: WS with $\langle k \rangle = 10$, $\beta = 0.06$ and $\langle cc \rangle = 0.557 \pm 0.007$; SBM-WS with 10 communities of size 100, each community has the following WS parameters: $\langle k \rangle = 10$, $\beta = 0.01$ and $p_{\text{add}} = 0.001$, $\langle cc \rangle = 0.553 \pm 0.004$ and $Q = 0.909 \pm 0.004$; SBM with 10 communities of size 100, a high modularity case ($p_{\text{cl}} = 0.1$, $p_{\text{add}} = 0.001$, $Q = 0.908 \pm 0.005$) and a low modularity case ($p_{\text{cl}} = 0.03$, $p_{\text{add}} = 0.008$, $Q = 0.220 \pm 0.007$) are depicted; ER with $p = 0.01$. Each data point is the average of 10^2 independent simulations. Bars represent the standard deviation σ .

Another consequence of this converging to one of the two opinions every single simulation, is the fact that the Erdős-Rényi network and the stochastic block model with a low modularity show a strong appearance of echo chambers for $T \leq 0.5$. This is not due to any network features, but a direct consequence of the usage of the majority model. As explained above, each simulation the system converges to one of the two opinions with as result a strong increase in the echo chambers around that opinion (as a matter of fact the whole system becomes kind of a huge, single echo chamber). The PR filtering algorithm seems to hamper this convergence to one opinion each run and hence, this artificial creation of echo chambers. This can be seen in Fig. 5.15 where the ER and the SBM with a low modularity do not show any creation of opinion clusters. Also note that the standard deviations when using the PR filtering algorithm are significantly smaller (of the order $\sigma \sim 50$) than those when using the REC/REF filtering algorithms. This is another indication that the PR filtering algorithm hampers the convergence

to a single opinion each simulation. If $T \geq 0.5$, it starts to have an impact. However, in Fig. 5.16 the effect of the threshold does not become visible until $T > 0.8$, after which we see a decrease in the formation of the echo chambers for all the network models until the echo chambers size reaches values equal to one for $T = 1$. At this point, none of the nodes can be convinced of another opinion and hence all the nodes keep their initial opinion. The number of echo chambers does not change over time, which results in an echo chamber size equal to one in the figure. A constant amount of echo chambers over time is represented by the black dotted line.

Fig. 5.17 illustrates the particular behavior of the majority model more clearly. The figure shows the evolution of the prevalence of opinion A for a single simulation (we always chose results that show an increase in the fraction of nodes with opinion A; the reason for this is that it makes a comparison of the results easier and more clear; it must however be emphasized that every simulation there is an equal probability of converging to opinion A as to opinion B, the opinion to which the system eventually converges is a consequence of random fluctuations). The figure shows the results for each of the four network models: ER, WS, SBM (high and low modularity) and SBM-WS. For each model the REC and PR filtering algorithms are compared. The threshold parameter is set equal to $T = 0$, so there is no effect of stubbornness.

The PR filtering algorithm hampers the convergence to a single opinion each independent simulation. Furthermore, the high clustering networks (WS and SBM-WS) hinder the convergence to one opinion, even for the REC filtering algorithm. This may indicate that a high clustering is a protective factor against the convergence to one opinion each independent simulation in case of the majority model. Having a clear community structure (high modularity) in case of the stochastic block model seems to be another hindering of this convergence, as can be seen in Fig. 5.17c. For the REC filtering algorithm, the high modularity stochastic block model converges to lower values than the low modularity stochastic block model. For the PR filtering algorithm, this is not really the case, but this is probably due to the fact that the PR filtering algorithm already strongly hampers the convergence to a single opinion; having a high or low modularity does not give an additional effect on top of this PR filtering effect.

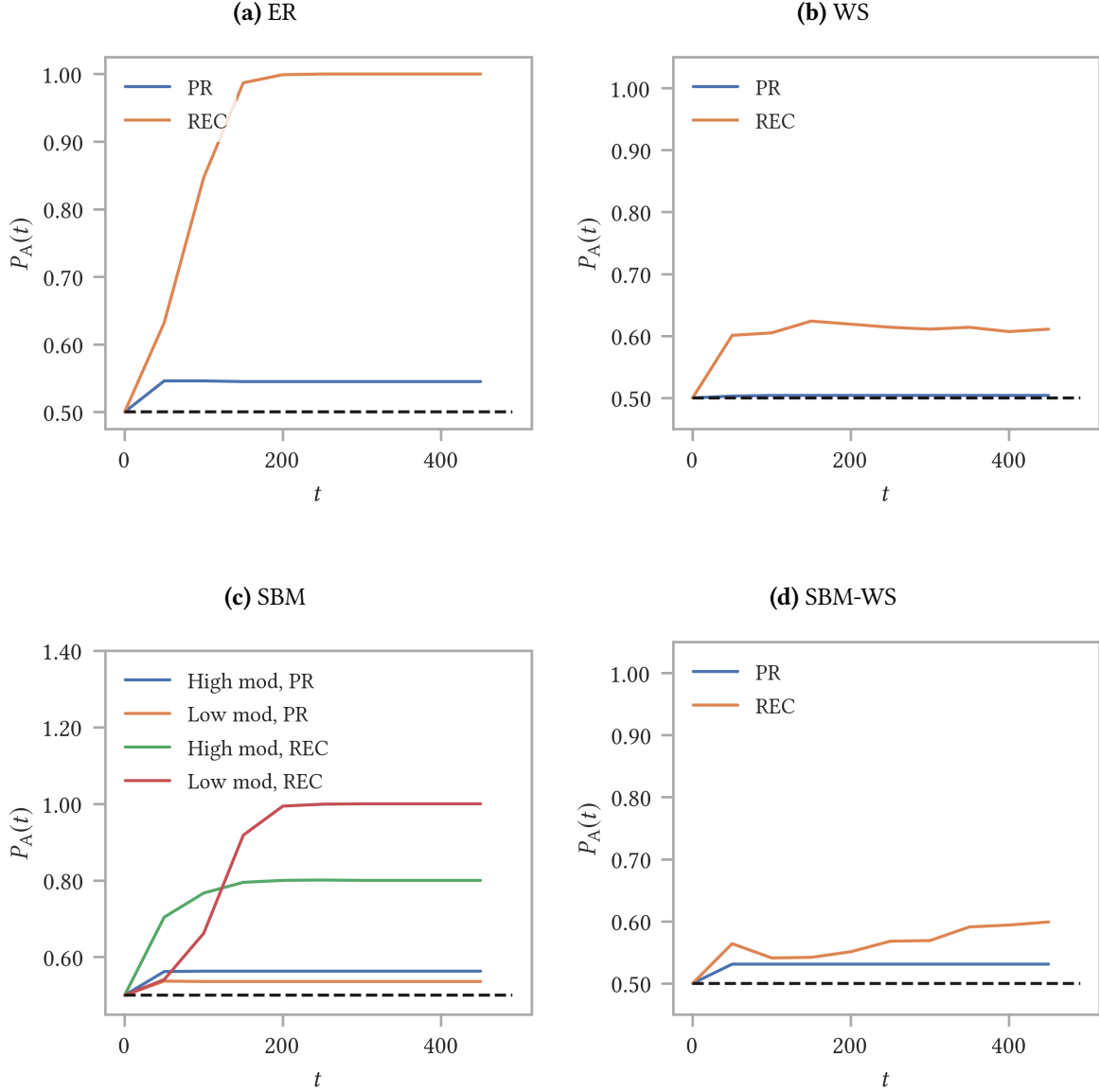


Figure 5.17: Evolution of the prevalence of opinion A ($P_A(t)$) over time for an initial 50/50 distribution. The majority threshold model is implemented with $T = 0$ and results are shown for a single simulation. Four different network models are used, each with average degree $\langle k \rangle \sim 10$ and $N = 10^3$: **(a)** ER, $p = 0.01$; **(b)** WS with $\langle k \rangle = 10$, $\beta = 0.06$ and $\langle cc \rangle = 0.557 \pm 0.007$; **(c)** SBM with 10 communities of size 100, a high modularity case ($p_{cl} = 0.1$, $p_{add} = 0.001$, $Q = 0.908 \pm 0.005$) and a low modularity case ($p_{cl} = 0.03$, $p_{add} = 0.008$, $Q = 0.220 \pm 0.007$) are depicted; **(d)** SBM-WS with 10 communities of size 100, each community has the following WS parameters: $\langle k \rangle = 10$, $\beta = 0.01$ and $p_{add} = 0.001$, $\langle cc \rangle = 0.553 \pm 0.004$ and $Q = 0.909 \pm 0.004$. For each model the REC and the PR filtering algorithms are compared.

5.3 Random versus community distributed opinions

This section is devoted to results regarding the way the opinions are distributed over the network. In all the previous results, the two opinions were, initially, randomly distributed across the network. It might however be more realistic if people with the same opinion are more or less grouped together initially. We did introduce a network model with a community structure (the SBM) to represent the group structures found in real-life systems. But we have not yet distributed the opinions according to those groups.

We study the stochastic block model (SBM) and we give a fraction of the communities a single opinion, namely opinion A. The remaining communities are given a 50/50 opinion distribution. This situation may, in an idealized way, represent the situation in which you have groups of people following the same idea together with groups where the two ideas coexist. The total opinion distribution over the entire network is no longer 50/50, but instead opinion A becomes the majority opinion (hence, opinion B becomes the minority opinion). The higher the fraction of single opinion A communities, the bigger the difference between this majority and minority opinion. The results will be compared to the corresponding case in which the total opinion distribution is randomly distributed over each community. Thus, eg. if we have 10 communities of size 100 and we make 10% of those communities single opinion A communities while the others get a 50/50 distribution, the total initial opinion distribution is 55/45. This situation is then compared to the case in which this 55/45 distribution is randomly distributed over each community.

We will study a network with a high modularity, representing the case of more or less isolated communities, and a network with a low modularity, representing a more blended community structure in which there is a lot of communication between the different communities. More specifically, the two stochastic block models that are implemented are: (i) SBM with 10 communities of size 100 with $p_{cl} = 0.1$ and $p_{add} = 0.001$ ($Q = 0.908 \pm 0.005$); and (ii) SBM with 10 communities of size 100 with $p_{cl} = 0.03$ and $p_{add} = 0.008$ ($Q = 0.220 \pm 0.007$). Both networks have a total number of nodes $N = 10^3$ and average degree $\langle k \rangle = 10.79 \pm 0.14$ and $\langle k \rangle = 10.17 \pm 0.14$, respectively.

The opinion dynamics model is described in Chapter 4, Section 4.3. The activation probability is set equal to $p_{act} = 0.1$ and the maximum length of the actual time-line is $S = 20$.

In subsection 5.3.1 we will discuss the results for the evolution of the prevalence of the opinions. Sub-section 5.3.2 will discuss the formation of echo chambers.

5.3.1 Evolution of the prevalence of the opinions

First, we discuss how the evolution of the opinions are impacted by distributing the opinions in communities instead of randomly distributing them.

Fig. 5.18 shows the results for the prevalence of opinion A versus time. A fraction equal to 0.1 of the communities is given a single opinion, opinion A, while the other communities get an initial 50/50 opinion distribution. The results are compared to the random case in which each community initially gets the corresponding total opinion distribution (55/45 in this case). The figure shows the results for

both the high and the low modularity case. For each modularity the REC and PR filtering algorithms are compared.

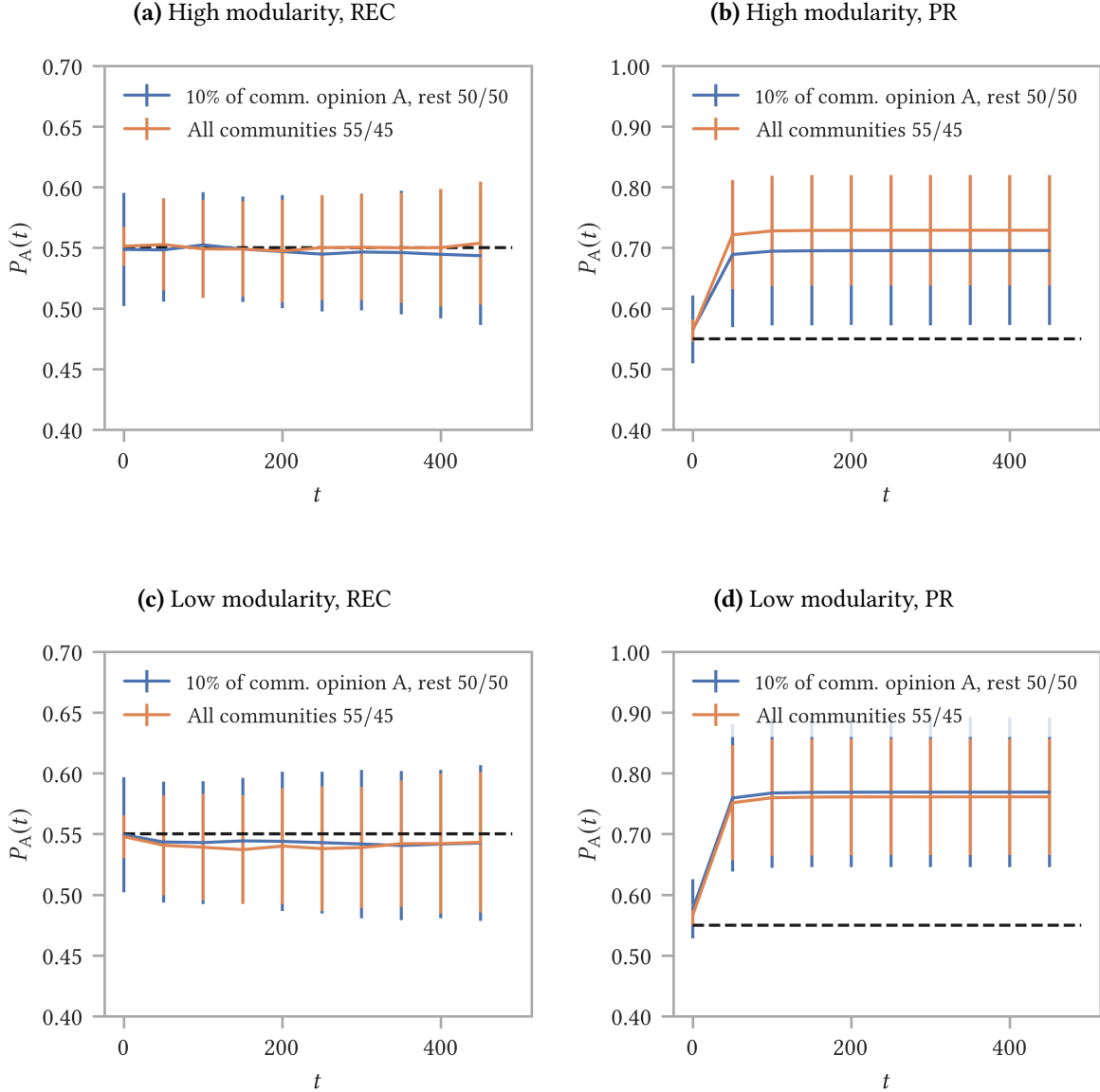


Figure 5.18: Evolution of the prevalence of opinion A ($P_A(t)$) over time for making a fraction equal to 0.1 of the communities single opinion A communities, while the others get an initial 50/50 opinion distribution. Results are compared to the case where the total initial opinion distribution (55/45) is randomly distributed over each community. The stochastic block model with 10 communities of size 100 is implemented with two different modularities: $Q = 0.908 \pm 0.005$ with $p_{cl} = 0.1$, $p_{add} = 0.001$, $\langle k \rangle = 10.79 \pm 0.14$ and $Q = 0.220 \pm 0.007$ with $p_{cl} = 0.03$, $p_{add} = 0.008$, $\langle k \rangle = 10.17 \pm 0.14$. $N = 10^3$ for both modularities. **(a)** High modularity, REC; **(b)** High modularity, PR; **(c)** Low modularity, REC; **(d)** Low modularity, PR. Each curve is the average of 10^2 independent simulations and data points are shown every 50 time steps to improve visualization. Bars represent the standard deviation σ .

In case of the REC filtering algorithm there is no difference between distributing the opinions randomly versus distributing them in communities. The prevalence of the majority opinion A remains unchanged over time. This result is the same for both the high and low modularity case, see Fig. 5.18a and Fig. 5.18c.

The PR filtering algorithm leads to an increase in the prevalence of the majority opinion in case of unbalanced starting conditions and if the opinions are randomly distributed. This is a result that was found in Section 5.1, Subsection 5.1.2, see eg. Fig. 5.3. If a fraction equal to 0.1 of the communities is given one opinion, opinion A, while the remaining communities get a 50/50 opinion distribution, we see from Fig. 5.18b that, in case of the high modularity network, the increase in the majority opinion is hampered compared to the randomly distributed case. This makes sense, since the single opinion communities are more or less isolated from the mixed opinion communities. This has as consequence that the mixed opinion communities live under the assumption that the opinion distribution is 50/50. They do not really feel that opinion A is a majority opinion, since they are isolated from these single opinion A communities. In case of the low modularity network, Fig. 5.18d, this isolation argument of the different communities no longer holds. This is also visible in the results since the hampering in the increase of the majority opinion is no longer present. The community distributed case behaves equivalent to the random distributed case. In the low modularity network, the community structure is not clearly present, but becomes blended. The different communities talk a lot to each other and there is a lot of communication between them. As a consequence, the mixed opinion communities clearly feel the presence of the single opinion communities and hence feel the majority of opinion A in the same way as if the opinions would be randomly distributed over the communities.

The results found in Fig. 5.18 for 10% of single opinion A communities remain valid if we increase the fraction of single opinion A communities. This can be seen in Fig. 5.19, which depicts the average prevalence of opinion A before (solid black line) and after (dotted lines) the time evolution versus the fraction of single opinion A communities. The community distributed cases are compared to the corresponding randomly distributed cases. Results are shown for both a high modularity and a low modularity network. Fig. 5.19a shows the results for the REC filtering algorithm. Fig. 5.19b shows those for the PR filtering algorithm.

The higher the fraction of single opinion A communities, the higher the initial average prevalence of opinion A. This is seen in both figures by the increase of the solid black line, which represents the initial prevalence of opinion A. In case of the REC filtering algorithm (Fig. 5.19a) the prevalence of opinion A remains the same before and after the time evolution for a fixed fraction of single opinion A communities. Giving a fraction of the communities a single opinion, opinion A, and the others an initial 50/50 opinion distribution does not make a difference compared to randomly distributing the same total initial opinion distribution. This result is valid for both the high and low modularity case.

The PR filtering algorithm (Fig. 5.19b) shows an increase in the prevalence of opinion A over time for a fixed fraction of single opinion A communities. Making a fraction of the communities single opinion A communities, while the other communities get a 50/50 opinion distribution, hampers this increase compared to the corresponding randomly distributed case, if we are dealing with a high modularity network with a clear and almost isolated community structure. The low modularity network

does not exhibit this hampering. The reason for this hampering in case of the high modularity network and the absence of it for the low modularity network was explained for Fig. 5.18 and has to do with whether or not the single opinion A communities can influence the 50/50 communities.

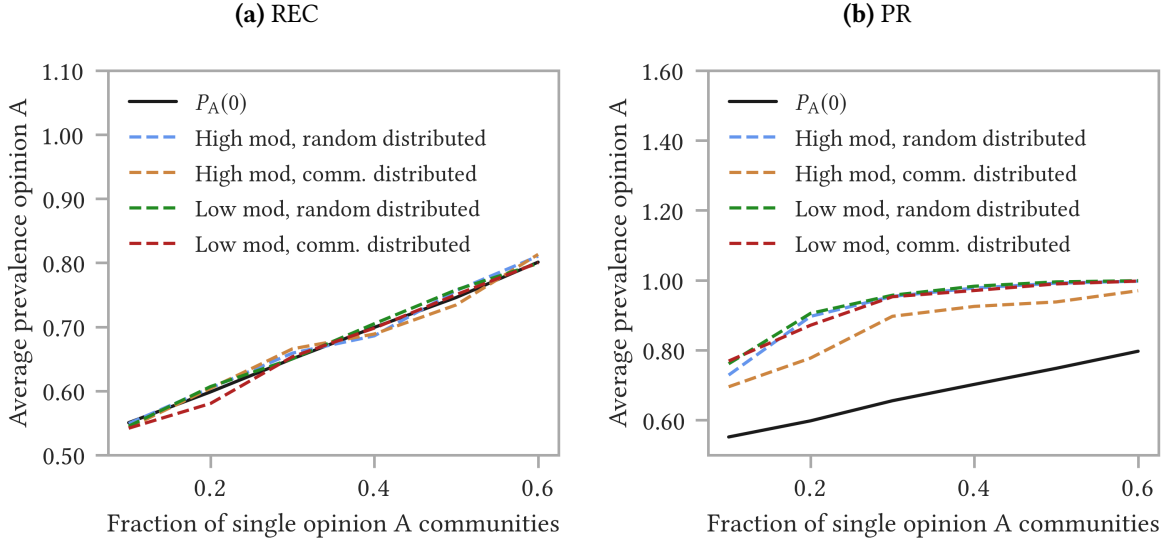


Figure 5.19: Average prevalence of opinion A before and after the time evolution versus the fraction of single opinion A communities. Community distributed cases are compared to the corresponding randomly distributed cases for both a high modularity ($Q = 0.908 \pm 0.005$ with $p_{cl} = 0.1$, $p_{add} = 0.001$ and $\langle k \rangle = 10.79 \pm 0.14$) and a low modularity ($Q = 0.220 \pm 0.007$ with $p_{cl} = 0.03$, $p_{add} = 0.008$ and $\langle k \rangle = 10.17 \pm 0.14$), both with $N = 10^3$. **(a)** REC filtering algorithm; **(b)** PR filtering algorithm. Each curve is the average of 10^2 independent simulations. Error bars are omitted for an improved visualization.

5.3.2 Echo chambers

We will investigate the effect of community distributing the opinions versus randomly distributing them on the formation of echo chambers.

Fig. 5.20 shows the distribution of the fraction of friends (nearest neighbors, nn) of node i with the same opinion B at $t = 500$ for the case where a fraction equal to 0.1 of the communities is made a single opinion A community while the other communities get an initial 50/50 opinion distribution. The value shown on the y -axis, $F_N(\langle P_1^{nn} \rangle)$, represents the result of dividing the average distribution of opinions in each neighborhood at $t = 500$ by its corresponding value at $t = 0$. The community distributed case is compared to the corresponding randomly distributed case (which is, in this case, an initial 55/45 opinion distribution). The formation of echo chambers in both the high and low modularity network are investigated. The REC and PR filtering algorithms are compared.

The results for the REC filtering algorithm are depicted in Fig. 5.20a. The community distributed case for the high modularity network shows a decrease in the formation of echo chambers around the majority opinion A (leftmost region on the x -axis, where the blue line drops under 1), with as re-

sult an increase in more mixed neighborhoods (bump in the blue line). The number of neighborhoods where all the nodes carry opinion A decreases in favor of neighborhoods where we find both nodes with opinion A and nodes with opinion B. Even though there is only a minor communication between the communities, this limited communication has the effect that the high number of echo chambers at $t = 0$, due to the fraction of single opinion A communities, reduces and that the opinions become more mixed. The prevalence of opinion A remains constant over time when using the REC filtering algorithm (Fig. 5.18a). The communities with the single opinion A see, however, a decrease in the prevalence of opinion A and become more mixed. We also observe a small increase in the number of echo chambers around the minority opinion B. This indicates that the minority opinion starts to group together. The randomly distributed case for the high modularity network shows an increase in both the echo chambers around opinion A and opinion B. Again, the opinion fractions remain constant over time, but are shifted from a random distribution to a more clustered situation. The increase remains however smaller than two, which indicates that there are less than twice as much echo chambers at $t = 500$ than at $t = 0$.

The community distributed case for the low modularity network does not really show a decrease in the formation of echo chambers around opinion A (which was observed for the community distributed, high modularity case). This is due to the fact that the number of echo chambers around opinion A at $t = 0$, originating from the fraction of single opinion A communities, is smaller for the low modularity network than for the high modularity network. The reason is the more blended community structure for the low modularity network. We still observe a small increase in the number of echo chambers around opinion B. This increase in the formation of echo chambers around the minority opinion B seems however hampered compared to the randomly distributed case. Remember that the increase in the number of echo chambers around the minority opinion for the SBM in combination with the REC filtering algorithm for unbalanced starting conditions that are randomly distributed was observed in Section 5.1, Subsection 5.1.2 (Fig. 5.5c).

The results for the PR filtering algorithm are depicted in Fig. 5.20b. They are different from those obtained with the REC filtering algorithm, which we just discussed and which are depicted in Fig. 5.20a.

Lets first focus on the high modularity network. The randomly 55/45 distributed case strongly resembles the results for the stochastic block model in combination with the PR filtering algorithm obtained in Section 5.1, Subsection 5.1.2, Fig. 5.5c (these results were obtained for an initial 20/80 opinion distribution). We observe a strong increase in the formation of echo chambers around the majority opinion A, with a corresponding decrease in all the neighborhoods that have a fraction of nodes with the minority opinion B. Remember from Fig. 5.18b that the PR filtering algorithm leads to an increase in the majority opinion A. If we, however, make 10% of the communities single opinion A communities while giving the remaining ones a 50/50 opinion distribution, we see that this increase in the formation of echo chambers around the majority opinion A is strongly hampered. This hampering is partly an artifact of the way the opinions are distributed. If we give entire communities only opinion A while others get a 50/50 distribution, we have a large number of echo chambers around opinion A at $t = 0$ due to these single opinion communities. Moreover, the number of opinion A echo chambers at $t = 0$ is higher than in the corresponding randomly distributed case. If we, however, would look at the absolute number of echo chambers around opinion A at $t = 500$, we would see that this number is lower for the commu-

nity distributed case than for the randomly distributed case. This shows that the observed hampering of the formation of echo chambers around the majority opinion A in the community distributed case compared to the randomly distributed case is a result of more than just an increase in the initial number of echo chambers. Remember from Fig. 5.18b that the high modularity, community distributed case hampers the increase of the majority opinion A (and thus the decrease of the minority opinion B); this hampering is probably one of the reasons for the lower absolute number of echo chambers around the majority opinion at $t = 500$ for the community distributed case versus the random distributed case. Beside this hampering of echo chambers around the majority opinion A, the community distributed case also shows an increase of echo chambers around the minority opinion B (which is not visible for the randomly distributed case). This may also be a consequence of the hampering in the decrease of the minority opinion for the community distributed case; hence, a significant fraction of minority opinion nodes (around 30%) is able to survive and they group together in opinion clusters.

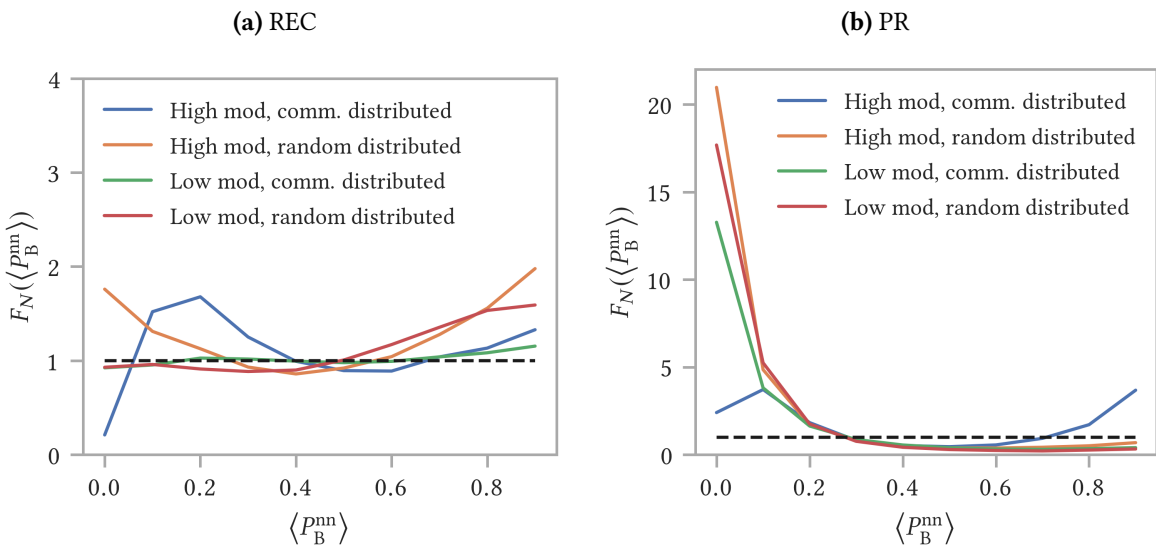


Figure 5.20: Distribution of the fraction of friends (nearest neighbors, nn) of node i with the same opinion B at $t = 500$. The distribution is normalized by dividing for the same quantity computed at $t = 0$. 10% of the communities is given a single opinion, opinion A, while the remaining communities get an initial 50/50 opinion distribution. The community distributed case is compared to the corresponding randomly distributed case (55/45) for both a high modularity ($Q = 0.908 \pm 0.005$ with $p_{\text{cl}} = 0.1$, $p_{\text{add}} = 0.001$ and $\langle k \rangle = 10.79 \pm 0.14$) and a low modularity ($Q = 0.220 \pm 0.007$ with $p_{\text{cl}} = 0.03$, $p_{\text{add}} = 0.008$ and $\langle k \rangle = 10.17 \pm 0.14$), both with $N = 10^3$. **(a)** REC filtering algorithm; **(b)** PR filtering algorithm. Each curve is the average of 10^2 independent simulations. Error bars are omitted for an improved visualization.

The low modularity network does not show such a discrepancy between the formation of echo chambers in the community distributed and the random distributed cases, as was observed for the high modularity network. Moreover the two cases show qualitatively the same behavior in the formation of echo chambers, with an increase in the number of echo chambers around the majority opinion A and a corresponding decrease in all the neighborhoods where a fraction of the nodes carry the minority opinion B. From Fig. 5.18d, it was made clear that, in case of the low modularity network, both the random

distributed and the community distributed case lead to a significant decrease of the minority opinion (when using the PR filtering algorithm). This decrease of the minority opinion is now also visible in the decrease of neighborhoods where a fraction of the nodes carry the minority opinion. The quantitative difference between the community distributed case and the randomly distributed case (smaller formation of echo chambers around the majority opinion for the former compared to those for the latter) lies partly in the slightly higher number of initial echo chambers around the majority opinion for the community distributed case. However, as for the high modularity case, if we would look at the absolute number of echo chambers around the majority opinion at $t = 500$, we would see that this number is lower for the community distributed case than for the randomly distributed case.

Fig. 5.21 shows a similar plot as Fig. 5.20. 50% of the communities is given opinion A, while the others get a 50/50 distribution. The results look more or less the same as for the case where 10% of the communities is given opinion A (Fig. 5.20).

The REC filtering algorithm, Fig. 5.21a, shows a decrease in the number of echo chambers around the majority opinion A with a corresponding increase in more mixed opinion neighborhoods for the community distributed, high modularity case. A difference with the case where 10% of the communities are single opinion A communities, is the fact that we no longer see an increase in the formation of echo chambers around the minority opinion B. Instead we observe a decrease in the number of echo chambers around the minority opinion. For the REC filtering algorithm, the initial opinion distribution remains unchanged, but we see that the opinions reorganize in such a way that the final situation mostly has mixed opinion neighborhoods with the majority of the nodes carrying the majority opinion A and a minority of the nodes carrying the minority opinion B.

The low modularity, community distributed case seems to wiggle around 1. If we look closely, we see that the results qualitatively resemble those for the high modularity, community distributed case (albeit with quantitative values that are a lot smaller). We observe a small decrease in the formation of echo chambers around the majority opinion A, with a small increase in more mixed opinion neighborhoods as result. We also observe a small decrease in the number of echo chambers around the minority opinion B. The REC filtering algorithm seems to force the system towards a more uniformly mixed opinion distribution in the case of 50% of the communities being single opinion A communities, while the others get a 50/50 opinion distribution.

The randomly distributed cases for both the high and low modularity strongly resemble the results for an initial, randomly distributed 20/80 opinion distribution depicted in Fig. 5.5c, see Section 5.1, Subsection 5.1.2. They show a small increase in the formation of echo chambers around the minority opinion, indicating the clustering of the nodes that carry this opinion.

Results for the PR filtering algorithm also strongly resemble those depicted in Fig. 5.20b, which were obtained for a fraction equal to 0.1 of single opinion A communities. The randomly distributed cases for both the high and low modularity are quite similar to those depicted in Fig. 5.5c for an initial, random 20/80 opinion distribution (see Section 5.1, Subsection 5.1.2). They show a strong increase in the formation of echo chambers around the majority opinion A.

The low modularity, community distributed case shows a small hampering in the increase of echo chambers around the majority opinion A, which was also observed in Fig. 5.20b.

The high modularity, community distributed case shows an even stronger hampering in the increase of echo chambers around the majority opinion A. This was also observed in Fig. 5.20b and is partly due to the fact that, for a high modularity network, giving a fraction of the communities a single opinion, namely opinion A, hampers the increase in this majority opinion compared to the randomly distributed case (Fig. 5.18b and Fig. 5.19b). The increase in the number of echo chambers around the minority opinion A that was visible in Fig. 5.20b is no longer present.

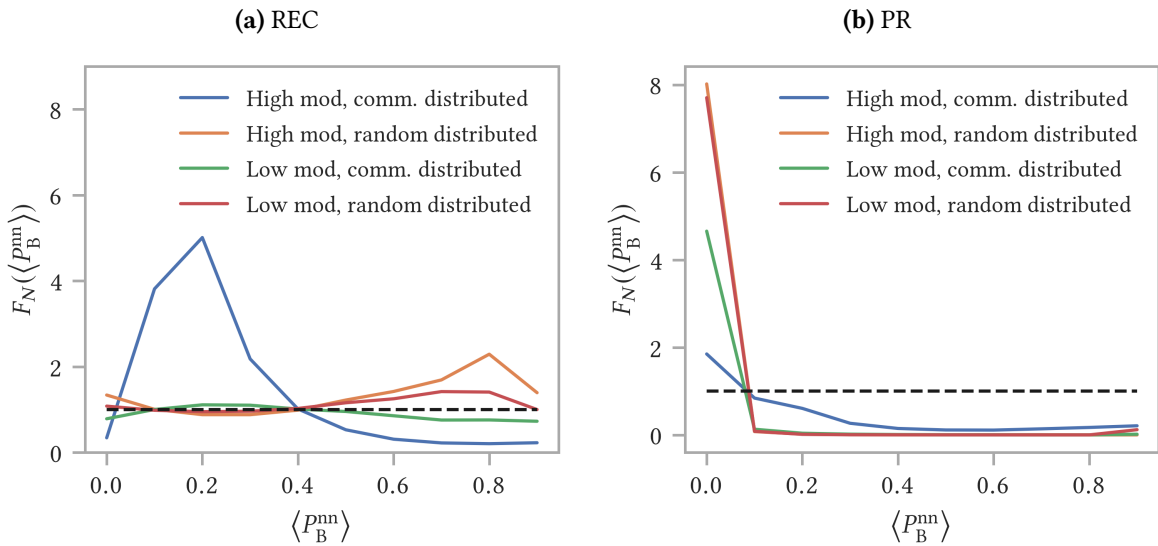


Figure 5.21: Distribution of the fraction of friends (nearest neighbors, nn) of node i with the same opinion B at $t = 500$. The distribution is normalized by dividing for the same quantity computed at $t = 0$. 50% of the communities is given a single opinion, opinion A, while the remaining communities get an initial 50/50 opinion distribution. The community distributed case is compared to the corresponding randomly distributed case (75/25) for both a high modularity ($Q = 0.908 \pm 0.005$ with $p_{\text{cl}} = 0.1$, $p_{\text{add}} = 0.001$ and $\langle k \rangle = 10.79 \pm 0.14$) and a low modularity ($Q = 0.220 \pm 0.007$ with $p_{\text{cl}} = 0.03$, $p_{\text{add}} = 0.008$ and $\langle k \rangle = 10.17 \pm 0.14$), both with $N = 10^3$. **(a)** REC filtering algorithm; **(b)** PR filtering algorithm. Each curve is the average of 10^2 independent simulations. Error bars are omitted for an improved visualization.

5.4 Real-world networks

The results of the two real-world networks: (i) the Last.fm on-line social network; and (ii) the PGP trust network, discussed in Chapter 4, Section 4.2, will be shared and discussed. For each real-world network, the results will be compared to results obtained from network models with similar average degree, clustering and/or modularity. We will mainly focus on the formation of echo chambers. We will only study balanced initial conditions and we will introduce a fraction of completely stubborn actors. For both real-world networks, the REC and PR filtering algorithms will be compared.

5.4.1 The Last.fm on-line social network

The formation of echo chambers versus the fraction of completely stubborn actors, fracRes , in the Last.fm on-line social network is studied. The results are compared to corresponding results from network models, all with $N = 8003$: (i) the Watts-Strogatz model with $\langle k \rangle = 4$, $\beta = 0.15$ and $\langle cc \rangle = 0.317 \pm 0.004$; (ii) the stochastic block model with 53 communities of size 151, $p_{\text{cl}} = 0.023$, $p_{\text{add}} = 0.0001$, $\langle k \rangle = 4.24 \pm 0.03$ and $Q = 0.811 \pm 0.004$; (iii) the stochastic Watts-Strogatz block model with 53 communities of size 151, each community has the following Watts-Strogatz parameters: $\langle k \rangle = 4$, $\beta = 0.025$; edges are added between communities with probability $p_{\text{add}} = 0.0001$, $\langle k \rangle = 4.77 \pm 0.01$, $\langle cc \rangle = 0.344 \pm 0.002$ and $Q = 0.833 \pm 0.003$. The results for the PR and REC filtering algorithms are shown in Fig. 5.22.

The PR filtering algorithm shows a decrease in the formation of echo chambers with an increasing fraction of stubborn actors. This is valid for both the real-world network and the network models. The stochastic Watts-Strogatz block model has similar clustering and modularity as the Last.fm network. The Last.fm network has, however, a smaller formation of echo chambers than the SBM-WS. This suggests that it is not only clustering and/or modularity that drives the formation of echo chambers. Other topologies must play a role as well. The biggest difference between the real-world Last.fm network and the stochastic Watts-Strogatz block model lies in the degree distribution: the Last.fm network has a heterogeneous degree distribution instead of a homogeneous degree distribution. It is probably this heterogeneous contact pattern that hampers the formation of echo chambers in the real-world network compared to a network model with similar clustering and modularity, but with a homogeneous degree distribution. This agrees with the result that Perra and Rocha [66] found: a heterogeneous contact pattern hampers the formation of echo chambers.

Another difference between the Last.fm and the SBM and SBM-WS network is the community structure. The Last.fm network has a community structure where the community sizes follow a heterogeneous distribution: plenty of small communities and a few large ones. The stochastic block model and stochastic Watts-Strogatz block model, that we used, only have communities of a single size. This does, however, not play a significant role in the formation of echo chambers, as can be seen in Fig. 5.23. In this figure, the distribution of echo chambers in the Last.fm network is compared to those in the SBM-WS network with similar clustering and modularity. The SBM-WS is modeled in two ways: (i) the communities all have a fixed size; (ii) the communities have the same heterogeneous sizes as in the Last.fm network. The PR and REC filtering algorithms are compared.

The results for the Watts-Strogatz model are similar to those for the stochastic Watts-Strogatz block model. The formation of echo chambers seems to be slightly smaller in the WS than in the SBM-WS network. It may be tempting to attribute this to the lack of community structure in the WS model. It must however be noted that the implemented WS model has a slightly smaller clustering coefficient ($\langle cc \rangle = 0.317 \pm 0.004$) than the SBM-WS ($\langle cc \rangle = 0.344 \pm 0.002$), which may also explain the somewhat smaller formation of echo chambers. Furthermore, it is interesting to notice that the Last.fm on-line social network coincides with the SBM with a similar modularity. It seems that the hampering of the formation of echo chambers due to a heterogeneous contact pattern is of the same size as the hampering due to a lack of high clustering.

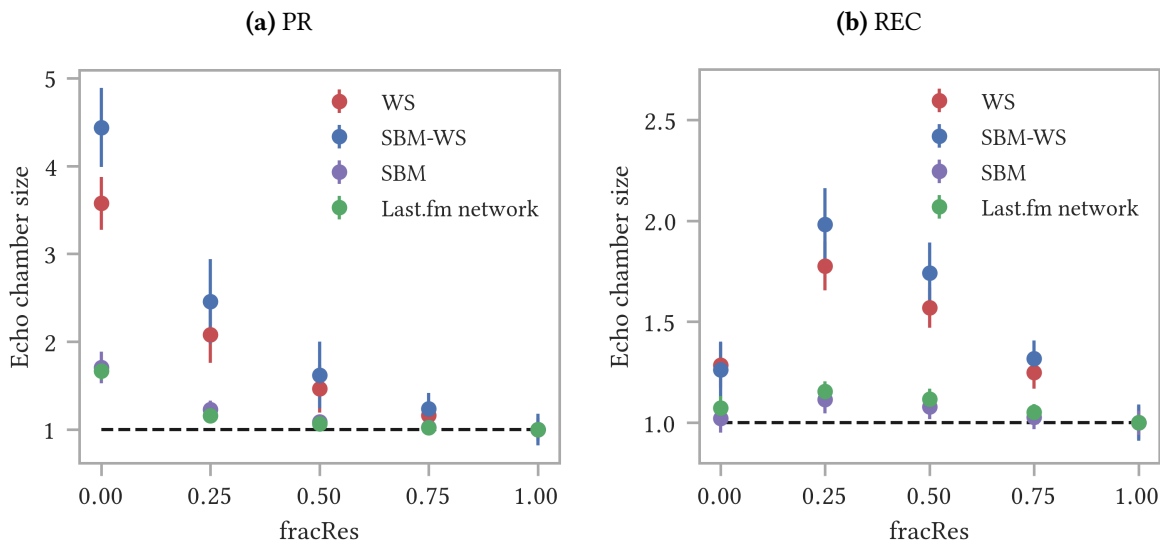


Figure 5.22: Formation of echo chambers versus the fraction of completely stubborn actors, $fracRes$, for an initial 50/50 opinion distribution. The Last.fm on-line social network is compared to corresponding network models: (i) WS with $\langle k \rangle = 4$, $\beta = 0.15$ and $\langle cc \rangle = 0.317 \pm 0.004$; (ii) SBM-WS with 53 communities of size 151, each community has the following Watts-Strogatz parameters: $\langle k \rangle = 4$, $\beta = 0.025$; edges are added between communities with probability $p_{add} = 0.0001$, $\langle k \rangle = 4.77 \pm 0.01$, $\langle cc \rangle = 0.344 \pm 0.002$ and $Q = 0.833 \pm 0.003$; (iii) SBM with 53 communities of size 151 with $p_{cl} = 0.023$, $p_{add} = 0.0001$, $\langle k \rangle = 4.24 \pm 0.03$ and $Q = 0.811 \pm 0.004$. **(a)** PR filtering algorithm; **(b)** REC filtering algorithm. The y -axis shows the average of the normalized fraction of nodes with all neighbors having opinion A and the normalized fraction of nodes with all neighbors having opinion B. This value represents the formation of echo chambers in the system (denoted with echo chamber size in the figure). Each data point is the average of 50 independent simulations. Bars represent the standard deviation σ .

The REC filtering algorithm enforces an increase in the formation of echo chambers when a small fraction of stubborn actors is introduced. If this fraction is further increased, the formation of echo chambers starts to decrease. The increase is the strongest for the high clustering network models (WS, SBM-WS). Even though the Last.fm network has a similar clustering as these high clustering models, the formation of echo chambers and the corresponding increase in that formation are significantly smaller. As for the PR filtering algorithm, this is probably a consequence of the heterogeneous degree pattern of the Last.fm network. The results for the Last.fm network coincide with those of the SBM.

This seems to suggest that the hampering in the formation of echo chambers due to a heterogeneous degree distribution is of a similar size as the hampering due to the lack of clustering.

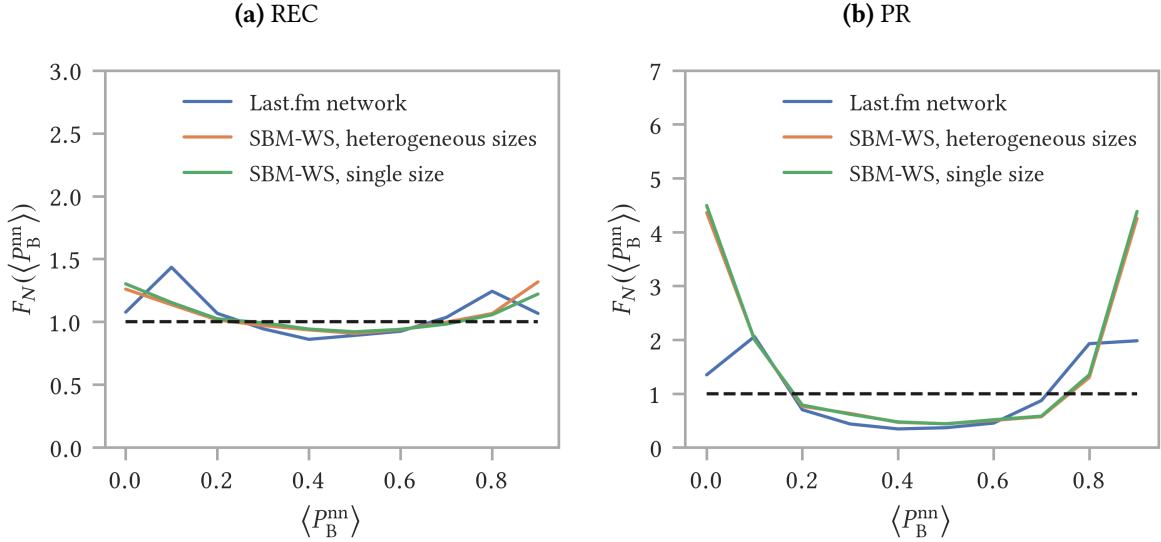


Figure 5.23: Distribution of the fraction of friends (nearest neighbors, nn) of node i with the same opinion B at $t = 500$. The distribution is normalized by dividing for the same quantity computed at $t = 0$. The SBM-WS with heterogeneous community sizes is compared to the SBM-WS with a single community size. Results are compared to the real-world Last.fm network with similar clustering and modularity. **(a)** REC filtering algorithm; **(b)** PR filtering algorithm. Each curve is the average of 50 independent simulations. Error bars are omitted for an improved visualization.

5.4.2 The PGP trust network

Results for the PGP trust network are compared to results for network models with similar average degree, clustering and/or modularity. The used network models are, all with $N = 10680$: (i) the Watts-Strogatz model with $\langle k \rangle = 4$, $\beta = 0.2$ and $\langle cc \rangle = 0.266 \pm 0.003$; (ii) the stochastic block model with 60 communities of size 178, $p_{cl} = 0.02$, $p_{add} = 0.00005$, $\langle k \rangle = 4.06 \pm 0.02$ and $Q = 0.868 \pm 0.002$; (iii) the stochastic Watts-Strogatz block model with 60 communities of size 178, each community has the following Watts-Strogatz parameters: $\langle k \rangle = 4$, $\beta = 0.12$; edges are added between communities with probability $p_{add} = 0.00007$, $\langle k \rangle = 4.74 \pm 0.01$, $\langle cc \rangle = 0.263 \pm 0.003$ and $Q = 0.842 \pm 0.002$.

In Fig. 5.24 the formation of echo chambers versus the fraction of completely stubborn actors (fracRes) is studied for the real-world PGP trust network and for the corresponding network models. This is done for both the PR and REC filtering algorithms.

The PR filtering algorithm (Fig. 5.24a) shows a decrease in the formation of echo chambers with an increasing fraction of completely stubborn actors for both the PGP trust network and the corresponding network models. The real-world PGP network has a significantly smaller formation of echo chambers compared to the network model with similar clustering and modularity (SBM-WS). This is most likely due to the heterogeneous degree pattern of the PGP network.

The REC filtering algorithm (Fig. 5.24b) shows an increase in the formation of echo chambers with an increasing fraction of stubborn actors, followed by a decrease if the fraction of stubborn actors is further increased. This is visible for both the PGP trust network and the network models. Again, the PGP network has a smaller formation of echo chambers than the network model with similar clustering and modularity (SBM-WS), due to its heterogeneous degree distribution. The data points for the SBM and the PGP trust network coincide, which may suggest that the hampering in the formation of echo chambers due to a heterogeneous degree distribution is of a similar size as the hampering due to a lack of clustering.

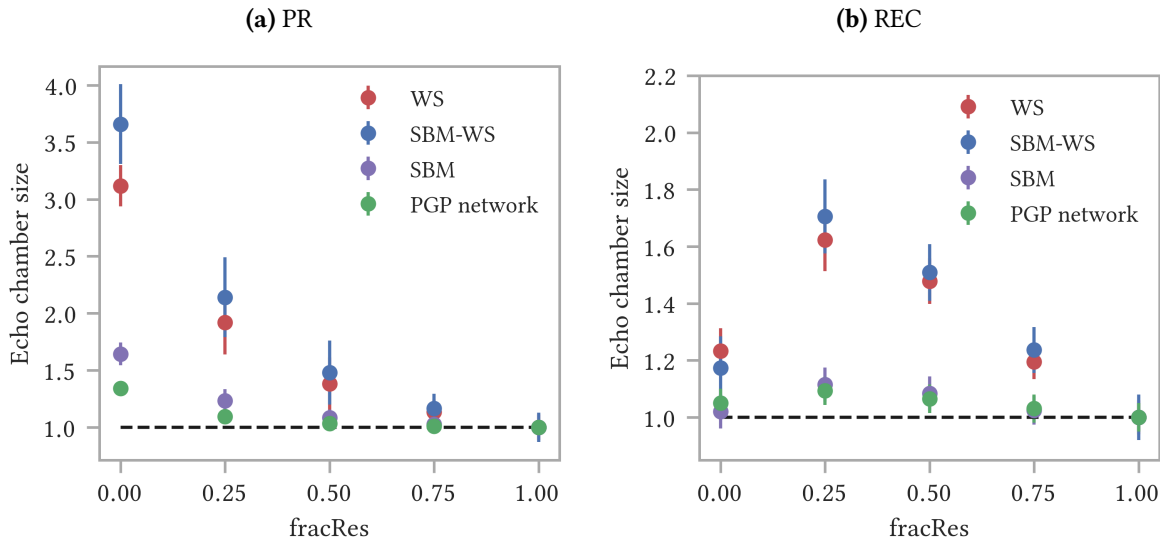


Figure 5.24: Formation of echo chambers versus the fraction of completely stubborn actors, fracRes , for an initial 50/50 opinion distribution. The PGP trust network is compared to corresponding network models: (i) WS with $\langle k \rangle = 4$, $\beta = 0.2$ and $\langle cc \rangle = 0.266 \pm 0.003$; (ii) SBM-WS with 60 communities of size 178, each community has the following Watts-Strogatz parameters: $\langle k \rangle = 4$, $\beta = 0.12$; edges are added between communities with probability $p_{\text{add}} = 0.00007$, $\langle k \rangle = 4.74 \pm 0.01$, $\langle cc \rangle = 0.263 \pm 0.003$ and $Q = 0.842 \pm 0.002$; (iii) SBM with 60 communities of size 178 with $p_{\text{cl}} = 0.02$, $p_{\text{add}} = 0.00005$, $\langle k \rangle = 4.06 \pm 0.02$ and $Q = 0.868 \pm 0.002$. **(a)** PR filtering algorithm; **(b)** REC filtering algorithm. The y -axis shows the average of the normalized fraction of nodes with all neighbors having opinion A and the normalized fraction of nodes with all neighbors having opinion B. This value represents the formation of echo chambers in the system (denoted with echo chamber size in the figure). Each data point is the average of 50 independent simulations. Bars represent the standard deviation σ .

Chapter 6

Discussion

We made use of simple toy models of real social media platforms to generate results regarding the evolution of the prevalence of the opinions and formation of echo chambers. These toy models consist of several layers, including a network layer and an opinion dynamics layer. Simple filtering algorithms were implemented to replicate and simulate the content curation used by real social media companies. Furthermore, a notion of stubbornness was introduced to investigate the interplay between individual resistance to change, network structure and filtering algorithm. For simplicity we only allowed two competing opinions (A and B). Furthermore, we studied two different settings: balanced starting conditions and unbalanced starting conditions.

We investigated the effect of the network structure on the dynamics of the opinions in the system. The main focus was put on the difference between networks with a high clustering coefficient and no community structure (WS) compared to networks with a clear community structure and a low clustering coefficient (SBM). It was found that a clear community structure enhances the formation of echo chambers (mainly when using the PR filtering algorithm) compared to a random network. This enhancement is however not as strong as for networks with a high clustering coefficient. Networks that have both a high clustering coefficient and a high modularity (clear community structure) (SBM-WS) behave similar as the high clustering networks (WS). This indicates that it is mainly the high clustering that drives the formation of echo chambers. There is a correlation between modularity and formation of echo chambers: a higher modularity results in a larger formation of echo chambers (in case of the PR filtering algorithm). The enhancement is just not as strong as the enhancement in the formation of echo chambers introduced by a high clustering.

When introducing a notion of stubbornness (with the help of a stubbornness parameter r), we found that the interplay between the PR filtering algorithm and this individual resistance resulted in a decrease in the formation of echo chambers for the both the high clustering (WS, SBM-WS) and the high modularity networks (SBM, SBM-WS). The REF and REC filtering algorithms, on the other hand, showed an increase in the formation of echo chambers with increasing stubbornness, followed by a decrease if the stubbornness was further increased. This is mainly seen in the high clustering networks, however a small bump can also be observed in the high modularity network. This interplay between the PR filtering algorithm and individual resistance versus the interplay between the REF/REC filtering algorithms

and stubbornness is seen for both balanced starting conditions and unbalanced starting conditions. It was also found that including stubborn actors hampers the increase in the majority opinion (and thus prevents the formation of a final consensus state) in case of unbalanced starting conditions combined with the PR filtering algorithm.

These results give us an insight in the interplay between network structure, filtering algorithms and individual resistance. These insights may be crucial to understand phenomena such as polarization in society and to determine the impact of social media on these phenomena. They teach us that even though semantic filtering (PR) strongly enhances the formation of echo chambers in the absence of stubborn actors, this enhancing does not stand on its own. An interplay between a network with a high clustering and/or community structure is needed to effectively see this increase in echo chambers induced by semantic filtering. A random network, combined with semantic filtering, does not enhance the formation of echo chambers. Furthermore, if there are no stubborn actors, recent or random filtering (REC/REF) seems to be more protective against the formation of echo chambers than semantic filtering. If there are, however, small fractions of stubborn actors in the system, this scenario changes: semantic filtering starts to hamper the formation of echo chambers, whereas recent or random filtering begins to enhance polarization. It is often assumed that algorithmic personalization, tailored to ones preferences (eg. semantic filtering), is one of the main reasons of the appearance of echo chambers on social media [38][56][70]. Our results may, however, suggest, that if there is some kind of stubbornness (which is probably the case in the real world), heterogeneous exposure (REF/REC) to different opinions may be more harmful than a homogeneous exposure (PR). Bail et al. found experimental results that may agree with this finding [5]. This is an interesting result, that should be investigated more thoroughly.

It was found that the initial distribution of the opinions over the communities in a network with community structure (SBM) makes a difference. We investigated a scenario in which a fraction of the communities was given a single opinion, opinion A, while the remaining communities were given an initial 50/50 opinion distribution. This scenario was then compared to the case in which the total opinion distribution was randomly distributed over the system. This was done for both a high modularity and a low modularity network and for both the REC and PR filtering algorithms.

The REC filtering algorithm did not show any difference in the evolution of the prevalence of the opinions between this (initial) community distributed and (initial) randomly distributed scenario. For the PR filtering algorithm it was found that the high modularity network hampers the increase in the majority opinion in the community distributed scenario compared to the randomly distributed scenario. For the low modularity network, such a discrepancy was not found.

Furthermore, it was found that, when using the REC filtering algorithm, the system evolves towards a more mixed opinion distribution in the community distributed scenario. This was found for both the high and low modularity network. If we make a fraction of the communities single opinion A communities, while giving the remaining communities a 50/50 opinion distribution, we initially have a large number of echo chambers around opinion A. Over time, these opinion A echo chambers decrease; even if there is only a limited amount of communication between the communities, it was found that the

single opinion A communities become more and more mixed. The total prevalence of opinion A is unchanged when using the REC filtering algorithm, so the initial 50/50 communities see a small increase in the prevalence of opinion A. The randomly distributed scenario does not evolve towards a mixed opinion distribution, instead there is a small increase in the formation of echo chambers around the minority opinion B (for both the high and low modularity network).

For the PR filtering algorithm, the randomly distributed scenario resulted in an increase in the formation of echo chambers around the majority opinion A. This was observed for both the low and high modularity networks. The community distributed scenario for the low modularity network hampers this increase. It was found that this is more than just a result of the increased number of initial opinion A echo chambers. For the high modularity network, the community distributed scenario showed an even larger hampering of the formation of echo chambers around the majority opinion A. This is probably the result of: (i) an even higher initial number of echo chambers around the majority opinion A than for the low modularity network; (ii) the hampering in the increase of the majority opinion A for the community distributed scenario in case of the high modularity network combined with the PR filtering algorithm.

Finally, results for real-world networks were compared to those obtain from corresponding network models. It was found that the formation of echo chambers in the real-world networks is smaller than those in a network model with similar clustering and modularity. The reason for this hampered formation of echo chambers was attributed to the heterogeneous degree pattern of the real-world networks. This hampering of echo chambers due to a heterogeneous degree distribution was also found by Perra and Rocha [66] when they compared a network model with a heterogeneous degree distribution to models with homogeneous contact patterns.

The formation of echo chambers in social networks/social media, and the enhancement of them when using algorithmic personalization such as semantic filtering, agrees with results found in literature (in the absence of stubborn actors) [11][17][62][72]. The enhancement of the formation of echo chambers in clustered communities is also found in literature on complex contagious processes [42]. Banisch and Olbrich showed that in a social feedback model polarization is increased in high modularity networks compared to an Erdős-Rényi network [6]. This agrees with our findings that a clear community structure enhances the formation of echo chambers.

The hampering in the increase of the majority opinion in case of unbalanced starting conditions combined with the introduction of stubborn actors for the PR filtering algorithm agrees partly with related research on continuous opinion dynamics models combined with stubborn actors [3]. In this research, Acemoğlu et al. showed that introducing stubborn actors (with different opinions) in an inhomogeneous stochastic gossip process of continuous opinion dynamics leads to a situation in which consensus can no longer be reached [3]. This result is also found in the majority opinion dynamics model and in the voter model combined with stubborn actors (equally distributed over the two opinions) [37][55][79]. In our case, the possible consensus around the majority opinion, that could have been reached when combining the PR filtering algorithm with unbalanced starting conditions, can no longer be obtained when introducing stubborn actors.

Wang et al. [77] proposed an agent based continuous opinion dynamics model in which they investigated the formation of echo chambers. They found that stubbornness of individuals protects them from the influence of centralized sources of influence; “A purely stubborn or conformist population may both be less susceptible to the emergence of two dominant and opposing echo chambers” (Wang et al., p.10, [77]). This agrees with our result that the PR filtering algorithm, combined with stubborn actors, hinders the formation of echo chambers.

It must be emphasized that there are limitations to our model and methods. First, the simpleness of the model, which on one hand can be seen as a strength, may also be one of the weaknesses. Real-life social behavior and opinion dynamics on social media may be far from simple. As a consequence, there may be many dynamics of real-life opinion formation that are not well-captured by our model. More empirical data is therefore needed to compare the results, obtained from our model, against. Other limitations may be the rather small system sizes that were used in our simulations ($N = 10^3$). It is unclear how the system size affects the results and it is recommended that the model is tested on both larger network models and real-world networks. Another possible shortcoming is the binary nature of the model. There are real-life cases in which people have to choose between two competing opinions. These situations, however, do not cover the complete range of possible opinion dynamics situations. It would be interesting to run the model on situations where more than two opinions are allowed or to switch to continuous opinion dynamics. We also did not differentiate between the agents in our model, except for non-stubborns versus stubborns. This combined with the homogeneous degree distribution of our networks models may be another limitation. Real-life social media platforms display a heterogeneous contact pattern, where the ‘hubs’ are often more influential than other users, not only by their larger reach, but also by their status. This may impact the spread of opinions [31][76]. We could adapt our model to mimic this real social media behavior more closely. Therefore, a heterogeneous network model should be introduced, combined with an influence parameter. This parameter should be used to determine the influence of an agent on others: the opinion of a more influential agent is easier adopted by the others. In the model, the high degree nodes should then be made more influential. As a final limitation, we mention the fixed stubbornness of the agents. Even though the stubbornness parameter r could be individualized to each node, we did not include the possibility to be more stubborn towards opinions coming from one friend than from another. This idea may be linked to the influence of certain friends/acquaintances: somebody may adopt another viewpoint more easily from certain friends than from others.

Some future investigation paths, linked to limitations of our model, were given in the previous paragraph. Other future directions may be: (i) investigating the distribution of the stubborn actors (community distributed versus random); (ii) making one opinion more stubborn than the other; (iii) investigating the effect of the activation mechanism: what happens if we switch to the heterogeneous activation mechanism (see Section 3.4)? and (iv) making the network temporal in the sense that it becomes possible to add and remove friends. Sasahara et al. investigated a model in which social influence was combined with social rewiring (unfriending) [68]. Their findings were that these processes of influence and unfriending enhanced the formation of echo chambers [68]. It might be interesting to incorporate their model features into our model with algorithmic personalization and stubbornness.

Chapter 7

Conclusion

Simple toy models were implemented to investigate the interplay between network structure, filtering algorithms and individual resistance to change in the evolution of two competing opinions. Our goal was to get a better understanding of the impact of social media and algorithmic personalization on phenomena such as polarization and formation of echo chambers (opinion clusters) in society.

We found that topological correlations such as high clustering strongly enhance the formation of opinion clusters. Beside clustering, community structure also favors the formation of echo chambers. Real-world networks have a lower formation of echo chambers than network models with similar clustering and modularity. The heterogeneous contact pattern of these real-world networks is most likely the cause of this hampering. If people are not stubborn, we found that semantic filtering and hence, a homogeneous exposure to information increases polarization in the system. This is an intuitive result: if you shield people from opposing views and strengthen them in their own beliefs, it feels natural that the system will evolve towards a more polarized state. It is then expected that a more heterogeneous exposure to information reduces this polarization. We found that this is indeed the case if people are not stubborn. If, on the contrary, people have some level of stubbornness, we found the surprising result that homogeneous exposure to information may be more protective against opinion clusters than heterogeneous exposure. This is an important result, since it may change our beliefs/assumptions that algorithmic personalization is at the root of the increase in polarization and extremism often seen on social media. More research on this topic is definitely needed in the near future. Finally, we found that distributing the opinions in communities instead of randomly distributing them may hinder the convergence towards the majority opinion in case of semantic filtering, if the modularity is high enough.

Our results strongly suggest that the effects of algorithmic personalization do not stand on their own. Instead, the interplay with certain network topologies may enhance or hamper these effects. Beside that, individual resistance strongly affects the impact of these filtering algorithms. It would therefore be incorrect to only point to algorithmic personalization as the cause of polarization. It is the interplay between many different aspects of the system (such as topological correlations, distribution of the opinions, individual resistance, content curration) that may potentially enhance or hamper the formation of opinion clusters.

Appendix A

Network measurements: Derivations

A.1 Modularity

A.1.1 Simple form of network modularity

Using [9]

$$Q_c = \frac{1}{2L} \sum_{(i,j) \in C_c} (A_{ij} - p_{ij}) , \quad (\text{A.1})$$

and [9]

$$p_{ij} = \frac{k_i k_j}{2L} , \quad (\text{A.2})$$

we can write the modularity of the whole network as [9]

$$Q = \frac{1}{2L} \sum_{i,j=1}^N \left(A_{ij} - \frac{k_i k_j}{2L} \right) \delta_{c_i, c_j} , \quad (\text{A.3})$$

where c_i represents the community to which node i belongs and the Dirac-delta function δ_{c_i, c_j} expresses the fact that only pairs of nodes that belong to the same community are taken into account. We can then rewrite the first term as a sum over communities [9]

$$\frac{1}{2L} \sum_{i,j=1}^N A_{ij} \delta_{c_i, c_j} = \sum_{c=1}^{n_c} \frac{1}{2L} \sum_{(i,j) \in C_c} A_{ij} = \sum_{c=1}^{n_c} \frac{L_c}{L} , \quad (\text{A.4})$$

where L_c is the number of edges in community C_c and the factor 2 disappears because each edge is counted twice in A_{ij} . Similarly, the second term in Eq. (A.3) can be rewritten as [9]

$$\frac{1}{2L} \sum_{i,j=1}^N \frac{k_i k_j}{2L} \delta_{c_i, c_j} = \sum_{c=1}^{n_c} \frac{1}{(2L)^2} \sum_{(i,j) \in C_c} k_i k_j = \sum_{c=1}^{n_c} \frac{k_c^2}{4L^2} , \quad (\text{A.5})$$

where k_c is the total degree of the nodes in community C_c . Combining Eq. (A.4) and Eq. (A.5) gives the final result [9]

$$Q = \sum_{c=1}^{n_c} \left[\frac{L_c}{L} - \left(\frac{k_c}{2L} \right)^2 \right]. \quad (\text{A.6})$$

A.1.2 Modularity change after merging two communities

Consider two communities A and B and denote with k_A and k_B the total degree of communities A and B respectively [9]. The change in modularity after merging the two communities is calculated as follows (using Eq. (A.6)) [9]

$$\Delta Q_{AB} = \left[\frac{L_{AB}}{L} - \left(\frac{k_{AB}}{2L} \right)^2 \right] - \left[\frac{L_A}{L} - \left(\frac{k_A}{2L} \right)^2 + \frac{L_B}{L} - \left(\frac{k_B}{2L} \right)^2 \right], \quad (\text{A.7})$$

where $L_{AB} = L_A + L_B + l_{AB}$ is the total number of edges in the merged community; L_A and L_B are the number of edges in communities A and B respectively and l_{AB} is the number of direct edges between communities A and B [9]. $k_{AB} = k_A + k_B$ is the total degree of nodes in the merged community; k_A and k_B are the total degree of the nodes in community A and B respectively [9]. Inserting the formulas for L_{AB} and k_{AB} in Eq. (A.7) gives

$$\Delta Q_{AB} = \frac{l_{AB}}{L} - \frac{k_A k_B}{2L^2}. \quad (\text{A.8})$$

Appendix B

Network models: Derivations

B.1 The Erdős-Rényi model

B.1.1 Degree distribution

The probability that a node is connected to k other nodes and not to the $N - 1 - k$ others is given by

$$p^k(1-p)^{N-1-k}. \quad (\text{B.1})$$

The number of ways to choose the k nodes among the $N-1$ possible candidates is given by the binomial coefficient

$$\binom{N-1}{k} = \frac{(N-1)!}{k!(N-1-k)!}, \quad (\text{B.2})$$

and the probability of being connected to exactly k other nodes becomes

$$P(k) = \binom{N-1}{k} p^k(1-p)^{N-1-k}. \quad (\text{B.3})$$

We thus derived the degree distribution of a random network.

B.1.2 Average degree

The expected mean degree is given by [81]

$$\begin{aligned} \langle k \rangle &= \sum_{k=0}^{N-1} k P(k) \\ &= \sum_{k=0}^{N-1} k \binom{N-1}{k} p^k(1-p)^{N-1-k}. \end{aligned} \quad (\text{B.4})$$

In order to simplify this equation we can make use of the following formula [81]

$$(p+q)^n = \sum_{k=0}^n \binom{n}{k} p^k q^{n-k}. \quad (\text{B.5})$$

Differentiating both sides of this equation (with respect to p) gives us [81]

$$\begin{aligned} n(p+q)^{n-1} &= \sum_{k=0}^n \binom{n}{k} kp^{k-1} q^{n-k} \\ &= \frac{1}{p} \sum_{k=0}^n \binom{n}{k} kp^k q^{n-k}. \end{aligned} \tag{B.6}$$

Finally, by substituting $q = 1 - p$, we get [81]

$$\begin{aligned} n(p + (1-p))^{n-1} &= \frac{1}{p} \sum_{k=0}^n \binom{n}{k} kp^k (1-p)^{n-k} \\ np &= \sum_{k=0}^n \binom{n}{k} kp^k (1-p)^{n-k}, \end{aligned} \tag{B.7}$$

where the right hand side is equal to Eq. (B.4) with $n = N - 1$ and we obtain $\langle k \rangle = (N - 1)p$.

B.1.3 Poisson form of the degree distribution

We begin with the exact binomial distribution (Eq.(2.30))

$$P(k) = \binom{N-1}{k} p^k (1-p)^{N-1-k}, \tag{B.8}$$

which characterizes a random graph. In the case $k \ll N$, we can simplify the binomial in the following way [7]

$$\binom{N-1}{k} = \frac{(N-1)(N-1-1)\dots(N-1-k+1)}{k!} \approx \frac{(N-1)^k}{k!}. \tag{B.9}$$

We also note the following equality [7]

$$\ln[(1-p)^{N-1-k}] = (N-1-k) \ln \left(1 - \frac{\langle k \rangle}{N-1} \right), \tag{B.10}$$

where we made use of the fact that $\langle k \rangle = (N - 1)p$. Using the series expansion [7]

$$\ln(1+x) = \sum_{n=1}^{\infty} \frac{(-1)^{n+1}}{n} x^n = x - \frac{x^2}{2} + \frac{x^3}{3} - \dots, \quad \forall |x| \leq 1, \tag{B.11}$$

we get [7]

$$\ln[(1-p)^{N-1-k}] \approx -(N-1-k) \frac{\langle k \rangle}{N-1} = -\langle k \rangle \left(1 - \frac{\langle k \rangle}{N-1} \right) \approx -\langle k \rangle, \tag{B.12}$$

which is valid if $k \ll N$. We thus find [7]

$$(1-p)^{N-1-k} = e^{-\langle k \rangle}. \tag{B.13}$$

Substituting Eq. (B.13) and Eq. (B.9) in Eq. (B.8) and using $\langle k \rangle = (N - 1)p$, we finally obtain the Poisson form of the degree distribution [7]

$$\begin{aligned} P(k) &= \binom{N-1}{k} p^k (1-p)^{N-1-k} = \frac{(N-1)^k}{k!} p^k e^{-\langle k \rangle} \\ &= \frac{(N-1)^k}{k!} \left(\frac{\langle k \rangle}{N-1} \right)^k e^{-\langle k \rangle} \\ &= e^{-\langle k \rangle} \frac{\langle k \rangle^k}{k!}. \end{aligned} \quad (\text{B.14})$$

B.1.4 Diameter

The expected number of nodes at a distance d from a starting node is [7]

$$N(d) = 1 + \langle k \rangle + \langle k \rangle^2 + \dots + \langle k \rangle^d = \frac{\langle k \rangle^{d+1} - 1}{\langle k \rangle - 1}. \quad (\text{B.15})$$

$N(d)$ cannot exceed the number of nodes N in the network. The maximum distance or diameter d_{\max} of the network can thus be found by setting [7]

$$N(d_{\max}) \approx N. \quad (\text{B.16})$$

If $\langle k \rangle \gg 1$, we can neglect the -1 terms in Eq. (B.15), which gives [7]

$$N \approx \langle k \rangle^{d_{\max}}, \quad (\text{B.17})$$

and thus the diameter of a random network becomes [7]

$$d_{\max} \approx \frac{\ln N}{\ln \langle k \rangle}. \quad (\text{B.18})$$

B.2 The Watts-Strogatz model

B.2.1 The regular ring lattice

Clustering coefficient

A triangle in the regular ring lattice requires two edge traversals in the same direction and one in the opposite direction [64]. In the regular ring lattice every node has a fixed degree K , this means that each node is connected to $K/2$ neighbors on its left and $K/2$ neighbors on its right. It is then clear that the final, backwards step can span at most $K/2$ nodes [64]; otherwise we would end up at a different node from which we started, which would definitely not form a triangle.

Hence, the number of triangles for a given node is given by choosing the two forward target nodes from the $K/2$ possibilities [64]

$$\binom{\frac{K}{2}}{2} = \frac{1}{4} K \left(\frac{K}{2} - 1 \right). \quad (\text{B.19})$$

The number of connected triples per node is given by choosing two nodes out of the K neighbors [64]

$$\binom{K}{2} = \frac{1}{2}K(K - 1). \quad (\text{B.20})$$

Since every node in the regular ring lattice is identical, we can easily find the total number of triangles and connected triples in the network by multiplying Eq. (B.19) and Eq. (B.20) by the number of nodes N . We then obtain the final result for the clustering coefficient in the regular ring lattice [64]

$$\langle cc \rangle = \frac{3 \cdot N \frac{1}{4} K \left(\frac{K}{2} - 1 \right)}{N \frac{1}{2} K (K - 1)} = \frac{3(K - 2)}{4(K - 1)}. \quad (\text{B.21})$$

Average distance

The general formula for the average distance is given by Eq. (2.11)

$$\langle d \rangle = \frac{1}{N(N - 1)} \sum_{i \neq j} d_{ij}, \quad (\text{B.22})$$

where the sum runs over the shortest path between every pair of nodes. Assume we have a regular ring lattice with N nodes and each node has K neighbors. We can then calculate the distance between node i and every other node in the ring lattice as follows: (i) There are K nodes adjacent to node i , so there are K nodes with a distance $d_{ij} = 1$; (ii) There are K nodes that are neighbors of the neighbors of node i , so there are K nodes with a distance $d_{ij} = 2$; (iii) ...; and (iv) There are K nodes that have a distance $d_{ij} = \frac{N}{K}$ between them and node i ; it's easy to see that these are the nodes that are the furthest away from node i .

So the average distance for node i becomes [1]

$$d_i = \frac{1}{N - 1} K \left(1 + 2 + 3 + \dots + \frac{N}{K} \right) \approx \frac{K}{N} \left(1 + 2 + 3 + \dots + \frac{N}{K} \right), \quad (\text{B.23})$$

where the last approximation holds for $N \gg 1$. Since every node in the regular ring lattice is identical we can easily find the average distance of the network [1]

$$\langle d \rangle = \frac{1}{N} \sum_i d_i = \frac{1}{N} N d_i \approx \frac{K}{N} \left(1 + 2 + 3 + \dots + \frac{N}{K} \right). \quad (\text{B.24})$$

Using [1]

$$1 + 2 + 3 + \dots + x = \sum_{i=1}^x i = \frac{x(x + 1)}{2} \approx \frac{x^2}{2}, \quad (\text{B.25})$$

where the last approximation holds for $x \gg 1$; we finally obtain [1]

$$\langle d \rangle \approx \frac{K}{N} \frac{\frac{N^2}{K^2}}{2} = \frac{N}{2K}. \quad (\text{B.26})$$

Bibliography

- [1] Chapter 9: Graphs and networks.
- [2] E. Abbe. Community detection and stochastic block models: Recent developments. *Journal of Machine Learning Research*, (18):1–86, Oct. 2018.
- [3] D. Acemoğlu, G. Como, F. Fagnani, and A. Ozdaglar. Opinion fluctuations and disagreement in social networks. *Mathematics of Operations Research*, 38(1):1–27, Feb. 2013.
- [4] R. Albert and A.-L. Barabási. Statistical mechanics of complex networks. *Reviews of Modern Physics*, 74(1):47–97, Jan. 2002.
- [5] C. A. Bail, L. P. Argyle, T. W. Brown, J. P. Bumpus, H. Chen, M. B. F. Hunzaker, J. Lee, M. Mann, F. Merhout, and A. Volfovsky. Exposure to opposing views on social media can increase political polarization. *Proceedings of the National Academy of Sciences*, 115(37):9216–9221, Aug. 2018.
- [6] S. Banisch and E. Olbrich. Opinion polarization by learning from social feedback. *The Journal of Mathematical Sociology*, 43(2):76–103, Oct. 2018.
- [7] A.-L. Barabási. Network science: Random networks. Sept. 2014.
- [8] A.-L. Barabási. *Network science*, chapter 4, pages 112–164. Cambridge University Press, July 2016.
- [9] A.-L. Barabási. *Network science*, chapter 9, pages 320–378. Cambridge University Press, July 2016.
- [10] A. Barrat and M. Weigt. On the properties of small-world network models. *Europ. Phys. J. B*, 547(13), 2000.
- [11] F. Baumann, P. Lorenz-Spreen, I. M. Sokolov, and M. Starnini. Modeling echo chambers and polarization dynamics in social networks. *Phys. Rev. Lett.* 124, 04830, June 2019.
- [12] I. Benjamini, S.-O. Chan, R. O’Donnell, O. Tamuz, and L.-Y. Tan. Convergence, unanimity and disagreement in majority dynamics on unimodular graphs and random graphs. *Stochastic Processes and their Applications*, 126(9):2719–2733, Sept. 2016.
- [13] M. Boguñá, R. Pastor-Satorras, A. Díaz-Guilera, and A. Arenas. Models of social networks based on social distance attachment. *Physical Review E*, 70(5), Nov. 2004.
- [14] E. Bozdag. Bias in algorithmic filtering and personalization. *Ethics and Information Technology*, 15(3):209–227, June 2013.

- [15] M. Buchanan. *The social atom: Why the rich get richer, cheaters get caught, and your neighbor usually looks like you*. BLOOMSBURY, June 2007.
- [16] C. Castellano, S. Fortunato, and V. Loreto. Statistical physics of social dynamics. *Reviews of Modern Physics*, 81(2):591–646, May 2009.
- [17] M. Cinelli, G. D. F. Morales, A. Galeazzi, W. Quattrociocchi, and M. Starnini. Echo chambers on social media: A comparative analysis. Apr. 2020.
- [18] A. Clauset. Inference, models and simulation for complex systems: Lecture 13. Oct. 2011.
- [19] A. Clauset. Network analysis and modeling, csci 5352: Lecture 6. 2017.
- [20] A. Clauset, E. Tucker, and M. Sainz. The colorado index of complex networks. <https://icon.colorado.edu/>, 2016.
- [21] P. Crucitti, V. Latora, M. Marchiori, and A. Rapisarda. Complex systems: Analysis and models of real-world networks.
- [22] L. da F. Costa. What is a complex network? (cdt-2). 2018.
- [23] L. da F. Costa, O. N. O. Jr., G. Travieso, F. A. Rodrigues, P. R. V. Boas, L. Antiqueira, M. P. Viana, and L. E. C. da Rocha. Analyzing and modeling real-world phenomena with complex networks: A survey of applications. Oct. 2007.
- [24] L. da F. Costa, F. A. Rodrigues, G. Travieso, and P. R. V. Boas. Characterization of complex networks: A survey of measurements. *Advances in Physics*, 56(1):167–242, Jan. 2007.
- [25] A. S. da Mata. Complex networks: a mini-review. *Brazilian Journal of Physics*, 50(5):658–672, July 2020.
- [26] G. Deffuant. Comparing extremism propagation patterns in continuous opinion models. *Journal of Artificial Societies and Social Simulation*, 9(3):8, 2006.
- [27] G. Deffuant, F. Amblard, G. Weisbuch, and T. Faure. How can extremism prevail? a study based on the relative agreement interaction model. *Journal of Artificial Societies and Social Simulation*, 5(4), Oct. 2002.
- [28] G. Deffuant, D. Neau, F. Amblard, and G. Weisbuch. Mixing beliefs among interacting agents. *Advances in Complex Systems*, 03(01n04):87–98, Jan. 2000.
- [29] S. N. Dorogovtsev and J. F. F. Mendes. Evolution of networks. *Advances in Physics*, 51(4):1079–1187, June 2002.
- [30] D. Easley and J. Kleinberg. *Networks, crowds, and markets: Reasoning about a highly connected world*. Cambridge University Press, 2010.
- [31] C. Fan, Y. Jiang, Y. Yang, C. Zhang, and A. Mostafavi. Crowd or hubs: Information diffusion patterns in online social networks in disasters. *International Journal of Disaster Risk Reduction*, 46, June 2020.

- [32] J. Fernández-Gracia, K. Suchecki, J. J. Ramasco, M. S. Miguel, and V. M. Eguíluz. Is the voter model a model for voters? *Physical Review Letters*, 112(15), Apr. 2014.
- [33] E. Ferrara. A large-scale community structure analysis in facebook. *EPJ Data Science*, 1(1), Nov. 2012.
- [34] N. E. Friedkin and E. C. Johnsen. Social influence and opinions. *Journal of Mathematical Sociology*, 15(3-4):193–205, 1990.
- [35] N. E. Friedkin and E. C. Johnsen. Social influence networks and opinion change. *Advances in Group Processes*, 16(1), Jan. 1999.
- [36] T. Funke and T. Becker. Stochastic block models: A comparison of variants and inference methods. *PLOS ONE*, 14(4), Apr. 2019.
- [37] S. Galam and F. Jacobs. The role of inflexible minorities in the breaking of democratic opinion dynamics. *Physica A: Statistical Mechanics and its Applications*, 381:366–376, July 2007.
- [38] Y. Ge, S. Zhao, H. Zhou, C. Pei, F. Sun, W. Ou, and Y. Zhang. Understanding echo chambers in e-commerce recommender systems. July 2020.
- [39] W. Goddard and O. R. Oellermann. Distance in graphs. In *Structural Analysis of Complex Networks*, pages 49–72. Birkhäuser Boston, Sept. 2010.
- [40] D. Gribel, T. Vidal, and M. Gendreau. Assortative-constrained stochastic block models. Apr. 2020.
- [41] A. Guggiola. *A statistical physics approach to different problems in network theory*. phdthesis, Ecole normale supérieure de Paris, Oct. 2015.
- [42] D. Guilbeault, J. Becker, and D. Centola. Complex contagions: A decade in review. Oct. 2017.
- [43] H. Heer, L. Streib, R. B. Schäfer, and S. Ruzika. Maximising the clustering coefficient of networks and the effects on habitat network robustness. *PLOS ONE*, 15(10), Oct. 2020.
- [44] R. Hegselmann and U. Krause. Opinion dynamics and bounded confidence models, analysis, and simulation. *Journal of Artificial Societies and Social Simulation*, 5(3), 2002.
- [45] P. Holme and J. Saramäki. Temporal networks. *Physics Reports*, 519(3):97–125, Oct. 2012.
- [46] H.-B. Hu and X.-F. Wang. Disassortative mixing in online social networks. *EPL (Europhysics Letters)*, 86(1), Apr. 2009.
- [47] A. Ioannis and T. Eleni. Statistical analysis of weighted networks. Apr. 2007.
- [48] S. Iyer, T. Killingback, B. Sundaram, and Z. Wang. Attack robustness and centrality of complex networks. *PLOS ONE*, 8(4), Apr. 2013.
- [49] A. Jędrzejewski and K. Sznajd-Weron. Statistical physics of opinion formation: Is it a SPOOF? *Comptes Rendus Physique*, 20(4):244–261, May 2019.

- [50] B. Karrer and M. E. J. Newman. Stochastic blockmodels and community structure in networks. *Physical Review E*, 83(1), Jan. 2011.
- [51] M. Latapy and C. Magnien. Measuring fundamental properties of real-world complex networks.
- [52] C. Lee and D. J. Wilkinson. A review of stochastic block models and extensions for graph clustering. *Applied Network Science*, 4(1), Dec. 2019.
- [53] Y. Li, Y. Shang, and Y. Yang. Clustering coefficients of large networks. *Information Sciences*, 382-383:350–358, Mar. 2017.
- [54] M. McGlohon, L. Akoglu, and C. Faloutsos. Statistical properties of social networks. In *Social Network Data Analytics*, pages 17–42. Springer US, 2011.
- [55] M. Mobilia, A. Petersen, and S. Redner. On the role of zealotry in the voter model. *J. Stat. Mech. P08029*, June 2007.
- [56] S. Mohseni and E. Ragan. Combating fake news with interpretable news feed algorithms. Nov. 2018.
- [57] L. Muchnik, S. Pei, L. C. Parra, S. D. S. Reis, J. S. A. Jr, S. Havlin, and H. A. Makse. Origins of power-law degree distribution in the heterogeneity of human activity in social networks. *Scientific Reports*, 3(1), May 2013.
- [58] M. E. J. Newman. Models of the small world: A review. *J. Stat. Phys.*, 101:819–841, Jan. 2000.
- [59] M. E. J. Newman. The structure and function of complex networks. *SIAM Review*, 45(2):167–256, Jan. 2003.
- [60] M. E. J. Newman. Power laws, pareto distributions and zipf's law. *Contemporary Physics*, 46(5):323–351, Sept. 2005.
- [61] V. X. Nguyen, G. Xiao, X.-J. Xu, Q. Wu, and C.-Y. Xia. Dynamics of opinion formation under majority rules on complex social networks. *Scientific Reports*, 10(1), Jan. 2020.
- [62] D. Nikolov, D. F. Oliveira, A. Flammini, and F. Menczer. Measuring online social bubbles. *PeerJ Computer Science*, 1, Dec. 2015.
- [63] H. Noorazar, K. R. Vixie, A. Talebanpour, and Y. Hu. From classical to modern opinion dynamics. *International Journal of Modern Physics C*, 31(7), July 2020.
- [64] K. Pelechrinis. Telcom2125: Network science and analysis, 2015.
- [65] N. Perra, B. Gonçalves, R. Pastor-Satorras, and A. Vespignani. Activity driven modeling of time varying networks. *Scientific Reports*, 2(1), June 2012.
- [66] N. Perra and L. E. C. Rocha. Modelling opinion dynamics in the age of algorithmic personalisation. *Scientific Reports*, 9(1), May 2019.
- [67] B. Saha, A. Mandal, S. B. Tripathy, and D. Mukherjee. Complex networks, communities and clustering: A survey. Mar. 2015.

- [68] K. Sasahara, W. Chen, H. Peng, G. L. Ciampaglia, A. Flammini, and F. Menczer. Social influence and unfollowing accelerate the emergence of echo chambers. *Journal of Computational Social Science*, 4(1):381–402, Sept. 2020.
- [69] P. Sobkowicz. Modelling opinion formation with physics tools: Call for closer link with reality. *Journal of Artificial Societies and Social Simulation*, 12(1):11.
- [70] B. Stark, D. Stegmann, M. Magin, and P. Jürgens. Are algorithms a threat to democracy? the rise of intermediaries: A challenge for public discourse. *Governing Platforms*, page 69, May 2020.
- [71] A. Sîrbu, V. Loreto, V. D. P. Servedio, and F. Tria. Opinion dynamics: models, extensions and external effects. 2016.
- [72] A. Sîrbu, D. Pedreschi, F. Giannotti, and J. Kertész. Algorithmic bias amplifies opinion polarization: A bounded confidence model. Mar. 2018.
- [73] G. Thedchanamoorthy, M. Piraveenan, D. Kasthuriratna, and U. Senanayake. Node assortativity in complex networks: An alternative approach. *Procedia Computer Science*, 29:2449–2461, 2014.
- [74] R. Toivonen, L. Kovanen, M. Kivelä, J.-P. Onnela, J. Saramäki, and K. Kaski. A comparative study of social network models: Network evolution models and nodal attribute models. *Social Networks*, 31(4):240–254, Oct. 2009.
- [75] M. A. Turner and P. E. Smaldino. Stubborn extremism as a potential pathway to group polarization.
- [76] Q. Wang, F. Miao, G. K. Tayi, and E. Xie. What makes online content viral? the contingent effects of hub users versus non–hub users on social media platforms. *Journal of the Academy of Marketing Science*, 47(6):1005–1026, July 2019.
- [77] X. Wang, A. D. Sirianni, S. Tang, Z. Zheng, and F. Fu. Public discourse and social network echo chambers driven by socio-cognitive biases. *Physical Review X*, 10(4), Dec. 2020.
- [78] D. J. Watts and S. H. Strogatz. Collective dynamics of ‘small-world’ networks. *Nature*, 393(6684):440–442, June 1998.
- [79] E. Yıldız, A. Ozdaglar, D. Acemoğlu, A. Saberi, and A. Scaglione. Binary opinion dynamics with stubborn agents. *ACM Transactions on Economics and Computation*, 1(4):1–30, Dec. 2013.
- [80] D. Zhang and G. Guo. A comparison of online social networks and real-life social networks: A study of sina microblogging. *Mathematical Problems in Engineering*, pages 1–6, 2014.
- [81] J. Zhang, D. Goldburt, and J. Hopcroft. Lecture 01: Large graphs. Jan. 2006.